GENOMIC DIVERSITY AND VIRULENCE OF ENTEROHEMORRHAGIC *ESCHERICHIA COLI*

By

Galeb Saif Abu-Ali

A DISSERTATION

Submitted to
Michigan State University
in partial fulfillment of the requirements
for the degree of

DOCTOR OF PHILOSOPHY

Comparative Medicine and Integrative Biology

2009

ABSTRACT

GENOMIC DIVERSITY AND VIRULENCE OF
ENTEROHEMORRHAGIC *ESCHERICHIA COLI*

By

Galeb Saif Abu-Ali

Enterohemorrhagic *Escherichia coli* (EHEC) strains have been shown to vary considerably in their ability to cause disease, although they share common sets of horizontally acquired virulence mechanisms. The basis for this variation has been explained, in part, by studies of evolutionary relatedness, which have resolved the EHEC pathotype into distinct genetic groups. Certain subpopulations of serotype O157:H7, the sole variant of the EHEC 1 pathogenic clone, have been associated with dramatically higher rates of severe human disease compared to other O157:H7 subpopulations. In addition to human infection, several serotypes of the EHEC 2 clone have also been implicated in bovine disease. The overall goal of this research is to characterize the extent of genetic variation among EHEC, and identify the differences in pathogenic potential among EHEC subpopulations. The specific aims are to: 1) evaluate the genomic diversity of the EHEC 2 pathogenic clone and its relatedness to EHEC 1; 2) identify differences in the colonization capacity and genome-wide expression profiles of epidemiologically different O157:H7 strains; and 3) determine if the phenotypic and transcriptional differences between O157:H7 strains are associated with the inherent genetic variability among O157:H7 subpopulations. Under specific aim 1, the gene content of the EHEC 2 clonal group was determined with comparative genomic microarrays, and the data were

subjected to phylogenetic analyses. In specific aim 2, infection of epithelial cells with O157:H7 was conducted to determine colonization phenotypes, and to examine whole-genome expression of O157:H7 strains under conditions that mimic the host-pathogen challenge. For specific aim 3, the colonization capacity and transcriptional responses were characterized for population samples representative of two distinct lineages of O157:H7. The phenotypic and transcriptional data were compared between O157:H7 strains of the same lineage, as well as between lineages. Appreciation of the genomic diversity of the EHEC 2 population will help focus future studies on EHEC 2 serotypes from which hypervirulent lineages are more likely to evolve. Observed differences in pathogenic potential between O157:H7 subpopulations will provide the basis for studying genetic factors, specific to hypervirulent lineages of EHEC, that mediate differential regulation of shared EHEC virulence mechanisms.

ACKNOWLEDGMENTS

I wish to thank my mentor, Thomas S. Whittam, for providing the resources and opportunities for me to acquire a broad range of scientific skills, and for his guidance, which was invaluable to the development of my intellectual courage. I thank my committee members, Paul Coussens, Matti Kiupel, Martha Mulks, Vincent Young, and my program director Vilma Yuzbasiyan-Gurkan for their advice and help; specially Martha Mulks who has guided me in the final stages of my studies.

My labmates have greatly helped my development with their positive attitude, critical discussions and technical assistance. I thank Teresa Bergholz, Scott Henderson, David Lacher, Shannon Manning, Adam Nelson, Lindsey Ouellette, Weihong Qi, James Riordan, Amber Springman, Sivapriya Kailasan Vanaja, and Lukas Wick.

My family has provided me with the support to complete my graduate studies. I wish to thank my parents, Saif and Milica, my brother Vladimir, and my wife Jovana, for their love and encouragement.

TABLE OF CONTENTS

LIST OF TABLES

LIST OF FIGURES

Figures in this dissertation are presented in color

ABBREVIATIONS

AEEC	Attaching and effacing *E. coli*
ANOVA	ANalysis Of Variance
APEC	Avian pathogenic *E. coli*
BSA	Bovine serum albumin
DAEC	Diffusely adherent *E. coli*
DMEM	Dulbecco's modified Eagle's medium
DMSO	Dimethyl-sulfoxide
EAEC	Enteroaggregative *E. coli*
EHEC	Enterohemorrhagic *E. coli*
EIEC	Enteroinvasive *E. coli*
EPEC	Enteropathogenic *E. coli*
ETEC	Enterotoxigenic *E. coli*
ExPEC	Extraintestinal *E. coli*
FAS	Fluorescent-actin staining
FBS	Fetal bovine serum
HC	Hemorrhagic colitis
HUS	Hemolytic uremic syndrome
LB	Luria-Bertani
LEE	Locus of enterocyte effacement
MAANOVA	MicroArray ANalysis Of Variance
MFI	Mean fluorescence intensity
MNEC	Meningitis-associated *E. coli*

ABBREVIATIONS

MOI	Multiplicity of infection
MOPS	morpholino-propanesulfonic acid
PAI	Pathogenicity island
PBS	Phosphate-buffered saline
PC	Preconditioned
qRT-PCR	Quantitative real-time PCR
SSC	Sodium chloride and sodium citrate
STEC	Shiga-toxin producing *E. coli*
Stx	Shiga toxin
TTSS	Type three secretion system
UPEC	Uropathogenic *E. coli*
UTIs	Urinary tract infections

CHAPTER 1

Literature Review

INTRODUCTION

Escherichia coli, the most common representative of *Enterobacteriaceae* in the intestinal microbiota, colonizes the gastrointestinal tract of humans and animals shortly after birth, and thereafter, the host and *E. coli* derive a mutual benefit. As a facultative anaerobe, *E. coli* persists in the mucous layer of the large intestine, where the predominantly anaerobic bacteria facilitate intestinal assimilation of some of the less digestible nutrients. Usually harmless, commensal *E. coli* strains cause disease only in the immuno-compromised host or when the mucosal barrier has been violated, allowing entry into sterile tissue (83, 193). Within the species, however, exist multiple pathogenic forms that cause a wide range of illnesses in humans and animals (79), significantly contributing to the clinical (212) and economic (287) burden of infectious disease in the US.

The capacity of pathogenic strains of *E. coli* to cause disease is attributable to their expression of a wide range of virulence factors, including various adhesins, toxins, secretion systems, iron scavenging proteins (siderophores), etc., that are otherwise absent in innocuous variants of the species (164, 220). These determinants of disease have been introduced into the *E. coli* genome mainly via horizontal transfer of pathogenicity islands (PAIs), DNA fragments of 'foreign' origin that confer virulence properties to the recipient strain (131). The ability of *E. coli* to acquire and maintain exogenous genetic material has earned this species a paradigm status for the evolution of microbial pathogens from commensal bacteria (193). The *en bloc* exchange of DNA

fragments can occur within as well as between species (230), via bacterial conjugation, phage transduction, or passive transformation, and, depending on the virulence factor conferred, arbitrates the ability of the recipient to cause different illnesses (Figure 1.1).

Repeated acquisition of foreign DNA fragments has resulted in considerable remodeling of the *E. coli* chromosome. Comparative genomic analysis of 17 commensal and pathogenic *E. coli* strains reveals a remarkably diverse species pan-genome, and indicates that the species 'core conserved' genome constitutes only about one-half the genome of a given *E. coli* isolate (252). Successful combinations of virulence traits, which have been permanently incorporated into the genome of certain strains, have resulted in the evolution of several highly specialized and adapted pathogenic lineages of *E. coli* (158, 164). Strains of pathogenic *E. coli* are differentiated by serologic typing of their O (somatic) and H (flagellar) antigens (220); however, serotype classification does not necessarily infer phylogenetic relatedness between strains nor does it unconditionally imply a common mode of pathogenesis (158).

Pathogenic subpopulations that utilize a shared set of virulence determinants and cause a similar disease are termed pathotypes, and the variety of clinical manifestations that are caused by these pathotypes can be broadly grouped into intestinal and extraintestinal disease (79). Extraintestinal pathogenic *E. coli* (ExPEC) include uropathogenic *E. coli* (UPEC),

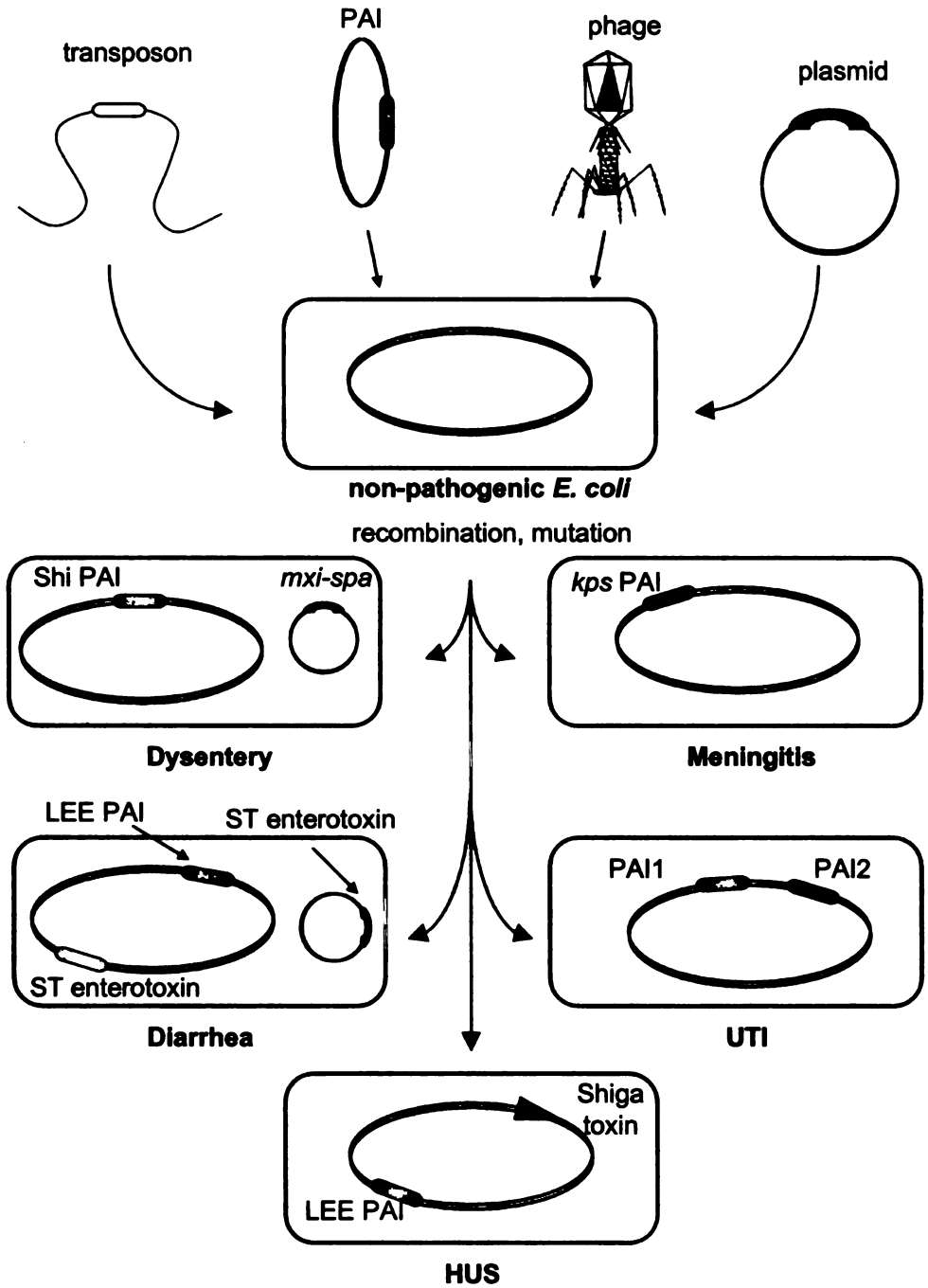

Figure 1.1. Evolution of pathogenic *E. coli* from commensal strains via acquisition of mobile genetic elements that encode virulence factors. Tn – transposon, PAI – pathogenicity island, UTI – urinary tract infection; HUS – hemolytic uremic syndrome. Adapted from (164).

which cause urinary tract infections (UTIs), and meningitis-associated *E. coli* (MNEC); avian pathogenic *E. coli* (APEC) cause respiratory infections, endocarditis and septicemia in poultry. The intestinal pathotypes are: attaching and effacing *E. coli* (AEEC), enteropathogenic *E. coli* (EPEC), Shiga-toxin producing *E. coli* (STEC), enterohemorrhagic *E. coli* (EHEC), enterotoxigenic *E. coli* (ETEC), enteroinvasive *E. coli* (EIEC), enteroaggregative *E. coli* (EAEC) and diffusely adherent *E. coli* (DAEC); disease manifestations and major virulence factors for the clinically most relevant pathotypes are reviewed in Table 1.1. Grouping by pathotype is not a clear delineation in every instance, as certain variants of pathogenic *E. coli* possess an arrangement of virulence factors that coincide with two pathotypes (Figure 1.2). The pathogenic potential of *E. coli* is extremely diverse and the continuous identification of new determinants of disease leads to discovery of potentially new pathotypes of *E. coli*, such as the recently proposed adherent-invasive *E. coli* pathotype that is associated with Crohn's disease (66). This review will focus on EHEC, the virulence attributes of which overlap between STEC and AEEC pathotypes.

EHEC

Pathotype attributes. According to a widely accepted definition, the main virulence factors that characterize EHEC strains are Shiga toxins, a type three secretion system (TTSS) and a 60-MDa plasmid (197, 198), which is also known as the EHEC plasmid (pEHEC). The cytotoxicity of Shiga toxin was first suggested by Kiyoshi Shiga, following an outbreak of dysentery in the late

Table 1.1. Clinical and virulence features of various *E. coli* pathotypes[a].

Pathotype	Clinical features	Epidemiological features	Virulence factors
EPEC	Watery diarrhea and vomiting	Infants in developing countries	Bundle-forming pilus TTSS for A/E Efa-1/LifA adhesin
EHEC	Watery diarrhea, hemorrhagic colitis, HUS	Food & water borne outbreaks in developed countries	Shiga toxins, TTSS for A/E Efa-1/LifA, ToxB adhesins StcE promotes adhesion enterohemolysin
ETEC	Watery diarrhea	Childhood diarrhea in developing countries, traveler's diarrhea	CFAs adhesins, LT, ST enterotoxins
EAEC	Diarrhea with mucous	Childhood diarrhea	Aggregative adherence fimbriae, ShET1 and Pet cytotoxins
EIEC	Dysentery, watery diarrhea	Food-borne outbreaks	IpaA, B, C, D, H invasins IcsA/VirG intracellular motility ShET1/2 enterotoxins aerobactin siderophore
UPEC	Cystitis, pyelonephritis	Sexually active women	Pap fimbrial adhesin IreA, IroN siderophores hemolysin cytotoxic necrotizing factor
MNEC	Acute meningitis	Neonates	K1 capsule (antiphagocytic) S fimbrial adhesin IbeA,B,C and AsiA invasin cytotoxic necrotizing factor
DAEC	Diarrhea? Poorly characterized	Infants >12 months	F1845 Dr fimbrial adhesin
STEC	HUS, piglet edema disease	Mostly sporadic cases of food & waterborne disease	Shiga toxins

a – this is not an exhaustive list of pathogenic *E. coli* pathotypes, but an overview of the most relevant pathotypes; TTSS – type 3 secretion system, HUS – hemolytic uremic syndrome, A/E – attaching and effacing. The data were summarized from (79, 164).

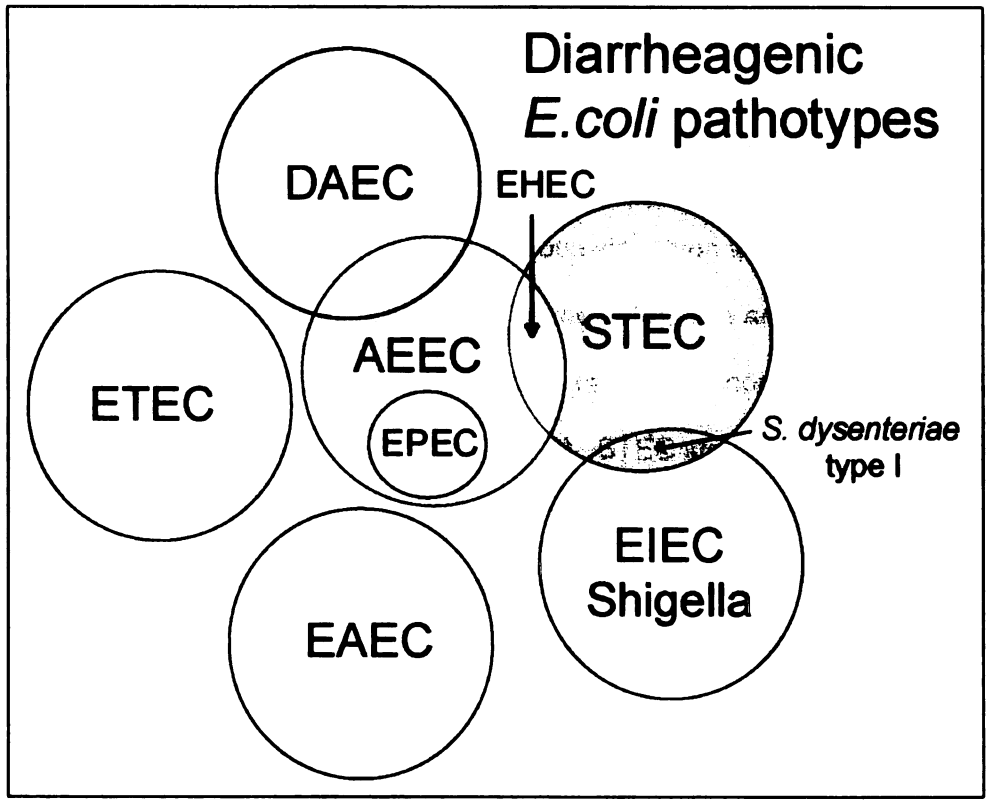

Figure 1.2. Venn diagram of the relationships of diarrheagenic *E. coli*. Note that EPEC are a subset of AEEC. Regions that overlap represent strains that share characteristics of different pathotypes. Modified from (78).

19th century (60, 101, 283). Kiyoshi Shiga characterized the dysentery bacillus, and described production of its cytotoxins, which was first named *Shigella* in the 1930 edition of *Bergey's Manual of Determinative Bacteriology* (320). Recently, analyses of evolutionary relatedness have shown that *Shigella spp.* are actually a variant of EIEC (158) and, hence, represent the first pathogenic form of *E. coli* to be identified. The 'rediscovery' of Shiga toxin was made in the 1970s (184), when the ability of other, non-invasive, *E. coli* to produce Shiga toxins was associated with a different life-threatening condition termed hemolytic uremic syndrome (HUS) (168, 169, 185, 329).

Tight adherence to the intestinal mucosa via a type III secretion system, which produces a histopathological lesion termed attaching and effacing (A/E), is the defining property of AEEC; EPEC are also capable of inducing A/E lesions and are, hence, a subset of AEEC (Figure 1.2). STEC strains that are capable of A/E lesion formation are known as EHEC (78). From almost 500 serotypes of STEC that have been identified, many were associated with illness (25, 27, 29, 33, 34, 129, 167, 315), but only a handful are responsible for the majority of outbreaks and sporadic cases of disease, and those are the serotypes that belong to the EHEC pathotype. In addition to Shiga toxin production and A/E lesion formation, several pEHEC-encoded ancillary virulence factors have also been characterized and are discussed below.

Pathophysiology of disease. Both pathotypes, STEC and EHEC, can trigger HUS and thrombotic thrombocytopaenic purpura in humans, and edema disease in postweaning piglets, which is attributable solely to the cytotoxicity of

Shiga toxin. Conversely, only EHEC can induce hemorrhagic colitis (HC) in humans and cattle (202), which is hypothesized to be a consequence of the combined effects of A/E lesions on the intestinal mucosa and the destruction of submucosal capillaries by Shiga toxin. Studies of human, bovine and swine infections with STEC that do not cause A/E lesions report an absence of a diarrheal prodrome (71, 146, 202, 247, 292, 322).

The pathognomonic lesion of HC includes edema and hemorrhage of the submucosal intestinal wall, which, in advanced cases, can be accompanied by inflammatory pseudomembranes that consist of focal necrosis and neutrophil infiltration (121). Microscopic inspection of the intestinal mucosa reveals A/E lesions, characterized by tight attachment of bacteria to enterocytes and effacement of enterocyte microvilli (220, 245); EHEC do not invade the host cell, in contrast to Shigella and other EIEC.

EHEC infections are not commonly accompanied by bacteriemia and fever. It is not fully understood why one patient develops HUS and another does not. Nevertheless, in approximately 15% of HC patients, HUS ensues within 5-13 days after onset of diarrhea (305). Originally described by Gasser *et al.* (116), HUS is characterized by thrombotic microangiopathy, non-immune hemolytic anemia, and acute renal failure. Vascular injury, mediated by Shiga toxins, elicits thrombin and fibrin formation, leading to thrombocytopenia; this is, in turn, followed by erythrocyte lysis resulting in hemolytic anemia. Irreversible damage of the glomeruli in the renal cortex, also mediated by Shiga toxins, constitutes the third component of HUS (172). In certain patients, activation and deposition

of immune complexes in the renal cortex can further exacerbate the illness (227, 246). Neurological symptoms may appear in 20-30% of HUS patients, and are prognostically ominous (315). Administration of antibiotics is not recommended in case of EHEC infections, as it leads to increased production of Shiga toxin. In fact, treatment is limited to supportive care, such as fluid management, and in cases of bilateral end-stage renal disease kidney transplantation may be the only option (227, 305).

Epidemiology. During the past several decades, EHEC pathogens have emerged from a zoonotic background, and have infiltrated and spread into the food supply of developed countries. Studies of patients with diarrhea in North America demonstrate that, depending on the geographic location and population investigated, EHEC are isolated at frequencies similar to those of other highly prevalent enteric pathogens, such as *Shigella* and *Salmonella* species (22, 37, 226). It has been estimated that EHEC cause over 110,000 illnesses and 90 deaths in the United States each year (212). The most serious sequelae of EHEC infection is HUS, which is usually preceded with a prodromal phase of hemorrhagic colitis (HC). HUS occurs most frequently in children under 10 years of age (246, 305) and is a major cause of end-stage kidney failure in childhood (122, 211).

EHEC, and other STEC, are transmitted mainly via the fecal-oral route; meat (3, 8), fresh produce (6, 143), and fruit juice (328) are the most common matrices that contribute to the dissemination of this foodborne pathogen. Person-to-person transmission, although well documented in institutional settings

(53, 256), mainly accounts for sporadic cases. Domestic ruminants, which are typically asymptomatic, represent the principal reservoir of STEC strains (27, 28, 110, 186). Although no age or diet related differences in colonization susceptibility have been determined *in vitro* (58), screening of dairy herds show calves to have the highest level of shedding (57), which may be a consequence of post-weaning stress.

The ability of *E. coli* serogroups O26, O118, and O111 to produce Shiga toxins was established in the 1970s, when Konowalchuk *et al.* compared the cytopathic effect of five different *E. coli* toxins and identified one that had a distinct and irreversible cytopathic effect on Vero cells (African green monkey kidney cells) (183, 184). However, it was not until the 1980s that EHEC became a public health problem of serious concern. In 1982, two outbreaks of hemorrhagic colitis in Michigan and Oregon, which were traced to hamburger patties contaminated with a then rare *E. coli* serotype O157:H7 (169, 259), were the first incidents of illness to gain widespread scientific and public interest in EHEC.

Serotype O157:H7 has since then emerged, in the epidemiological sense, as the most frequent serotype associated with EHEC disease in many parts of the world. In the US alone, O157:H7 contributes to approximately 75,000 human infections (212) and 17 outbreaks (250) each year. In Argentina, which has the highest incidence of HUS in the world (12.2 cases/100,000 population), O157:H7 is also the most common EHEC isolated from HUS patients (261). Serotype

O157:H7 is also reported as the predominant variant associated with EHEC infections in Europe and Japan (179, 225, 315).

Consecutive epidemiological surveys have, however, demonstrated that non-O157 EHEC, namely serotypes O26:H11, O111:H8, O121:H19, O103:H2 and O118:H16, also frequently cause sporadic cases of diarrhea and hemorrhagic colitis, can cause severe illness including HUS (13, 26, 30, 42, 96, 117, 147, 166, 200, 273, 319) and have been implicated in multiple outbreaks (Table 1.2). The US Council of State and Territorial Epidemiologists included infections caused by non-O157 EHEC in the National Notifiable Diseases Surveillance System in 2000 (42).

Retrospective epidemiological examination of non-O157 EHEC indicated that the perceived low frequency of non-O157 EHEC disease was due to inadequate surveillance, and not a true presentation of non-O157 incidence (Figure 1.3). Although O157:H7 is the leading cause of outbreaks of EHEC disease in North America, reports of diarrheal cases imply that non-O157 EHEC can be at least as prevalent as O157:H7 in certain parts of the US (96, 156). In addition, studies of EHEC carriage in cattle show that frequencies of non-O157 EHEC isolated from beef carcasses can be the same or higher than those of O157:H7 (20, 150); this indicates that the potential for the dissemination of non-O157 serotypes is equally threatening as that for O157:H7.

In Europe, non-O157 EHEC are isolated with a median 4-fold higher rate than O157:H7, however, although there is wide variation among studies (9). Serogroups O26, O111, O103 and O145 have been reported in 11, 11, 7, and 5

Table 1.2. Confirmed outbreaks of non-O157 EHEC serotypes world-wide.

Date	Serotype[a]	Location	Vehicle[b]	Number affected[c]	HUS (death)[d]	Ref.
1986	O111:H-	Japan	ND	22/9	1 (1)	(302)
1990	O111:NM	OH, USA	ND	5	-	(18)
1992	O111:NM	Italy	ND	9	9 (1)	(50)
1994	O104:H21	MT, USA	Milk	18/4	-	(7)
1995	O111:H8	Australia	Sausage	23	23 (1)	(1)
1996	O118:H2	Japan	Salad	126	-	(134)
1996	O103:H2	Japan	Calf-person	3	-	(268)
1997	O26:H11	Japan	ND	32	-	(144)
1999	O111:H8	TX, USA	ice	58/22	2	(2)
1999	O121:H19	CT, USA	Water	11	3	(208)
2000	O26:H11	Germany	Beef	11	-	(335)
2001	O111:NM	SD, USA	ND	3	-	(52)
2002	O26:H-	Austria	Raw milk	2	2	(13)
2002	O26:H11	Germany	ND	3	3	(216)
2003	O26:H11/ O103:H2	Argentina	Person-person	14	1	(119)
2006	O103:H25	Norway	Mutton sausage	17	10 (1)	(275)

a – NM, non-motile;
b – ND, not determined;
c – diarrhea and hemorrhagic colitis cases.
d – number of HUS and cases of death.

European countries, respectively (51). According to the 2008 Annual Report from the European Centre for Disease Prevention and Control, the proportion of non-O157 EHEC associated with disease is continually increasing, accounting for almost half of reported EHEC infections in Europe (4). In Australia, EHEC serogroup O111 is a much more important cause of human disease than O157:H7 (88). The explanation for the differing serotype distributions is not currently known; i.e. whether this is a consequence of improved and extended surveillance measures or represents a true difference in the spread and increase in the incidence of non-O157 EHEC lineages.

Probably the most striking epidemiological observation is that although both O157:H7 and non-O157 EHEC persist in the bovine gut, only non-O157 EHEC have been implicated in overt disease in cattle, including diarrhea and HC. Serotypes O26:H11, O111:H8, O118:H16, O103:H2 and O5:H- have been linked to both outbreaks and sporadic cases of calf diarrhea (scours) (126, 132, 195, 203, 214, 240, 339); isolates from bovine scours cases have been deposited in the strain collection of STEC Reference Center, Michigan State University.

The pathogenicity of these serotypes has also been validated with experimental infection of calves (217, 221, 278, 296). In Germany and Belgium, for example, EHEC O118:H16 are the most prevalent STEC in calves (340), with evidence of zoonotic transmission (26, 224). In contrast, O157:H7 has been shown to induce diarrhea only in experimentally infected colostrum-deprived calves below 3 weeks of age (43, 69, 70, 342). The mechanisms that underlie

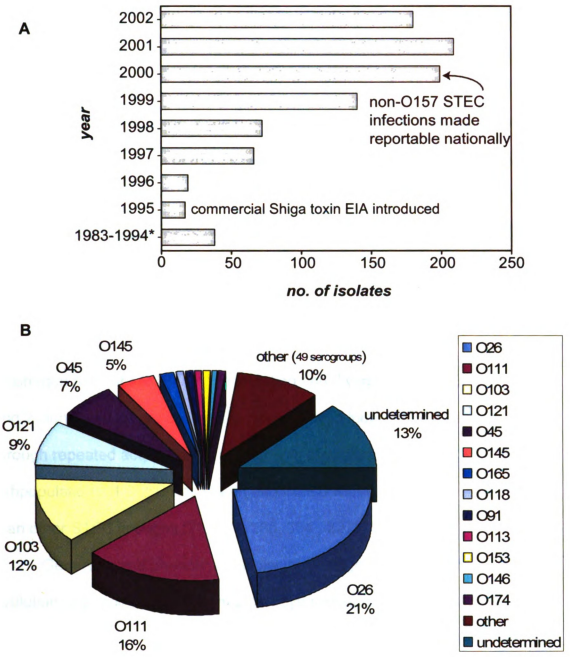

Figure 1.3. Human isolates of non-O157 STEC submitted to the USA Centers for Disease Control and Prevention between 1982-2002 (n = 940). A – *only 38 isolates were submitted between 1983-1994. Note the increase in frequency after the introduction of Shiga toxin Enzyme Immuno-sorbent Assay and especially after non-O157 STEC infections were made reportable nationally. B – breakdown of 940 isolates by serotype. Isolates are categorized as STEC in the referenced article, but over 84% of these isolates tested positive for intimin and 86% for enterohemolysin, which classifies them as EHEC. Adapted from (42).

the differences in the capacity of EHEC strains to cause disease in different hosts are unknown.

Evolutionary aspects. Phylogenetic analyses of conserved metabolic genes have revealed some of the basis for the variation in virulence among EHEC strains. Analyses of multi-locus enzyme electrophoresis and of sequence variation in conserved metabolic genes has classified EHEC into two distinct and distantly related clonal complexes: EHEC 1, which includes serotype O157:H7 and its close relative O55:H7, and EHEC 2, which includes strains of several serotypes (O26, O111, O103, O118, etc.). The shared genotype of strains belonging to a particular clone is believed to be the result of recent descent from a common ancestor (336). In the radiation and diversification of *E. coli*, EHEC 1 and 2 clonal groups are believed to have evolved independently and in parallel through repeated acquisition of related sets of virulence genes (255). These 2 subpopulations of STEC have been associated with disease more frequently than other STEC lineages (25, 221, 238, 304 , 337).

Genotypic and phenotypic studies have engendered a model of stepwise evolution of *E. coli* O157:H7 from a non-cytotoxigenic EPEC-like O55:H7 ancestor, involving multiple acquisition of mobile genetic elements (Figure 1.4) (95). Comparison of genome sequences of outbreak strains of O157:H7, Sakai and EDL 933, with the avirulent *E.coli* K12 MG1655 has revealed that O157:H7 strains possess approximately 1600 additional genes, which account for the 25% larger O157 chromosome (Figure 1.5). Low G + C content and codon usage analysis between the conserved 'backbone' and strain-specific genes provides

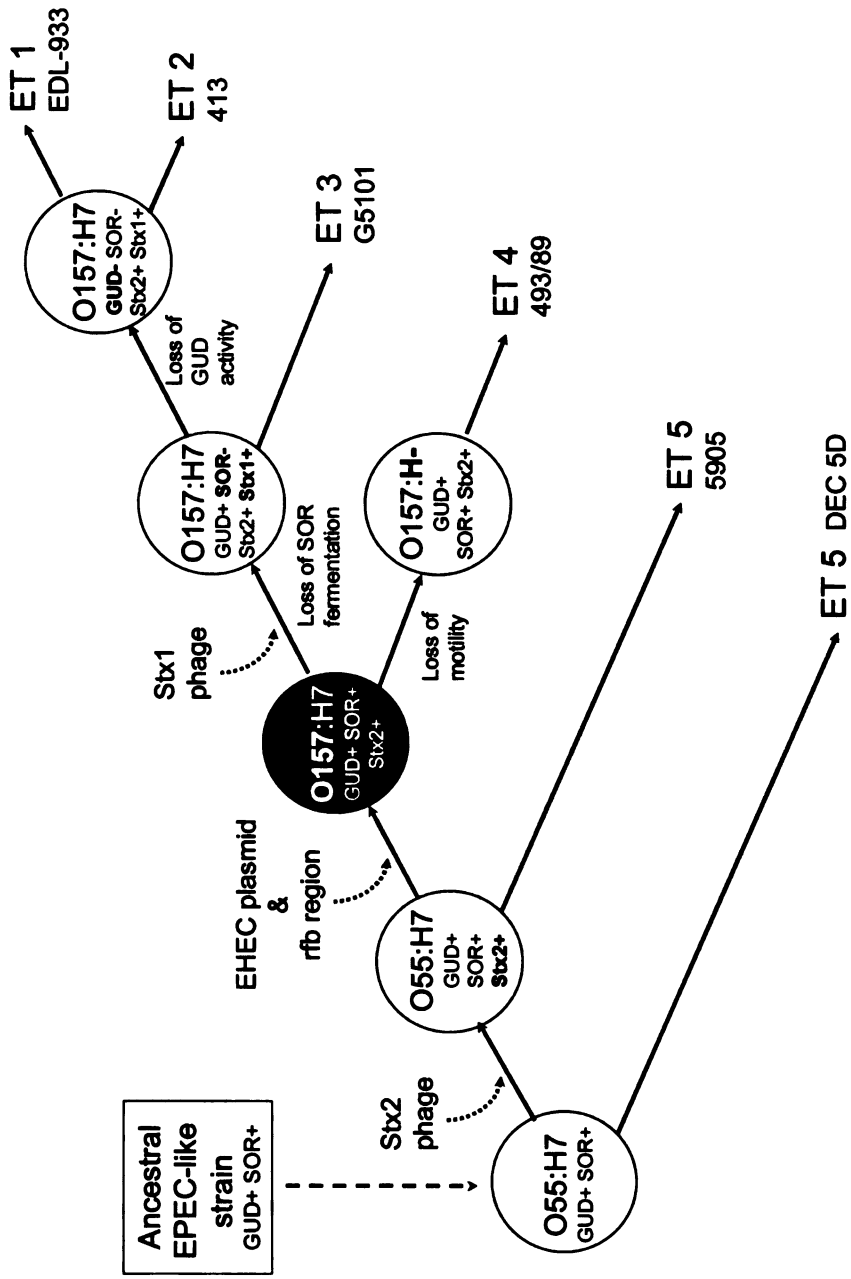

Figure 1.4. Proposed evolutionary model for emergence of the O157:H7 complex based on mutations in *uidA*, Stx production, SOR and GUD phenotypes, and multilocus enzyme electrophoretic profiles of *E. coli* O157:H7 and its relatives. Phenotypes of ancestors A1–A6 are shown; changes predicted to have occurred are in bold. Representative isolates are given below each electrophoretic type (ET). Strain with tracts of ancestor A3 (shaded circle) has not been reported (95).

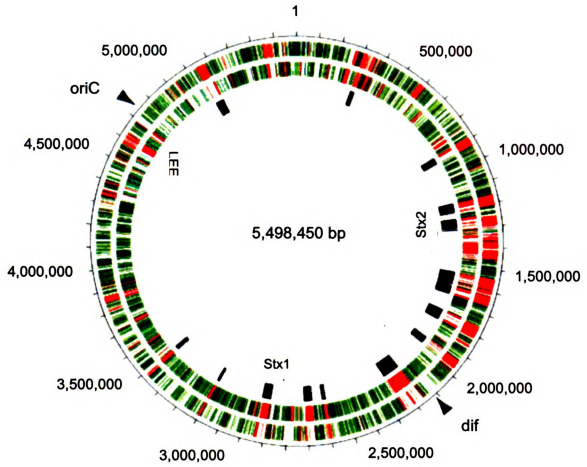

Figure 1.5. Comparison of the O157:H7 Sakai chromosome with K12 MG1655. Numbers in the first circle represent chromosomal location in bp. The second and third circle represent ORFs transcribed in the clockwise and counter clockwise direction, respectively. In green are ORFs conserved in K12 and in red are ORFs absent in K12. The fourth circle depicts Sakai prophages (Sp1-18). LEE – locus of enterocyte effacement, Stx – Shiga toxin. Modified from (136).

strong evidence of their foreign origin (136, 242). The bulk of these genes are organized into coordinately regulated operons, many of which are associated with virulence and constitute various pathogenicity islands (PAIs).

Microarray comparisons have shown that the divergence in gene content between O157:H7 and its most recent ancestor is ~140 times greater than the divergence at the nucleotide sequence level (338). The radiation and divergence of O157:H7 was reiterated in a recent assessment of the heterogeneity of this serotype. Single nucleotide polymorphism (SNP) genotyping of > 500 clinical strains has resolved the extant genomic diversity of the O157:H7 population into genetically distinct groups (clades 1-9) (205). Epidemiological analysis of O157:H7 outbreak severity indicate that these clades also differ in their ability to cause overt disease (205). More importantly, the findings of this report warn about emerging hyper-virulent lineages and the 'relentless evolution' (262) of EHEC.

Shiga toxins. As previously mentioned, the Shiga toxin-producing property of EHEC is conveyed by transfection with heterogeneous lambda-phages that integrate its DNA into the chromosome of bacteria (phage lysogeny); these phages can occupy different sites in the bacterial chromosome depending on insertion site availability and alignment with the phage integrase sequences (281). Induction of the lytic cycle (phage replication), and subsequent toxin release, is mainly stimulated by the bacterial SOS pathway in response to various DNA damaging agents, such as antibiotics, or reactive oxygen species

released by neutrophils following oxidative bursts (141); this is the reason that antibiotic therapy is strongly contraindicated in STEC/EHEC disease.

Shiga toxin (Stx) is a two-component toxin with an A1-B5 holotoxin structure, similar to that of the *Vibrio cholerae* toxin. The A subunit is the cytotoxic enzyme, while the B subunit mediates receptor binding with the host cell. Single copies of the A and B subunit genes are transcribed as a one unit, but the B subunit is translated in multiple copies due to a stronger ribosomal binding site. There are two main families of Stx, Stx1 and 2, with Stx1 being virtually identical in amino acid and nucleotide sequence to the Shiga toxin of *Shigella dysenteriae*, while Stx2 shares just over 50% homology with Stx1 and is immunologically distinct (239). The nomenclature and sequence homology of Stx variants is given in Table 1.3.

EHEC strains that harbor only Stx2 are more frequently associated with severe disease, than strains that contain both or just Stx1 (91, 239). A recent study of Stx phage biology implies that presence of more than one Stx-harboring lambda-phage in the bacterial chromosome reduces phage lysis, which is proportional to Stx production, thereby diminishing the virulence of the host bacterium (280). The increased potency of Stx2 was indicated by *in vitro* cytotoxicity assays using endothelial cells (155). Further, comparative toxicity studies of Stx1 and 2 using mice demonstrated that the lethal dose (LD_{50}) of Stx2 is 400 times lower than that of Stx 1, following intravenous and intraperitoneal injection of purified toxin (313). Similarly, intravenous injection of non-human primates with purified Stx2 induced progressive HUS and a strong cytokine

Table 1.3. Nomenclature and properties of Shiga toxin variants found in EHEC.

Protein	Gene	Homology of A/B subunits[a]	Receptor	Comments
Shiga toxin	*stx*		Gb_3	From S. dysenteriae
Shiga toxin 1	*stx1*	Identical to *stx*	Gb_3	
Shiga toxin 2	*stx2*	57/60%[b]	Gb_3	Immunologically distinct from Stx1; Most frequently associated with severe EHEC disease
Shiga toxin 2c	*stx2c*	100/95%[c]	Gb_3	Not as common in EHEC strains as Stx1 and 2
Shiga toxin 2d	*stx2d*	95/87%[c]	Gb_3	Incubation with intestinal mucus elastase increases Vero cell toxicity by 10-1000 fold; seldom associated with human disease
Shiga toxin 2e	*stx2e*	94/79%[c]	Gb_4	Causes piglet edema disease; seldom associated with human disease
Shiga toxin 2f	*stx2f*	63/75%[c]	unknown	Isolated from feral pigeons, one report of association with human diarrhea (288)

a – nucleotide sequence homology,
b – homology with *stx1*,
c – homology with *stx2*
Gb – globotriaosylceramide.
Data summarized from (106, 213, 239, 288, 298, 315).

response, while animals given Stx1 showed no clinical or histopathological signs of overt disease (285).

Stx toxins enter the cell via receptor mediated endocytosis, following binding of the B5 subunit to the Stx receptor globotriaosylceramide (Gb_3) on the surface of host cells. The A subunit is then separated from B5 and free to cleave a purine residue from the 28S rRNA, analogous to the RNA *N*-glycosidase activity of ricin, irreversibly inhibiting protein synthesis and ultimately leading to cell death (272); as this process is enzymatic, a single Stx molecule can inactivate many ribosomes.

Stx also trigger several facets of the immune response that directly and indirectly contribute to renal failure. In response to Stx, renal proximal tubule epithelial cells, mesangial cells, and macrophage/monocytes secrete proinflammatory cytokines that induce increased expression of Gb_3 leading to increased uptake of toxin. Moreover, these cytokines render the renal endothelium more prothrombotic and adherent to neutrophils (15, 59). Studies of autopsy and biopsy explants of renal cortices from HUS patients and of mice renal samples following infection with *E. coli* O157:H7 demonstrated the ability of Stx toxins to induce apoptotic cell death of renal cells (172). Apoptosis was shown to be augmented following treatment of renal epithelial cells with tumor necrosis factor alpha (172); this cytokine is induced with lipopolysaccharide (LPS) of gram negative bacteria and leads to enhanced Stx toxicity, as demonstrated in mice that were pretreated with LPS prior to injection with Stx (234).

Several types of human cells express Gb_3 (40, 199, 227, 301), though, endothelial cells, particularly those of the microcirculation, contain the highest levels of Gb_3 (40, 201, 229). As Stx localization is relative to the distribution of Gb_3, capillaries of the renal cortex, the GI tract, and less frequently the brain suffer the most damage. However, it is not clear why other organs with dense capillary networks are not affected. Mice may be the most feasible animal models to study the pathogenesis of HUS; however, murine renal pathology following EHEC infection is more concentrated in the proximal tubules whereas the primary site of Stx insult in human kidneys is the glomerular endothelium (86, 330, 331). Mapping of Stx distribution in mice, using radioactively labeled Stx, imply that Stx1 localizes mostly in the endothelial cells of the lung, while Stx2 targets the epithelium of proximal tubules of the kidney (266).

Several other animal models of HUS have been suggested with varying levels of success (113, 127, 171, 217, 234, 260, 285, 311, 321, 323). Gnotobiotic piglets infected with *E. coli* O157:H7 develop diarrhea and neurologic symptoms, but not HUS (17). With baboons as a model, the colitis phase of disease is not consistent in its presentation, following infection with Stx, but renal impairment is very similar to that in humans (311); however, using non-human primates as a model may encounter ethical and fiscal problems. Rabbits challenged with Stx react with non-bloody diarrhea and CNS signs, but do not progress to HUS (258); except in the case of Dutch-Belted rabbits that following a natural occurrence of EHEC O153:H- infection developed HUS that is very similar to human HUS (113), and appears to be reproducible (112).

Translocation of Stx from the gut into the bloodstream is not entirely clear. Initial *in vitro* work implicates platelets and leukocytes in this process (148, 173), but little progress has been made to elucidate the circulation of Stx in the blood and its pathway from the gut that ultimately results in renal impairment.

Locus of enterocyte effacement. The ability of EHEC to induce A/E lesions on the host epithelium is conferred by a laterally acquired PAI termed the locus of enterocyte effacement (LEE). The LEE is composed of 41 genes, organized into 5 coordinately regulated operons (*lee1-5*) (Figure 1.6), half of which encode a TTSS that serves to export LEE- and non LEE-encoded effector proteins. Also coded by the LEE are the adhesin intimin and the translocated intimin receptor (Tir), the interaction of which is central to bacterial attachment, and several LEE regulators. Intimin, which is transported to the periplasm by the general secretory pathway and then inserted into the outer membrane, binds to Tir that localizes on the host cell surface, following its translocation via the TTSS. Intimin-Tir binding triggers filamentous actin rearrangements that result in pedestal formation which abut the adherent bacteria , followed by the effacement of absorptive microvilli (115).

Although the mechanism leading to of diarrhea in EHEC infections is not entirely clear, studies of EPEC indicate that, in addition to A/E lesions, the TTSS subverts the intestinal mucosa in a number of ways through the action of effector proteins, ultimately leading to watery diarrhea and inflammation (115). The hemorrhagic component of illness originates from destruction of underlying mesenteric capillaries by Shiga toxins. In EPEC interactions with the host cell,

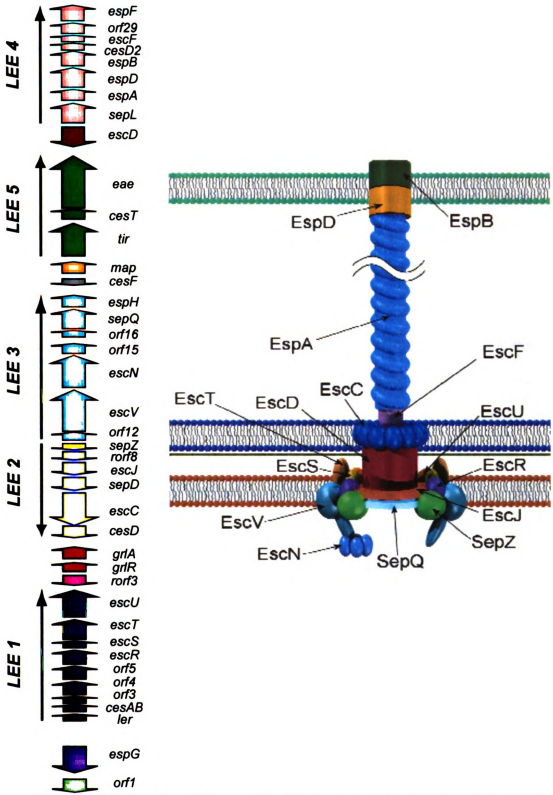

Figure 1.6. The LEE and type three secretion system of O157:H7. Left, genetic organization of 41 genes of the LEE into *LEE* operons, modified from (293). Right, 3-D representation of the type three secretion system. Adapted from (235).

the cooperative action of translocated TTSS effectors Map, EspF, Tir, and the intimin adhesin lead to inactivation of the sodium-D-glucose cotransporter, which is responsible for the daily uptake of 6 L of fluid from the small intestine (68). This process is not linked to effacement of the brush border, however, the precise mechanisms of this process are not resolved. EPEC and EHEC LEE-encoded effectors, Tir, Map, EspF, EspG, EspH, SepZ, and EspB, also disrupt the intestinal epithelial tight junctions causing increased permeability of the intestinal lining, disrupt transepithelial membrane potential and, stimulate secretion of chloride ions by enterocytes (115).

Recently, additional 39 non-LEE encoded effectors that are translocated by the LEE-encoded TTSS were identified in O157:H7 (317). Several of these have been characterized, including TccP involved in actin accumulation beneath adherent EHEC bacteria (114), the cycle inhibiting factor Cif (206), and NleA that is indicated to have an important, but unidentified, role in virulence (123). The function of the majority of non-LEE effectors remains unknown; these effectors resemble those of the plant pathogen *Pseudomonas syringae* in nucleotide sequence, inviting speculation that they target some unknown but conserved aspects of the eukaryotic cell biology (317).

The LEE is postulated to have been acquired independently and in parallel by different lineages of AEEC, including EHEC 1 and 2, and also, different lineages of EPEC (255). This island has, subsequently, diversified in the different backgrounds, with *lee1-3* being more conserved while *lee4* and *lee5* have diverged considerably among different lineages (54, 103). The latter two

operons code for proteins that are exposed to the extracellular environment or, more so, directly interact with the eukaryotic cell and, therefore, elicit an antibody response in HC and HUS patients (170, 236). The co-variation of intimin and Tir alleles is hypothesized to be a means of immune evasion, while retaining the adhesin-receptor interaction (236). Despite its immunogenicity, attempts to develop a LEE-subunit vaccine that would decrease persistence of EHEC in cattle have not been successful (325). The allelic variation of intimin (190) has also been implicated in mediating tissue specificity (97, 133).

Tissue tropism. Current knowledge of the tissue tropism of EHEC in the human gut is not definitive and is based on data derived from animal models and *in vitro* organ cultures (IVOC) of intestinal explants. Although the intestinal insult caused by EHEC infection is concentrated in the colon, it is not clear whether this pathology originates from adherent bacteria or is caused by Stx released into the lumen. EHEC O157:H7 colonization studies with gnotobiotic piglets support the assumption that the large intestine is the site of EHEC colonization (321). Conversely, based on human intestinal IVOC studies, A/E lesions caused by O157:H7 are limited to the follicle-associated epithelia (FAE) of Peyer's patches in the terminal ileum (245).

This site-specificity was demonstrated to be dependent on the particular gamma-intimin allele expressed by O157:H7; well over 20 alleles of intimin have been identified in EHEC and EPEC so far (190), however only three have been studied in the context of tissue tropism. EPEC serotype O127:H6, for example, has alpha-intimin and efficiently colonizes any region of the small intestine (97).

EHEC 2 strains have a different intimin allele than that in EHEC 1, beta-intimin, and initial *ex vivo* studies infer that tight attachment of EHEC 2 is also concentrated on the FAE, with little adherence to non-FAE explants (56, 99). However, extrapolating EHEC colonization trends from *ex vivo* studies to *in vivo* conditions should not be categorical, as IVOC infection assays are monitored over not more than 8 h. It is possible that Peyer's patches may serve as a site of initial colonization from which EHEC then spread to surrounding tissue. FAE is known to act as a 'docking' location for other *Enterobacteriacae*, including *Yersinia* and *Salmonella* species (133), and *Citrobacter rodentium* (341).

In the gastro-intestinal tract of cattle, as in the human intestine, the FAE of the recto-anal junction (rich in lymphoid follicles) is the preferred colonization spot of O157:H7 (222). EHEC 2 strains, however, were found to colonize and to form A/E lesions in both the small and large intestine (126, 240, 295, 333); the reasons for these differences are not fully understood. Studies using signature-tagged mutagenesis to identify mutants of O157:H7 and O26:H- unable to colonize calves reiterate different site specificities and infer alternate colonization strategies, but do not shed light on the molecular mechanisms that underlie the differences in colonization capacity or pathogenic potential between the two representatives of EHEC 1 and 2 (85, 326).

Intimin can, in addition to binding with Tir, also interact with eukaryotic cell receptors. The binding of intimin to integrin (102) and nucleolin (286) *per se* is still of unknown biological significance, however, the ability of intimin to interact with host receptors likely plays an important role for site-specificity in the gut. It

may represent an initial loose pairing of the bacterium with the host cell, allowing bacteria to recognize a favorable site prior to tight attachment through Tir (104, 133). However, intimin type is not the only factor to mediate tissue or host specificity. Several studies hint that EHEC 2 and EPEC strains from animals may have an increased affinity to adhere to cells of animal origin over human (98, 133, 228, 340).

Finally, site-specific colonization of the intestinal tract may be influenced by intrinsic differences in the regulation of the LEE island. In addition to 3 LEE-encoded regulators, this PAI is manipulated by multiple chromosomal and extra-chromosomal (plasmid) elements that inherently vary among different lineages and, consequently, alter LEE expression in assorted ways. Circuits that govern LEE expression are finely tuned to distinguish and respond to a wide range of stimuli, which can originate from the environment (pH, temperature, glucose, osmolarity, electrolytes, etc.), are produced by bacteria (quorum sensing), or are secreted by the eukaryotic host (epinephrine) (164, 265, 289, 327). Furthermore, there is evidence, albeit weak, which support the hypothesis that LEE of O157:H7 is expressed in a host-specific fashion (251).

Several important differences in LEE regulation have been detected between O157:H7 (EHEC 1) and O127:H6 (EPEC 1) (289). One such distinction is the necessity of the EPEC adherence factor (EAF) plasmid-encoded PerC regulator for full activation of the *lee1* operon in EPEC, making LEE expression in EPEC dependent on factors that activate the plasmid borne *per* regulon (162); EHEC possess a homologue of this regulator that is located on the chromosome.

Another dissimilarity is the suggested existence of a 'checkpoint', which is not-LEE encoded, for fine-tuning the expression of *lee4* and *lee5* operons in EHEC (264). This checkpoint, which is absent in EPEC, is hypothesized to allow formation of the membrane-bound part of the TTSS but to restrict assembly of the needle complex until further signals are received by the bacteria; signals such as contact with the host cell (137). As EHEC 1 is phylogenetically more distant from EHEC 2 than from EPEC 1 (304) and differs from EHEC 2 in the insertion site of LEE (255), it would be interesting to learn more about the regulation of LEE expression in EHEC 2. This will not be feasible until completed genome sequences of EHEC 2 representatives become available.

EHEC plasmid. Sequencing of the pEHEC in O157:H7 identified 100 open reading frames (46), some of which encode proteins associated with virulence. One such protein is enterohemolysin (EHEC-HlyA), a RTX (Repeats in ToXin), β-hemolytic, pore-forming toxin encoded by the *hlyCABD* operon. Lysis of red blood cells by EHEC-HlyA is suspected to provide iron necessary for growth of EHEC in the gut; its cytotoxicity extends to other cell types and, EHEC-HlyA has been shown to induce proinflammatory cytokine production (239, 303). However, despite its cytotoxicity and detection of antibodies specific to EHEC-HlyA in sera from patients recovering from HUS (276), the significance of this factor to the pathogenesis of EHEC disease remains questionable (36).

The immuno-reactive StcE/TagA protease (237) has been implied to increase intimate adherence of EHEC to epithelial cells, through its mucinase and anti-inflammatory activity (124, 125, 194). StcE is secreted by the type II

secretion apparatus (194), which is another pEHEC element encoded by a 14-gene *etpC-O* operon that by itself contributes to intestinal colonization (145). Lastly, ToxB/LifA indirectly stimulates translocation of *lee4*-encoded proteins (294, 307). As with EHEC-HlyA, however, the *in vivo* importance of these factors requires further investigation (294).

GOALS OF CURRENT STUDY

In the last two decades, the field of diarrheagenic *E. coli* studies has greatly furthered our knowledge about the pathogenesis and evolution of the EHEC 1 clonal group. Based on the incidence of disease caused by EHEC 2 serogroups O26, O111, and O118, and the distinct cladogenesis of this subset of EHEC, it is clear that exploration of the genomic composition of EHEC 2 strains is necessary. Working under the hypothesis that the acquisition of common virulence genes on mobile elements accounts for similar ability of O157:H7 and EHEC 2 to cause disease in humans, the first part of the research described here is an evaluation of the overall genetic similarity of EHEC 1 and EHEC 2 clonal groups. Also, the aim of this study is to understand how the distribution and subsequent diversification of laterally acquired PAIs have influenced the genomic diversity of EHEC 2 lineages that are most frequently associated with human and bovine disease.

A recent outbreak of O157:H7 infection was characterized by a remarkably high rate of severe disease, based on the frequency of HUS and hospitalization, even though O157:H7 strains share the same arsenal of virulence factors. The third chapter describes phenotypic and whole-genome

expression differences of two outbreak strains, which vary considerably in their epidemiological characteristics, under conditions that mimic the host-pathogen challenge. The working hypothesis of this study is that differences in the clinical burden between the two outbreaks are associated with differences in the pathogenic potential between the outbreak strains, and not merely a consequence of variable transmission rates in different food matrices, or host predisposition.

The fourth chapter is a follow-up to the third and describes the investigation of the pathogenicity of two distinct lineages of O157:H7, at a population level. Based on epidemiological analysis, the O157:H7 clade 8 lineage is hypothesized to be hypervirulent compared to clade 2. This hypothesis is tested by characterizing the colonization potential and virulence gene expression of clade 8 and 2 populations that were exposed to epithelial cells. It is the aim of this study to determine whether the variation in virulence is solely attributable to the presence of different Stx variants among EHEC O157:H7 strains, or are there lineage-specific differences in colonization capacity and in expression of shared virulence genes between clades of O157:H7.

The fifth chapter describes the gene expression of O157:H7 following treatment with culture media that has been preconditioned with epithelial cells, or with co-cultures of epithelial cells and EHEC or non-pathogenic *E. coli*. Since quorum sensing is known to influence virulence gene expression, determining whether O157:H7 can distinguish between signaling molecules that are secreted following an infection of the host cell with O157:H7, O26:H11, or non-pathogenic

K12 can contribute to our knowledge of the dynamics of mixed infections.

Conclusions and future considerations are presented in chapter 6.

CHAPTER 2

Genomic Diversity of Pathogenic *Escherichia coli* of the EHEC 2 Clonal Complexes

Abu-Ali, G. S., Lacher, D. W., Lukas M. Wick, L. M., Qi, W., and T. S. Whittam

Submitted to *J. BMC Genomics*, December 18th 2008

CHAPTER 2

Genomic Diversity of Pathogenic *Escherichia coli* of the EHEC 2 Clonal Complexes

Abu-Ali, G. S., Lacher, D. W., Lukas M. Wick, L. M., Qi, W., and T. S. Whittam

Submitted to *J. BMC Genomics*, December 18th 2008

SUMMARY

Background: Evolutionary analyses of enterohemorrhagic *Escherichia coli* (EHEC) have identified two distantly related clonal groups: EHEC 1, including serotype O157:H7 and its inferred ancestor O55:H7; and EHEC 2, comprised of several serogroups (O26, O111, O118, etc.). These two clonal groups differ in their virulence and global distribution. Although several fully annotated genomic sequences exist for strains of serotype O157:H7, much less is known about the genomic composition of EHEC 2. In this study, we analyzed a set of 24 clinical EHEC 2 strains representing serotypes O26:H11, O111:H8/H11, O118:H16, O153:H11 and O15:H11 from humans and animals by comparative genomic hybridization (CGH) on an oligoarray based on the O157:H7 Sakai genome. Results: Backbone genes, defined as genes shared by Sakai and K-12, were highly conserved in EHEC 2. The proportion of Sakai phage genes in EHEC 2 was substantially greater than that of Sakai-specific bacterial (non-phage) genes. This proportion was inverted in O55:H7, suggesting that a subset of Sakai bacterial genes is specific to EHEC 1. Split decomposition analysis of gene content revealed that O111:H8 was more genetically uniform and distinct from other EHEC 2 strains, with respect to the Sakai O157:H7 gene distribution. Serotype O26:H11 was the most heterogeneous EHEC 2 subpopulation, comprised of strains with the highest as well as the lowest levels of Sakai gene content conservation. Of the 979 parsimoniously informative genes, 15% were found to be compatible and their distribution in EHEC 2 clustered O111:H8 and O118:H16 strains by serotype. CGH data suggested divergence of the LEE

island from the LEE1 to the LEE4 operon, and also between animal and human isolates irrespective of serotype. No correlation was found between gene contents and geographic locations of EHEC 2 strains.

Conclusions: The gene content variation of phage-related genes in EHEC 2 strains supports the hypothesis that extensive modular shuffling of mobile DNA elements has occurred among EHEC strains. These results suggest that EHEC 2 is a multiform pathogenic clonal complex, characterized by substantial intra-serotype genetic variation. The heterogeneous distribution of mobile elements has impacted the diversification of O26:H11 more than other EHEC 2 serotypes, which suggests that this population is more likely to give rise to hyper-virulent lineages.

INTRODUCTION

Enterohemorrhagic *Escherichia coli* (EHEC), the intersection of Shiga toxin producing *E. coli* (STEC) and attaching and effacing *E. coli* (AEEC), comprise a group of pathogenic *E. coli* that cause a variety of human and animal illnesses ranging from diarrhea to hemorrhagic colitis (HC), and the multifactorial hemolytic uremic syndrome (HUS) (78). Intimate adherence to the intestinal epithelium resulting in characteristic attaching and effacing (A/E) lesions, and the destruction of capillary walls via production of phage borne Shiga toxins (Stx 1, 2, and variants) are hallmarks of EHEC pathogenesis. A/E lesion formation is dependent upon a type three secretion system (TTSS), which is encoded on the laterally acquired locus of enterocyte effacement (LEE) (164).

E. coli O157:H7 is the dominant EHEC serotype in the United States, Argentina, Great Britain, and Japan (5, 315). However, multiple reports have shown that other EHEC, including serogroups O26, O111, O103, and O118, frequently cause sporadic cases of human illness (13, 26, 30, 96, 117, 166, 273, 319), and have been implicated in numerous outbreaks (2, 41, 50, 208, 216). In Australia and parts of Europe, infections with serogroups O26 and O111 are prevailing while the incidence of O157:H7-associated disease appears to be declining (9, 32, 87, 88). In contrast to *E. coli* O157:H7, EHEC serogroups O26, O111, O118, O103, and O5 are commonly linked to outbreaks and sporadic cases of calf diarrhea (scours) and HC (126, 132, 195, 203, 214, 240, 339), which has been validated from experimental infections in calves (217, 221, 278, 296). In Germany and Belgium, for example, EHEC O118 is the most prevalent

type of STEC associated with diarrhea in calves (340), with evidence for zoonotic transmission (26, 224).

Phylogenetic analyses of conserved metabolic genes have revealed some of the basis for the variation among EHEC strains. Multilocus enzyme electrophoresis (336) and partial sequencing of 13 housekeeping genes (304) classified EHEC into two distantly related clonal groups: EHEC 1 includes serotype O157:H7 and its inferred ancestor O55:H7, whereas EHEC 2 includes numerous serogroups (e.g., O26, O111, O118). The key virulence factors shared between EHEC 1 and EHEC 2 clonal complexes were postulated to have been introduced through multiple and parallel acquisitions of mobile elements (255). A comparison of *E. coli* O157:H7 genomes has also revealed the extent and significant impact of horizontal transfer on the evolution of virulence (136, 242). Furthermore, array comparative genomic hybridizations (CGH) have shown that the divergence in gene content among closely related O157 strains is ~140 times greater than the divergence at the nucleotide sequence level (338). Although recent evidence indicates the emergence of highly virulent lineages among non-O157 EHEC, notably the O26 serogroup (32, 42), little is known about the gene content, genetic diversity and evolution of virulence in members of the EHEC 2 group.

The function of ancillary virulence determinants is somewhat characterized in O157:H7 (164, 317), however, the relevance as well as the distribution of these factors in EHEC 2 is not clear. To systematically investigate the gene content variations within the EHEC 2 clonal group. we analyzed a set of

24 clinical EHEC 2 strains representing serotypes O26:H11, O111:H8/H11, O118:H16, O153:H11 and O15:H11 from humans and animals using array-based CGH. Because there are no EHEC 2 genome sequences available, a multi-genome spotted oligoarray containing probes for 5,978 ORFs from O157:H7 Sakai, O157:H7 EDL933, and K-12 MG1655 was used to examine the distribution of these *E. coli* genes in our collection of EHEC 2 strains. The findings of this study shed light on the diversification of horizontally acquired elements in a group of pathogens that represent recent evolutionary branches of EHEC clonal groups.

MATERIALS AND METHODS

Bacterial strains and DNA isolation. Since genome sequences for tested strains are not available, two-color hybridizations between sequenced strains of *E. coli* O157:H7 RIMD 0509952 (Sakai) (136) and K-12 MG1655 (35) were used as references. A total of 24 EHEC 2 strains including serotypes O26:H11 (*n*=8), O111:H8 (*n*=6), O111:H11 (*n*=2), O118:H16 (*n*=6), O153:H- (*n*=1), and O15:H11 (*n*=1), originally isolated from human and animal cases of STEC-associated disease, were used in this study (Table 2.1) and were selected based on the serotype and source. The study also included an EHEC 1 O55:H7 strain, isolated from a human diarrhea case. Bacterial DNA was prepared from overnight LB cultures grown at 37°C using the Puregene genomic DNA isolation kit (Gentra Systems, Minneapolis, MN).

Multilocus sequence typing (MLST) and Shiga toxin (Stx) genes. The detailed MLST protocol and multiplex PCR conditions for characterizing the Stx genes (*stx1*/*stx2*) can be found at the STEC Reference Center website (http://www.shigatox.net). Briefly, MLST was performed on seven conserved housekeeping genes (*aspC*, *clpX*, *fadD*, *icdA*, *lysP*, *mdh*, and *uidA*), and sequence type (ST) assignments were made based on phylogenetic analyses of the concatenated sequences.

Oligonucleotide arrays. The Qiagen (Valencia, Calif.) spotted multi-genome arrays containing probes specific for 5,978 ORFs from *E. coli* K-12 MG1655, O157:H7 Sakai and EDL933 were utilized. Of these probes, a total of 5,943 were 70-mer oligonucleotides and 35 ranged from 41-69 bp. The probes

Table 2.1. Properties of strains used in this study sorted by serotype.

Strain[a]	Serotype[b]	Host	Clinical[c]	Location	Date[d]	*stx*	ST[e]	Source[f], Ref.
DEC 9f	O26:[h11]	Human	diarrhea	USA, SD	1974	-	106	1, (140)
DEC 10e	O26:H11	Calf	scours	USA, SD	1989	1	106	2, (254)
F5863	O26:H11	Human	diarrhea	USA, NE	1998	1	106	3, (96)
97-3250	O26:H11	Human	HUS	USA, ID	1997	1,2	104	4, (111)
413/89-1	O26:[h11]	Calf	diarrhea	Germany	1998	1	106	5, (72)
DA-22	O26:[h11]	Human	diarrhea	USA, DC	1999	1	106	6
03-ST-296	O26:H11	Human	b.d.	USA, MI	2003	1	106	7, (204)
CB 7505	O26:H11	Calf	no data	Germany	1998	1	106	8, (196)
DEC 8c	O111:[h11]	Calf	scours	USA, SD	1986	1	107	2, (140)
DEC 8d	O111:H11	Human	diarrhea	Cuba	1953	-	106	9, (157)
C408	O111:[h8]	Calf	diarrhea	Scotland	1993	1	106	10, (100)
BCL71	O111:[h8]	Calf	diarrhea	USA, CA	1993	1,2	106	11
ML178190	O111:[h8]	Human	diarrhea	USA, NE	1998	1,2	106	3, (96)
W29104	O111:H8	Human	diarrhea	USA, NE	1998	1,2	106	3, (96)
EK34	O111:[h8]	Human	diarrhea	USA, WA	1999	1	106	12, (180)
EK35	O111:H8	Human	diarrhea	USA, WA	2001	1	106	12, (180)
RW2030	O118:[h16]	Calf	diarrhea	Germany	1994	1	106	5, (340)
RW1302	O118:[h16]	Calf	diarrhea	Germany	1994	1	106	5, (340)
666/89	O118:H16	Calf	diarrhea	Germany	1989	1	106	5, (340)
05482	O118:H16	Human	HUS	Germany	1996	1	106	8, (84)
EK36	O118:H16	Human	diarrhea	USA, WA	2001	1	106	12, (180)
EK37	O118:H16	Human	diarrhea	USA, WA	2000	1	106	12, (180)
RDEC-1	O15:[h11]	Rabbit	diarrhea	USA, SC	1970s	-	681	13, (254)

Table 2.1, continued

Strain[a]	Serotype[b]	Host	Clinical[c]	Location	Date[d]	*stx*	ST[e]	Source[f], Ref.
02-3751	O153:[h11]	Rabbit	HUS	USA, MA	2002	1	104	14, (112)
97-3256	O55:H7	Human	diarrhea	USA, MI	1997	2	73	4, (111)

a. designations assigned to strains deposited in the STEC Reference Center
b. [h] - flagellar allele determined by *fliC* gene sequencing; H - expression of flagellar type confirmed by reaction to antisera. To avoid confusion in text, flagellar type will be denoted as H, regardless whether it was determined by sequencing or serologic typing.
c. b. d. - bloody diarrhea; HUS - hemolytic uremic syndrome; scours - neonatal calf diarrhea.
d. Year of isolation.
e. ST - sequence type based on MLST of 7 housekeeping genes (*aspC*, *clpX*, *fadD*, *icdA*, *lysP*, *mdh,* and *uidA*).
f. Strains were obtained from: 1 – CDC, 2 – Francis, D., 3 – Fey, P., 4 – O'Brien, A., 5 – Wieler, L., 6 – Acheson, D. W., 7 – Michigan Dept. of Community Health, 8 – Beutin, L., 9 – Orskov, F., 10 – Hart, C. A., 11 – Love, B.C., 12 – Tarr, P., 13 – *E. coli* Reference Collection, 14 – Fox, J.

were printed in duplicate on UltraGaps glass slides (Corning Inc., NY) at the Research Technology Support Facility at Michigan State University. The array also contained 384 spots representing 12 randomized negative control 70-mer probes. All probes were assigned ORF designations (b- =MG1655, ECs- =Sakai, or Z- =EDL933 numbers) or intergenic region labels based on the RefSeq database available on the National Center for Biotechnology Information (NCBI) website (14).

***In silico* analysis of microarray probe specificity.** To verify the probes with the up-to-date genome annotations, we compared all 5,990 probe sequences against the three *E. coli* genomes (MG1655, Sakai, and EDL933) by BLASTN available on NCBI, and recorded the two highest hits for every probe (top hit and second hit) for each genome. A probe was considered to be specific for a target when the top hit demonstrated ≥80% identity to the probe sequence stretch in the strain. Probes with nonspecific hybridization and multiple target hybridizations within MG1655 or Sakai DNA were excluded from the data analysis of MG1655 and Sakai hybridizations. These included probes that had multiple top hits with 75% overall identity or probes that had multiple top hits between 50% and 75% of overall identity with alignments containing a stretch of nucleotides with 100% identity, in which the stretch was 20% of the probe length. With respect to the MG1655 and Sakai genomes, out of 5,978 probes, 12 had no target (EDL933 specific), 731 showed nonspecific hybridization or had multiple targets, and 5,235 matched single genome targets. Of these, 3,803 targeted both genomes, with 1,002 targeting only Sakai and 430 targeting only K-12.

DNA labeling and microarray hybridization. Genomic DNA was sheared into 500 to 5,000 bp fragments in a cup sonicator (Heat Systems Ultrasonics W-225, 20 KHz, 200W) and 250 ng of sheared DNA was labeled with aminoallyl-dUTP (Sigma, St. Louis, Mo.) using the Invitrogen (Carlsbad, Calif.) DNA labeling system, as previously described (338). Equal amounts of DNA from Sakai and test strains were suspended and combined in a final volume of 44 µL of SlydeHyb Buffer #1 (Ambion, Inc., Austin, TX). Qiagen *E. coli* spotted oligo-arrays were hybridized and washed according to the manufacturer's instructions for hybridization using coverslips. Test strains were hybridized twice with Sakai as a reference: once with the Cy5 labeled test strain and Cy3 labeled Sakai and once with the Cy3 labeled test strain and Cy5 labeled Sakai to correct for dye incorporation bias.

Data collection and analyses. Arrays were scanned with the Genepix 4000B array scanner (Axon Instruments, Union City, Calif.) and probe intensities (median pixel intensities) were retrieved using Genepix 6.0 (Axon Instruments). Data quality was assessed by viewing plots of M versus A [$M = \log_2$ (test/reference); $A = \log_2$ (test x reference)] (Appendix Figure 1), and by checking for spatial effects with Genepix 6.0 and GeneTraffic (Iobion, La Jolla, Calif.) as described previously (338). Because genome sequences of tested strains were not available, microarray data were not normalized to avoid biasing the gene content of tested strains. Instead, microarray images showing spatial bias were discarded and hybridizations were repeated until control parameters were appropriate. Duplicate probes for each gene were averaged prior to analyses.

Probes with median pixel intensities higher than the median of the randomized negative controls were analyzed as the distribution of the two-color signal ratios using the "GACK" program (176). Analysis of the $\log_2$ (test strain/reference strain) distribution ($GACK_1$) as well as of the reciprocal ratio, $\log_2$ (reference strain/test strain) ($GACK_2$), were performed for Sakai versus MG1655 hybridizations to determine a cutoff. Genes with a $GACK_1$ value of ≥ 0.1 were classified as present, whereas genes with a $GACK_1$ value of < 0.1 were classified as divergent/absent. At this cutoff, maximum sensitivity (98.8%) and specificity (96%) were achieved for the MG1655/Sakai dye-swap hybridizations, and therefore, this cutoff was used to interpret the data from Sakai versus EHEC 2 hybridizations. The term 'present' is used to indicate that a gene was detected by CGH, and does not necessarily imply that the whole gene is conserved or functional; likewise, the term 'divergent/absent' indicates that a gene was not detected by CGH.

Phylogenetic analyses. Strains were assigned to clonal groups based on STs and bootstrap analyses as described previously (189, 304). A neighbor-joining tree of the concatenated MLST sequences was constructed using the Kimura 2-parameter distance method with 1000 bootstrap replications in MEGA 3.1 (187). The tree includes other enteropathogenic *E. coli* (EPEC) and EHEC STs as well as the lab-derived K-12 (ST173) and the uropathogenic *E. coli* CFT073 (ST27) for comparison; an *E. albertii* strain was used as the outgroup. For phylogenetic analyses of the microarray data, a total of 144 genes (from all array hybridizations) with probe intensities below those of negative controls were

excluded from the set of 4,944 genes. Neighbor-net phylogenies highlighting the distribution of Sakai genes in EHEC 2 strains, for which the presence or absence of genes was coded as 0 (divergent/absent) or 1 (present), were constructed using the uncorrected *p* distance in Splitstree 4.3 (149). The number of Sakai genes whose distribution in EHEC 2 was parsimoniously informative were determined in MEGA 3.1 (187), and the set of Sakai genes in EHEC 2 whose distribution was compatible with a single phylogeny was identified using the clique module of PHYLIP (94).

RESULTS

Sequence types (STs) and *stx* profiles of EHEC 2 strains.

Phylogenetic analyses of multi locus sequence typing (MLST) data grouped the 24 EHEC 2 strains (Table 2.1) into four STs. The most common was ST 106, which was found in 20 strains, while the remaining three STs each differed from ST 106 by a single nucleotide polymorphism (SNP) in almost 4,000 bp of the concatenated MLST sequence. MLST data revealed a lack of nucleotide sequence diversity in house keeping genes among these EHEC 2 strains. The neighbor-joining phylogeny based on concatenated MLST allelic sequences grouped the EHEC 2 strains into a distinct cluster, with 100% bootstrap support, which was more closely related to the EPEC 2 group (100% bootstrap support) than to members of EHEC 1 (Figure 2.1). Most of these EHEC 2 strains (n=17) were PCR positive for only *stx1*, whereas four strains had both *stx1* and *stx2*, and three strains were negative for both *stx* genes (Table 2.1).

Gene content of EHEC 2 strains. Binary classification of genes as present or divergent/absent, inferred by GACK analyses of the CGH data, was used to determine the gene content of all 24 EHEC 2 strains (Table 2.2) and of each individual strain (Table 2.3). Because all CGH experiments were performed with Sakai as the reference strain, our analyses focused on probes targeting genes present in the Sakai genome. The oligo probes were classified to represent backbone genes (shared by Sakai and K-12), and Sakai-specific genes (note that the term "Sakai-specific" is used here only in comparison to K-12). The Sakai-specific genes were further classified in Sakai phage genes (phage-

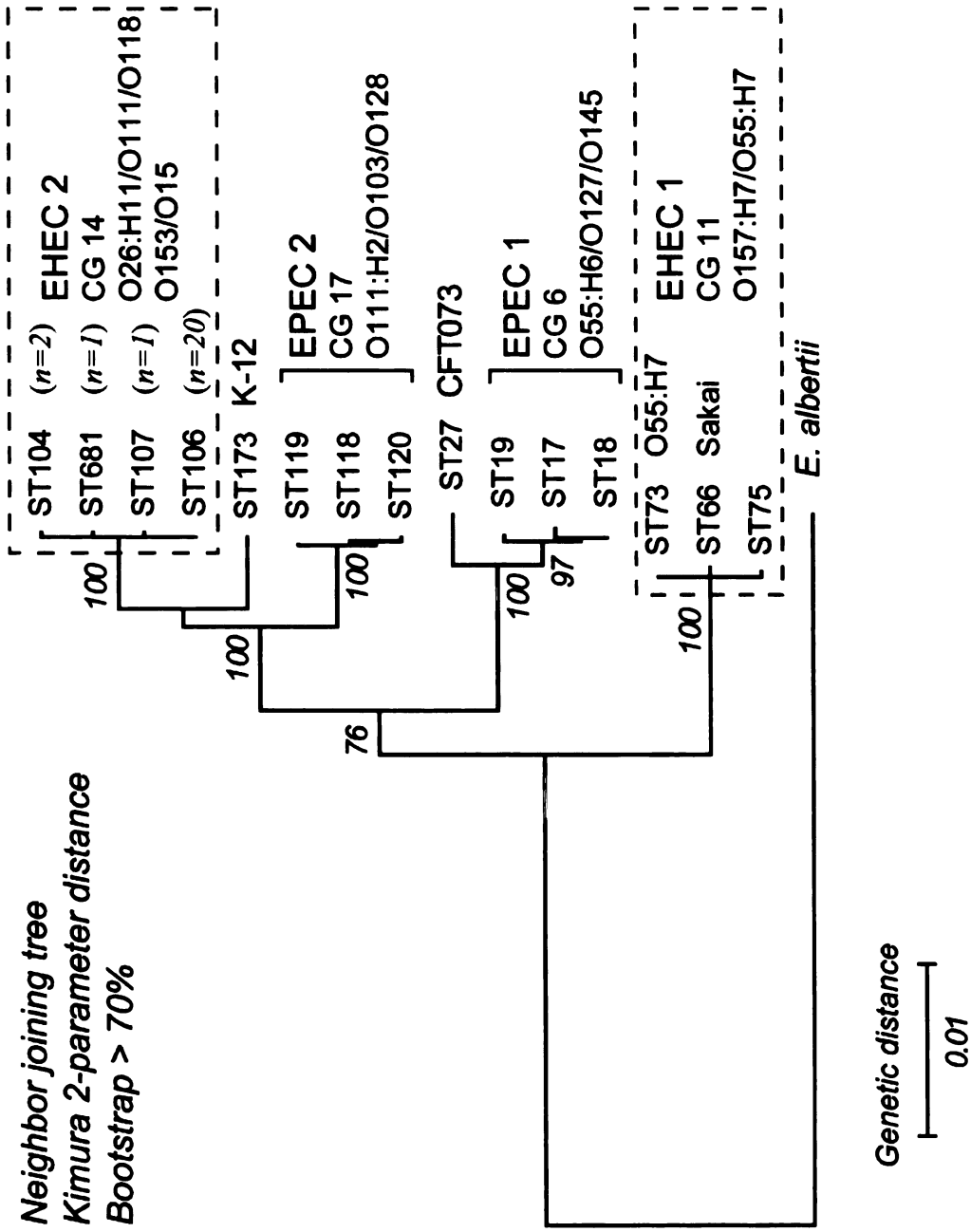

Figure 2.1. Phylogenetic relationships of EHEC and EPEC sequence types. The sequence types (STs) of EHEC 2 belong to a clonal group (CG 14), which is more closely related to EPEC 2 (CG 17), than EHEC 1 STs (CG 11). The phylogenetic tree was constructed using the Neighbor-joining algorithm based on the Kimura 2-parameter distance matrix of nucleotide substitution. Bootstrap confidence values were based on 1000 replicates. Only those higher than 70% are shown.

Table 2.2. Percentage of Sakai genes that are present, divergent/absent or variably absent or present (VAP) in all 24 EHEC 2 strains.

	Backbone genes	Sakai specific genes	
	(shared with K-12)	phage-related	bacterial
	n = 3696	*n* = 814	*n* = 434
Present	80.9%	5.8%	6.5%
Absent/divergent	1.1%	9.5%	53.0%
VAP[a]	18.0%	84.7%	40.5%

a – genes that were detected in at least one of the 24 EHEC 2 strains, but not in all EHEC 2 strains.

related genes present in Sakai but absent in K-12) and Sakai bacterial genes (non-phage-related genes present in Sakai but absent in K-12) (136). Of the 3,696 backbone genes, 80.9% were shared by all EHEC 2 strains, whereas only 5.8% of the Sakai phage genes (*n*=814) and 6.5% of the Sakai bacterial genes (*n*=434) were found in every tested EHEC 2 strain. While 84.7% of the Sakai phage genes were found in at least one of the 24 EHEC 2 strains, a whole 53% of the Sakai bacterial genes were not found in any of the these strains (Table 2.2).

In each individual EHEC 2 strain, approximately 95% of the 3,696 backbone genes were found (Table 2.3, Figure 2.2), with little variation (95.5% ± 1.2%, range 93% - 97%). In contrast, about 52% of the Sakai phage genes were found, but with a much greater variability across EHEC 2 strains (52.1% ± 8.2%, range 30% - 65%); Sakai bacterial genes were found less frequently in EHEC 2 strains (22.7% ± 2.3%, range 19% - 30%). Serotype O26:H11 showed the most interstrain variation, whereas O111:H8 and O118:H16 were more uniform with respect to Sakai gene distribution. The O55:H7 representative also had a high percentage of backbone genes (96.6%). Furthermore, 33% of the 814 Sakai phage genes and 70% of the 434 Sakai bacterial genes were conserved in O55:H7, suggesting an inverse trend relative to that observed in EHEC 2 strains (Table 2.3).

Identification of potential EHEC-specific genes. From the 1,248 Sakai-specific genes represented on the microarray, 152 (12.2%) were conserved in 23

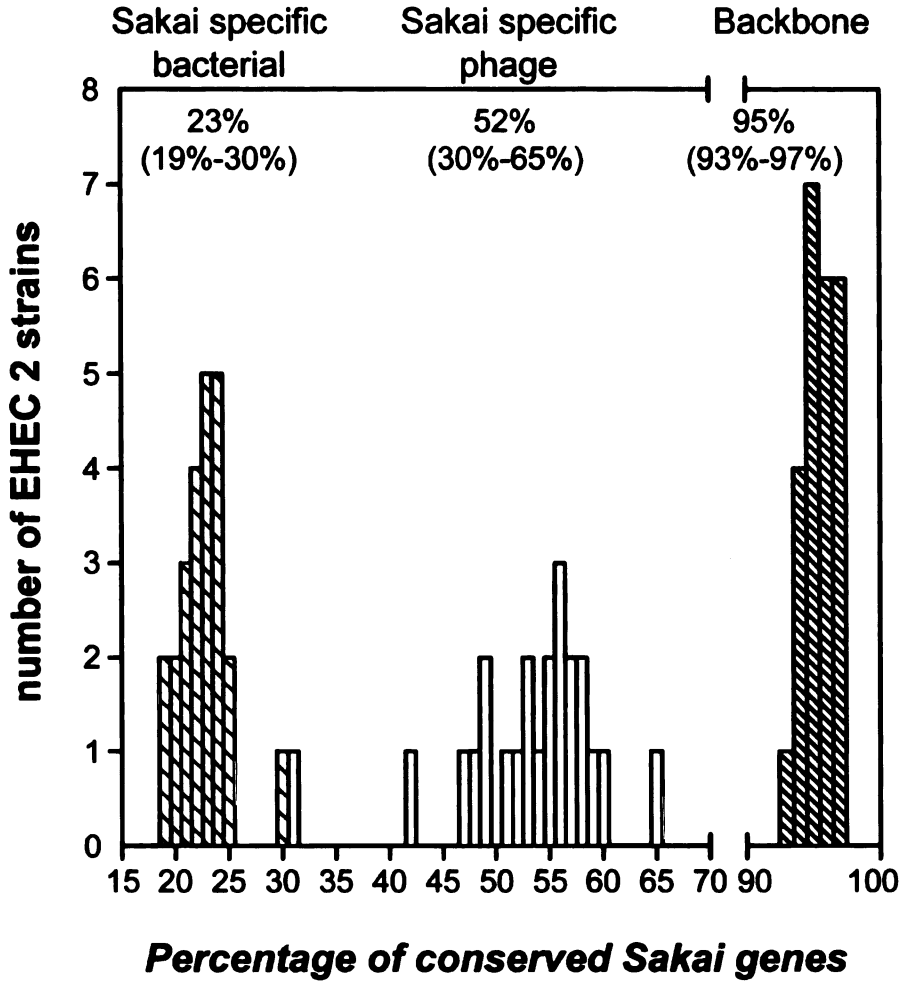

Figure 2.2 Distribution of Sakai genes among individual EHEC 2 clinical strains. The three histograms represent distribution trends of three Sakai gene groups in EHEC 2 strains: Sakai bacterial genes (left histogram – hatched bars), Sakai phage genes (middle histogram, open bars), and backbone genes (right histogram – hatched bars). The levels of Sakai gene content conservation were calculated for each EHEC 2 strain by dividing the number of Sakai genes, from a particular gene group, found in a strain by the total number of Sakai genes from the respective gene group, represented on the oligoarray; these values were expressed as percentages. Each bar represents the number of EHEC 2 strains that were found to have the same percentage of Sakai gene content conservation. Each strain is represented on each histogram and the bars in each histogram add up to 24, the total number of strains investigated. One exception is the bar representing Sakai phage gene content conservation in strain DEC9f, which is hidden by the hatched bar representing the Sakai bacterial gene content conservation in strain CB7505. As can be seen in Table 3, strain DEC9f has 30% of Sakai phage genes and strain CB7505 has 30% of Sakai bacterial genes, causing the bars to overlap. Numbers above each plot represent the average for each group of genes and the range of the distribution is given in parentheses.

Table 2.3. Percentages of Sakai genes found in tested EHEC 2 strains.

Serotype	Strain	Sakai genes on array *n* = 4,944	Backbone (shared with K-12) *n* = 3,696	Sakai-specific	
				phage-related *n* = 814	bacterial *n* = 434
O26:[h11]	DEC 9f	78%	94%	30%	20%
O26:H11	DEC 10e	82%	96%	51%	22%
O26:H11	F5863	84%	97%	56%	25%
O26:H11	97-3250	85%	97%	65%	23%
O26:[h11]	413/89-1	83%	96%	56%	20%
O26:[h11]	DA-22	84%	97%	57%	24%
O26:H11	03-ST-296	84%	97%	54%	22%
O26:H11	CB 7505	84%	96%	59%	30%
O26:H11	*Average*	83%	96%	54%	23%
	Stan. Dev.[a]	2.2%	1%	10.3%	3.2%
O111:[h11]	DEC 8c	82%	94%	55%	19%
O111:H11	DEC 8d	77%	93%	31%	21%
O111:[h8]	C408	82%	95%	49%	24%
O111:[h8]	BCL71	83%	95%	58%	24%
O111:[h8]	ML178190	82%	95%	52%	23%
O111:H8	W29104	81%	95%	48%	23%
O111:[h8]	EK34	81%	95%	47%	24%
O111:H8	EK35	80%	94%	49%	23%
O111:H8	*Average*	82%	95%	51%	24%
	Stan. Dev.	1%	0.4	4%	0.5%
O118:[h16]	RW2030	84%	96%	58%	23%
O118:[h16]	RW1302	82%	95%	56%	19%

Table 2.3, continued

Serotype	Strain	Sakai genes on array n = 4,944	Backbone (shared with K-12) n = 3,696	Sakai-specific	
				phage-related n = 814	bacterial n = 434
O118:H16	666/89	83%	95%	57%	21%
O118:H16	05482	82%	96%	53%	22%
O118:H16	EK36	83%	96%	53%	21%
O118:H16	EK37	84%	97%	55%	25%
O118:H16	*Average*	83%	96%	55%	22%
	Stan. Dev.	0.9%	0.8%	2.1%	2%
O153:[h11]	02-3751	84%	97%	60%	24%
O15:[h11]	RDEC-1	80%	94%	42%	22%
O55:H7	97-3256	84%	97%	33%	70%

a – Stan. Dev., standard deviation.

of the 24 EHEC 2 strains; 102 of these were phage-related. Sixty-four genes encode hypothetical proteins of unknown function, and the remainder consisted mostly of genes responsible for various prophage and other mobile element functions. Nucleotide sequences of these 152 genes were compared against five non-EHEC pathogenic *E. coli* (536, APEC O1, B171, CFT073, UTI89) and six *Shigella* (Sf2a 2457T, Sf2a 301, Sf5 8401, Ss046, Sb227, Sd197) published genomes, using BLAST. With a minimum of 80% nucleotide sequence identity in a minimum of 80% query coverage as the cutoff value to identify conserved genes, 26 of the 152 genes were not found in any of the 11 queried non-EHEC genome sequences. The 26 gene sequences were then "BLASTed" against the entire GenBank database with the same cutoff value. Only three of these 26 genes were not found in any other organisms and therefore could be considered as specific to EHEC strains: ECs1561 (Sakai prophage (Sp) 6); ECs1763, and ECs1822 (Sp 9). All three genes encode hypothetical proteins of unknown function.

Genomic relatedness of EHEC 2 strains. We used the split decomposition method to infer the strain relatedness based on gene content data. We first analyzed all the 4,800 genes whose probe intensities were higher than those for negative controls. As expected, the analysis showed a network like phylogeny (Figure 2.3), in which the parallel edges reflected incompatible signals in the data that were indicative of parallel gene gain/loss due to multiple transduction events or past recombination. All O111:H8 strains were clustered

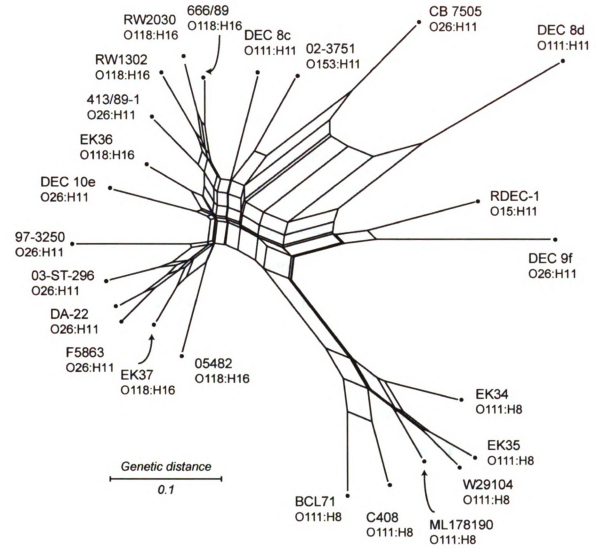

Figure 2.3. Phylogenetic network representing the distribution of Sakai genes in 24 EHEC 2 strains. The network was generated based on the distribution of 4800 Sakai genes among 24 EHEC 2 strains. 144 genes were excluded because their probe intensities were below those of randomized negative controls in the various Sakai/EHEC 2 hybridizations. Node labels refer to strain names (listed in Table 2.1). Parallel edges represent phylogenetic incompatibilities in the data set, which are indicative of parallel gene gain, loss, or divergence events. The network was generated in Splitstree 4.3, using neighbor net with the uncorrected *p* distance. Scale bar represents number of gene differences (present or divergent/absent) per gene site.

closely and branched away from the remaining EHEC 2 strains, which formed a loose cluster without any recognizable concordance to serotypes, hosts, or locations (Figure 2.3). The pairwise homoplasy index (PHI) (44), generated in Splitstree, confirmed that there was significant evidence of recombination (*p*-value = 0.0).

Among the 4,800 genes whose probe intensities were higher than those for negative controls, 70.8% were found to be either present or divergent/absent in all 24 strains, and therefore, phylogenetically uninformative. Compatibility analysis of the 979 parsimoniously informative (PI) genes identified 147 PI genes to be phylogenetically compatible with each other, but not compatible with the rest of the PI genes (the distribution of these genes is shown in Appendix Table 1). For the second split decomposition analysis, these 147 genes were combined with 421 singleton genes (genes found present or divergent/absent in only one of the 24 EHEC 2 strains). Singletons were added to generate terminal edges of the network and to help distinguish strain-specific changes. The analysis with this set of genes showed a more tree like phylogeny with a better separation of EHEC 2 strains (Figure 2.4). Six O111:H8 strains and six O118:H16 strains formed two tight and distinct clusters, while the twelve O26:H11, O111:H11, O153:H11, and O15:H11 strains were dispersed throughout the network. The O111:H8 cluster was visibly distinct from the rest, reiterating its particular pattern of gene content conservation across all 4,800 genes (Figure 2.3). The two O111:H11 strains did not cluster with O111:H8 strains, which is not unusual since the O111 serogroup has been suggested to

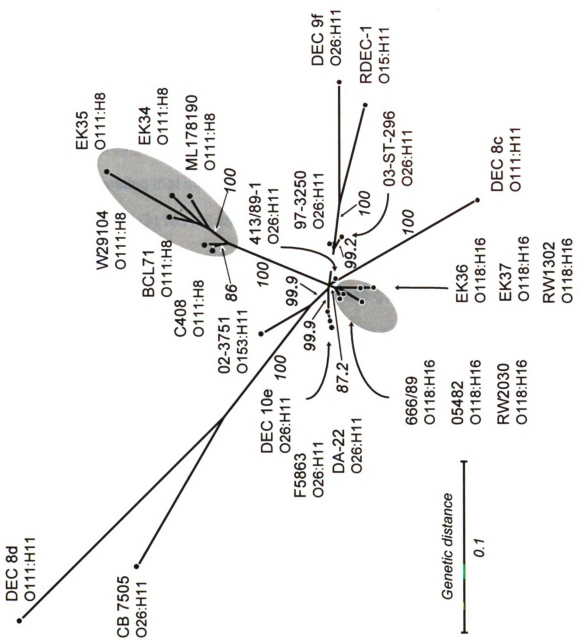

Figure 2.4. Split decomposition analysis of compatible parsimony informative genes and singleton genes in 24 EHEC 2 strains. Gray ovals encompass serotype-specific clusters of O118:H16 and O111:H8 strains. Node labels refer to strain names (listed in Table 1). The network was generated in Splitstree 4.3, using neighbor net with the uncorrected *p* distance. Scale bar represents number of gene differences (present or divergent/absent) per gene site. Percent bootstrap confidence values based on 1000 replicates are shown for selected edges.

include several lineages (48). In this analysis, the O118:H16 strains appear to be more closely related to most of the O26:H11 strains than any other EHEC 2 serotype. Nonetheless, there was a short edge separating the O118:H16 serotype from O26:H11, followed by strain-specific splits within O118:H16 that were based on singleton genes. The eight O26:H11 strains did not cluster together, suggesting that strains of this serotype are considerably more diverse than O111:H8 and O118:H16 strains.

Prophages. To visualize gene content of the 814 Sakai phage genes within the EHEC 2 clonal group, we classified these genes by Sakai phage groups (Sakai prophages Sp1-18, and prophage-like elements SpLE1-6) and sorted the genes in each group by chromosomal order (based on ECs numbers). This classification does not necessarily infer that these genes are present in EHEC 2 within the same phage or order as they are in Sakai, but simply allows an assessment of gene content variation of laterally acquired genes known to be linked in the Sakai chromosome. Dendrograms based on pairwise comparison of gene content were used to identify EHEC 2 strains with similar gene content (Figure 2.5). Overall, there was no common pattern of gene distribution for all phage groups (Figure 2.5), which was also implied by additional split decomposition networks (data not shown). Some similarity was detected among O111:H8 strains for Sp5, Sp15 and Sp8 genes, with more Sp5 and Sp15 genes being conserved in the O111:H8 serotype than in other EHEC 2 strains. Conversely, Sp8 was well-conserved in all but the O111:H8 strains (data not shown), in which Sp8 genes were virtually absent except for two short gene

segments, ECs1638-43 and ECs1656-63, which encode tail and hypothetical proteins, respectively.

Stx converting prophages. The CGH data confirmed the *stx1*/*stx2* profile of the EHEC 2 strains determined by PCR. In Sp15 (*stx1*-prophage), a block of genes at the beginning of the phage (ECs2940-2952) was conserved in most strains (Figure 2.5). These genes encode tail proteins and the putative outer membrane protein Lom precursor (ECs2942). Adjacent is a group of genes (ECs2953-2963) encoding two tail proteins, a putative terminase large subunit and several unknown proteins, which are fully conserved in O111:H8 strains but almost completely divergent/absent in the rest. Two regions in the Sp15 phage, ECs2984-2988 and ECs2998-3006, were well conserved in all strains positive for the *stx1* gene, except in O111:H8 strains. Excisionase and integrase genes (ECs3012 and ECs3013) were divergent/absent in most of the EHEC 2 strains. Overall, the gene content of Sp15 in strains negative for the *stx1* gene was different from those in *stx1* positive strains (Figure 2.5).

Strains positive for the *stx2* gene, mostly representing serotype O111:H8, had more Sp5 (*stx2*-phage) genes. Integrase and excisionase genes (ECs1160 and ECs1161), and the block of genes at the beginning of the phage, ECs1160-1187, were missing from most strains. The rest of Sp5 genes, which encode replication proteins O and P, NinE and NinG, Shiga toxin 2, antirepressor proteins, antitermination protein Q, outer membrane precursor proteins, terminases, tail proteins, and a number of hypothetical proteins, were present in

five of the six O111:H8 strains as well as in the O26:H11 strain containing both *stx1* and *stx2* (Figure 2.5).

Locus of enterocyte effacement (LEE) island. Of the 41 genes in the Sakai LEE island that are located on SpLE4, all except *escU* were present in the O55:H7 strain. This includes genes that were categorized as present after the initial GACK cutoff was relaxed by 20%. Since dye-swap genomic microarrays represent competitive hybridizations between two populations of DNA, there were instances when a small difference in the nucleotide sequence of the tested strain resulted in weaker probe signal intensity. For example, both of the two known SNPs present between the variable regions of γ intimin in O55:H7 and O157:H7 (210) are located in the middle region of the 70-mer probe for *eae*. Hence the signal intensity for this gene was just below the cutoff (gray shading in Figure 2.5). Based on the level of divergence of EHEC 2 LEE genes from O157 LEE genes, strains clustered into two major groups (Figure 2.5). The top group of the dendrogram is composed of human strains, which have a high level of similarity to O157 LEE genes, whereas the bottom cluster represents 11 animal and 3 human strains that have a lower level of similarity to the O157 LEE genes. The level of divergence was also found to be heterogeneous between LEE operons (Table 2.4). The genes that encode the type III secretion system (TTSS), *escRSTUCJVNDF*, were detected in 14 to 24 strains, with the exception of *escR* and *escC*, which were found in 11 and 5 strains, respectively. The needle filament gene, *espA*, was present in 23 strains, whereas *espB* and *espD* were divergent/absent in all. The *tir* and γ intimin genes were also

divergent/absent in EHEC 2; the γ intimin was conserved only in the O55:H7 representative, an expected result because the 70-mer probe was designed to detect the variable (allele-specific) part of *eae*.

Other phage gene groups. Most genes form SpLE1, which encodes the tellurite resistance and adherence island (TAI), were divergent/absent from two EHEC 2 strains and from the O55:H7 representative, but present in the rest of the EHEC 2 strains (Figure 2.5). The diverse trend in retention or loss of laterally acquired genes was emphasized by the arrangement of Sp10 genes. CGH data inferred three patterns of Sp10 gene content conservation in EHEC 2 (Figure 2.5). In the first 14 strains (top to bottom), Sp10 genes were found to be present or divergent/absent in an *en bloc* fashion. The middle branch of the dendrogram represents six strains in which virtually all Sp10 genes were present. In the remaining five strains, Sp10 genes appeared to have a mosaic structure with individual genes present or divergent/absent. In contrast, Sp18 was either entirely divergent/absent or nearly completely present. There was no correlation between the distribution of Sakai phage genes in EHEC 2 and geographic location of the EHEC 2 isolates.

Non-LEE encoded effectors. The gene content of non-LEE encoded effectors, which are predicted to be secreted by the LEE-encoded TTSS (317) in EHEC 2, varied from totally divergent/absent to present in every strain. Genes *espY1*, *nleD*, *espX2*, *espY4*, *espL3'*, *espX3'*, *espL4*, and *nleB2-1* were divergent/absent from EHEC 2, whereas a set of 15 genes (*espX1*, *espX5*, *espX6*, *espY3*, *espK*, *nleA*, *nleE*, *nleG*, *nleG2-2*, *nleG6-1*, *espM1*, *espM2*, *espR1*,

espL1, and *espW*) were present in at least 22 EHEC 2 strains. The *nleG7* gene, which was recently found to be conserved in a group of non-O157 EHEC strains (231), was also divergent/absent in all EHEC 2 examined in this study.

Figure 2.5.A. Distribution of Sakai phage genes and the LEE island in EHEC 2 strains. Sakai phage genes inferred as present or divergent/absent were grouped and sorted according to the Sakai annotation. Colormaps, with dendrograms, of individual phages were generated in R software (v 2.4.0.), using the 'gplots' package (v 2.3.2). Present genes are depicted as black, absent/divergent as white. Gray squares symbolize genes that have been classified as present after the cutoff was relaxed for 20%, representing a 'low' level of gene divergence. Dendrogram labels refer to strain names (Table 2.1). Panels: A – Stx1-converting phage; B – Stx2-converting phage, labels with asterisks in the Sp15 and Sp5 colormaps refer to strains that were positive for *stx1* and *stx2* genes, respectively; C – LEE island, labels with open boxes in the LEE colormap represent animal strains, and arrows and numerals atop the LEE colormap represent operons and the direction of their transcription; D – TAI island, E – Sp10, F – Sp18. Sp – Sakai prophage, SpLE – Sakai prophage-like element, TAI – tellurite resistance and adherence island.

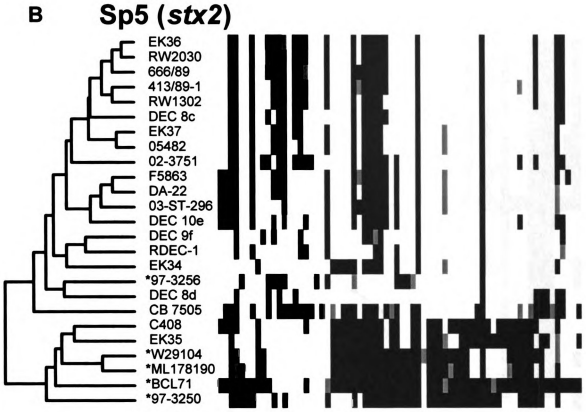

Figure 2.5.B. Distribution of Sakai phage genes and the LEE island in EHEC 2 strains.

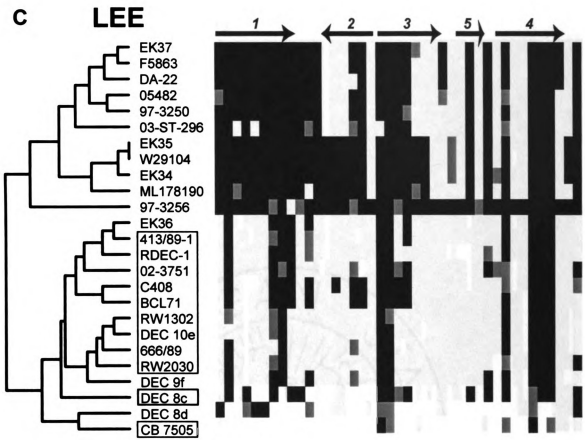

Figure 2.5.C. Distribution of Sakai phage genes and the LEE island in EHEC 2 strains.

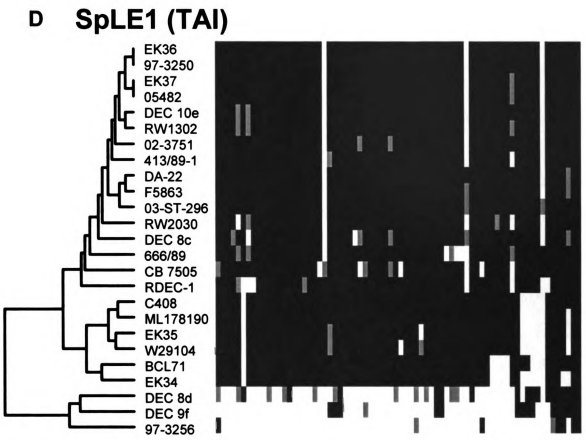

Figure 2.5.D. Distribution of Sakai phage genes and the LEE island in EHEC 2 strains.

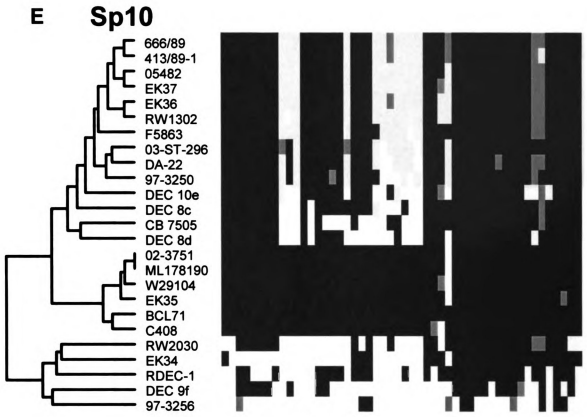

Figure 2.5.E. Distribution of Sakai phage genes and the LEE island in EHEC 2 strains.

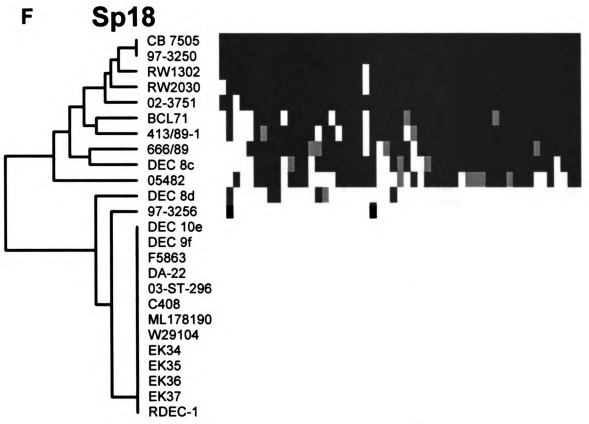

Figure 2.5.F. Distribution of Sakai phage genes and the LEE island in EHEC 2 strains.

Table 2.4. Conservation of O157 LEE operons in a set of 24 EHEC 2 strains.

	lee 1 (9)[a]	*lee 2* (6)	*lee 3* (7)	*lee 5* (3)	*lee 4* (8)
Human[b]	8.8 ± 0.6	3.1 ± 1.7	4.8 ± 1.1	1.0 ± 0.0	4.4 ± 0.5
Animal[c]	3.2 ± 1.2	0.6 ± 0.9	2.7 ± 0.9	0.1 ± 0.2	3.8 ± 0.9

a. The number of genes in each operon is given in parentheses.
b. Refers to the 10 human isolates in the top branch of the dendrogram in the LEE image in Figure 2.5, not including O55:H7. Values represent average number of genes in an operon, with standard deviation.
c. Refers to the 11 animal and 3 human isolates in the bottom branch of the dendrogram in the LEE image in Figure 2.5. Values represent average number of genes in operon, with standard deviation.

DISCUSSION

Comparative analysis of genomes from 17 commensal and pathogenic *E. coli* strains has revealed a diverse species 'pan-genome', while the *E. coli* 'core conserved' genome was calculated to be about one-half of the genome of a given *E. coli* isolate (252). Although EHEC utilize similar virulence mechanisms, this pathotype is comprised of phylogenetically distinct lineages that vary in their ability to cause disease in both humans and animals. Clearly, the genome of a single strain cannot reflect how the genomic diversity among EHEC strains influences pathogenesis of the EHEC population. Because no strains from the EHEC 2 clonal group have been sequenced, the genetic variability of 24 EHEC 2 strains were examined in relation to the distribution of genes from O157:H7 Sakai, which belongs to the EHEC 1 clonal group. The Sakai genome was used in this study, as its annotation is suggested to include more strain-specific genes compared to EDL933 (252). Genes specific to the EHEC 2 group have yet to be described. Some genes shared with Sakai might have been missed in our study, if the gene sequence had diverged to a point where the 70-mer oligonucleotide probes and the stringency of competitive hybridization preclude detection. Although this study allowed screening of known genes only, the gene content data still offered new insight on strain relatedness and the distribution and subsequent diversification of mobile elements within the EHEC 2 clonal group.

The CGH data presented here indicate that there are two distinct trends, which reflect the bacterial (vertical) and phage (lateral) origin of genes, impacting the genomic divergence of EHEC 2. Virtually the entire set of backbone genes

was present within the EHEC 2 clonal group (Tables 2.2 and 2.3). CGH inferences pertaining to the distribution of backbone genes can vary depending on array type, sample size, and strain diversity (231). For example, Anjum *et al.* have proposed that the O26 serogroup exhibits greater genetic homogeneity than was observed in our study (16); however, the microarray platform used in that study was limited to the genome of K-12 MG1655. Despite these differences, the degree of conservation among backbone genes in this CGH investigation was similar in previous studies (76, 107, 231). The distribution of Sakai-specific genes in EHEC 2 was, not surprisingly, noticeably lower than that of the backbone, which restates established findings about intraspecies genomic variability (192, 334, 338). The conservation of Sakai phage genes was, however, found to be more than 2-fold higher when compared to Sakai bacterial genes (Figure 2.2 and Table 2.3). In O55:H7, the inferred ancestor of O157:H7 (95), the proportion of Sakai phage to bacterial gene conservation was opposite from the proportion observed in EHEC 2; this suggests that Sakai bacterial genes have been vertically acquired from the O55:H7 progenitor and are not disseminated among the EHEC 2 clone. Cursory assessment of K-12-specific genes suggests a homogenous distribution in EHEC 2, with less than half of the genes present; most K-12 phage-related genes were found to be uniformly divergent/absent from the entire EHEC 2 population. Assessing the conservation of K-12 specific genes was, however, beyond the scope of this study, as K-12 MG1655 is a non-pathogenic laboratory-derived strain that is distantly related to EHEC (Figure 2.1).

The increased presence of Sakai phage genes in the EHEC 2 group compared to Sakai bacterial genes reveals independent acquisition and exchange of similar mobile elements. For example, of the 152 Sakai-specific genes present in EHEC 2, only 26 genes were not found in 11 completed non-EHEC *E. coli* and *Shigella spp.* genomes. About one-half of the 26 "EHEC only" genes were found in *stx1*-encoding phages BP-4795 and CP-1639 from STEC O84:H11 and O111:H-, respectively (61, 62). Sakai genes identified by BLASTN as present on BP-4795 are disseminated on phages Sp6, 9, 10, and 12, which is in agreement with the evidence for recombination between phages (45). Although the number of phage genes shared by all tested strains was low, the percentage of those that were VAP was high (Table 2.2), which may reflect sequence heterogeneity in prophage genomes with similar modular structures (45, 61, 253), and not true absence of genes.

Phylogenetic network analysis implied a serotype-specific uniformity of O111:H8 strains, unlike other EHEC 2 strains (Figure 2.3), which can also be inferred from the arrangement of Sakai phage genes in O111:H8 strains (Figure 2.5). Interestingly, these six EHEC 2 representatives are the only strains with the θ intimin allele while the remaining eighteen EHEC 2 strains had β intimin, as determined by PCR-based RFLP typing of *eae*; the method for *eae* typing was described previously (190). By contrast, members of the EHEC 1 clonal group (i.e., O157:H7 and O55:H7) typically had the γ allele. Although intimin θ has been found in an atypical EPEC O55:H7 and a non-EHEC 2 strain (GenBank Acc. No. AJ833638 and AF253561), O111:H8 is, to the best of our knowledge,

the only EHEC 2 serotype with this intimin allele, providing further support for the hypothesis that O111:H8 represents a distinct grouping.

Based on the distinguishing distribution of Sakai genes (Figures 2.3 and 2.4), serotype O26:H11 appears to be considerably more diverse compared to the distinct and more uniform O111:H8. This suggests that the genetic make-up of O26:H11 is such that it allows more frequent lateral exchange of DNA elements, which can result in acquisition of novel fitness and virulence genes by O26:H11 more commonly than by other EHEC 2. For example, O26:H11 possess the *Yersinia spp.* high pathogenicity island (HPI) that encodes the iron-uptake siderophore yersiniabactin and the pesticin receptor, whereas other EHEC serotypes, including O157:H7, O111:H-, O103:H2, and O145:H-, do not have this HPI (165). The diversity of O26:H11/H- has also been implied with other methods (344).

A proportion of the EHEC 2 hybridization data (15% of the PI genes) were identified as genes that are phylogenetically compatible with each other, i.e., having no homoplasy. Although this represents a small number of genes, it is remarkable that the distribution pattern grouped EHEC 2 O111:H8 and O118:H16 strains by serotype (Figure 2.4). The pathogenic *E. coli* used in this study represent tips of phylogenetic branches, where high frequencies of recombination strongly impact the shaping of genomic content (128) and eventually lead to erosion of the phylogenetic signal between clonal complexes (93). Thus, the set of genes shared with EHEC 1 O157:H7 whose pattern of

presence and absence in EHEC 2 infers compatibility and is not random, but coincides with serotype, warrants further investigation.

The heterogeneity of Stx phages has been demonstrated (141, 253), even within the O157:H7 lineage itself (109, 232), so it is not unexpected to find such variation between different EHEC 2 strains. In addition, Ogura *et al.* propose that Stx phages have alternative integration sites in EHEC 2 (231); this may explain our lack of detection of integrase genes, as integration site specificity is dependent on the alignment of the phage integrase with the attachment sequence in the bacterial chromosome (281). Strains that were *stx* negative in our study were, nevertheless, found to carry genes from the Sp15 and Sp5 phages, which is a common effect of frequent modular shuffling of sequences between phages of related enteric hosts (45, 138, 139). The significance of the unique conservation patterns of Sp10 and Sp18 phage genes is not clear. Sp10 is perhaps more conserved as it harbors non-LEE effector genes (317), all 3 of which were detected in at least 22 out of 24 EHEC 2 strains. Absence of the entire Sp18 was also detected among O157:H7 strains (232), one of which belongs to a hyper-virulent lineage of the O157:H7 population (205).

Incongruent divergence of LEE operons has been previously suggested. Studies indicate that this island is a dynamic region (271), and that different selective pressures act on different parts of the LEE (54). The sequence diversity of the LEE, both at the nucleotide and amino acid level, increases along the length of the island from the LEE1 to the LEE4 operon (54, 103). A comparable trend can be observed in the CGH data presented here, as there

was greater conservation of the content of genes that encode the secretion apparatus (LEE1-3). However, differences in the content of O157:H7 Sakai LEE genes between human and animal EHEC 2 strains of the same serotype (Figure 2.5 and Table 2.4) suggest that the LEE has diverged between EHEC 2 strains in a host dependent manner, possibly due to host species adaptive pressure. This result was not expected and its implications are not supported by the current literature. Multiple, parallel acquisitions of the LEE by different clonal groups have been inferred (159, 241, 255, 308). Muniesa *et al.* suggest that the LEE genes associated with serogroup O26 are present more commonly in STEC than the LEE genes associated with EHEC O157:H7 or EPEC O127:H6 (219). Yet, there is no clear evidence to support the hypothesis that LEE divergence within a lineage results from positive adaptive pressure in different host species. In fact, when several LEE genes from strain RDEC-1 were compared to those from other AEEC, the variation appeared to be associated with evolutionary lineage and not host specificity (345). Even so, given the heterogeneous diversification of this island and the recent inference about host-specific expression of *espA* and *eae* in O157:H7 (251), it would be interesting to compare complete LEE sequences from a larger sample of EHEC 2 strains of human and animal origin.

CONCLUSIONS

Here, we present an assessment of the gene content of a set of EHEC 2 clinical strains of animal and human origin, isolated from the USA and Europe. The small subset of phylogenetically compatible genes represent potential markers that will aid in the investigation of the relatedness and cladogenesis of the EHEC 2 clonal group. In this study, serotype O26:H11, the most frequent EHEC 2 serotype associated with overt disease, represented the most diverse EHEC 2 population. Compared to the more homogeneous O111:H8 strains, O26:H11 strains may have an increased propensity to laterally exchange DNA, which may ultimately give rise to hyper-virulent lineages within EHEC 2 O26:H11. Furthermore, the identification of several EHEC-specific genes could potentially be used as novel genetic markers to identify strains belonging to this pathotype.

ACKNOWLEGDMENTS

The authors thank Shannon Manning, James Riordan, Sivapriya Kailasan Vanaja, Linda Mansfield, Martha Mulks, and Jillian Tietjen for critically reviewing earlier versions of the manuscript; Lindsey Ouellette for technical assistance with MLST; and those investigators who supplied strains for use in the study. This project was funded in part by the MSU foundation and the NIAID, NIH, DHHS, under NIH research contract N01-AI-30058 (TSW), which supports the STEC Center.

CHAPTER 3

Increased Adherence and Virulence Gene Expression of the Spinach Outbreak Strain of Enterohemorrhagic *Escherichia coli* O157:H7

Abu-Ali, G. S., Ouellette, L. M., Henderson, T. S., and Whittam, T. S.

Submitted to *J. BMC Microbiology*, April 1st 2009

SUMMARY

Background: The *Escherichia coli* O157:H7 TW14359 strain was implicated in a multi-state USA outbreak in 2006, which resulted in remarkably high rates of severe disease when compared to previous outbreaks of illness caused by *E. coli* O157:H7. In this study, we hypothesized that the elevated pathogenic potential of this strain is associated with increased virulence gene expression. To test this hypothesis, we performed epithelial cell association assays and global gene expression measurements, following O157:H7 challenge of epithelial cells, with O157:H7 TW14359 and O157:H7 RIMD0509952 (Sakai), a well-studied outbreak strain.

Results: Epithelial cell assays revealed a 2.47 ± 0.27-fold increase in association of the TW14359 strain relative to Sakai. Whole-genome microarrays detected significant differential expression of 914 genes between the two O157:H7 strains, 206 of which had a fold change ≥ 1.5. In particular, the locus of enterocyte effacement (LEE) was upregulated in TW14359, whereas Sakai overexpressed flagellar and chemotaxis genes (flg and fli operons, and cheB, tar, and tsr), suggesting unsynchronized expression of the LEE and flagella in the two strains, possibly via the GrlA regulatory switch. The TW14359 strain also showed elevated expression of Shiga toxin 2 mRNA as well as of several pO157-encoded genes that promote adherence, including, type II secretion genes, and their effectors stcE and adfO. Of the 24 non-LEE effector genes that were differentially expressed, 16 were upregulated in Spinach. The relative

expression differences of LEE, flagella, and Shiga toxin 2 genes were verified by quantitative PCR.

Conclusions: This study revealed the overexpression of major and ancillary virulence genes in the O157:H7 TW14359 strain, under conditions that mimic the host-pathogen challenge. Moreover, the increased association of O157:H7 TW14359 with epithelial cells suggests that this strain is a more efficient colonizer of the intestines. Altogether, these findings indicate that an increased pathogenic potential exists for the O157:H7 TW14359 strain, and are consistent with the severe post-infection sequelae of the 2006 USA outbreak. Since these two strains were recently classified into genetically distinct O157:H7 subpopulations, this study also implies lineage-specific differences in the regulation of shared virulence traits.

INTRODUCTION

Enterohemorrhagic Escherichia coli (EHEC) O157:H7 are food- and waterborne pathogens of zoonotic origin that cause a range of clinical complications that include diarrhea, hemorrhagic colitis and a grave systemic condition termed hemolytic uremic syndrome (HUS). HUS is characterized by the triad of thrombotic microangiopathy, hemolytic anemia and acute renal failure (79, 305). EHEC O157 contributes to 17 outbreaks (212) as well as 75000 cases of sporadic illness (250) in the US each year. Variation in the frequency of severe disease, as indicated by hospitalization and HUS rates, have been reported between O157:H7 outbreaks (250). One recent example is the high rate of hospitalization (51%) and HUS (15%) (92) observed in the 2006 outbreak, linked to contaminated spinach, compared to the low rate of hospitalization (3-5%) and HUS (0-3%) (205) in the 1996 outbreak in Sakai, Japan, associated with contaminated radish sprouts. Although the Sakai outbreak affected roughly 25-60 times more people than the spinach outbreak and is considered the largest O157:H7 outbreak to date (108, 142, 215), the difference in the frequency of severe disease between outbreaks is puzzling.

One explanation for the variation in disease severity between the Sakai and spinach O157:H7 outbreaks could be ascribed to host susceptibility, or different concentration of bacteria in the food vehicle (163). Alternatively, this discrepancy may be attributable to intrinsic genetic variation between the two outbreak strains. Evidence supporting the latter hypothesis comes from the finding that the RIMD0509952 (Sakai outbreak) and TW14359 (spinach

outbreak) O157:H7 genomes differed by 10% in nucleotide sequence of 2,741 conserved genes that were examined (205). The spinach genome sequence analysis also uncovered genetic material not present in the Sakai genome, including a variant of the Shiga toxin 2 gene (stx2c) and the lysogenic bacteriophage 2851 that encodes it (205).

The spinach and Sakai outbreak strains may vary in their ability to colonize host epithelial cells as well as to express virulence genes. Both, colonization of the intestinal mucosa via a type three secretion system (TTSS), and the production of Shiga toxin(s) (Stx1, 2, and variants) are critical for O157:H7 disease pathogenesis (164). Shiga toxins are phage-borne, two-component cytotoxins that block protein synthesis via depurination of eukaryotic 28S rRNA (89, 141, 272). Interestingly, Shiga toxin 2, the variant that is most commonly associated with severe complications of O157:H7 infection (36, 91, 233), has been shown to be differentially expressed between different Shiga toxin producing E. coli (67), as well as between distinct subpopulations of O157:H7 (82). Similarly, expression of the laterally acquired locus of enterocyte effacement (LEE) (209), which encodes the TTSS in O157:H7 and enteropathogenic E. coli, is influenced by several distal regulators, chromosomal and plasmid borne, which act on the LEE-encoded regulators Ler, GrlA, and GrlR (164, 289). Together, these observations imply that the expression of integral O157:H7 virulence factors can vary depending on differences in the genetic background of O157:H7 strains.

Coordinate regulation of LEE operons (lee1-5) is required to mediate intimate attachment of O157:H7 to the mucosal epithelium. This process yields attaching/effacing (A/E) lesions, which are characterized by formation of actin pedestals that abut the bacteria and by effacement of the epithelial microvilli (115, 181). Studies have shown that expression of O157:H7 LEE genes is downregulated following intimate adherence to the eukaryotic cell (23, 65). Similarly, transcription of *Salmonella enterica* invasion genes is turned off following macrophage invasion (90). This suggests that potential differences in the transcription of colonization factors are more likely to be detected prior to bacterial adhesion/invasion of the eukaryotic cell.

This study examines the ability of EHEC O157:H7 TW14359 (Spinach) and RIMD0509952 (Sakai) outbreak strains to associate with epithelial cells, and investigates genome-wide expression patterns of the two strains following their exposure, but preceding intimate adherence, to MAC-T bovine epithelial cells. The overall goal is to determine whether these O157:H7 outbreak strains differ in their potential to colonize the epithelium and in expression of virulence genes, under conditions that mimic the host-pathogen challenge. Resolving phenotypic and transcriptional differences among outbreak strains of O157:H7 will advance our understanding of the molecular mechanisms that underlie the remarkably variable epidemiology of O157:H7.

MATERIALS AND METHODS

Bacterial strains and growth conditions. *E. coli* O157:H7 strains RIMD0509952 (Sakai), implicated in a radish sprout outbreak (215), TW14359 (Spinach), implicated in a spinach outbreak (6), and the lab-derived K12 MG1655 (35) were stored at -70 °C in Luria-Bertani (LB) broth + 10% glycerol. From freezer stocks, strains were inoculated into 10 ml of LB broth and grown to OD_{600} = 0.1 – 0.15, allowing revival of cells in rich media prior to transfer to morpholino-propanesulfonic acid (MOPS)-buffered minimal media. MOPS (10×) minimal media was prepared as described by Neidhardt et al. (223). LB cultures of O157:H7 strains were transferred to 50 ml of MOPS minimal media with 0.1% glucose at a ratio of 1:100, and grown to stationary phase (OD_{600} = 1) at 37 °C with shaking. Cultures in MOPS were transferred to 100 ml of MOPS at a ratio of 1:200 and grown for 10 h. Prior to infection of MAC-T epithelial cells, O157:H7 cultures in MOPS were transferred to Dulbecco's Modified Eagle's Medium (DMEM) (pH 7.4, without phenol-red, 0.45% glucose, 0.37% $NaHCO_3$) (Sigma, St. Louis MO) for adaptation, at a ratio of 1:40 and grown for 3 h ($(5 \pm 0.5)\times10^8$ CFU/ml) at 37 °C with shaking. Reproducible steady-state growth of O157:H7 cultures in MOPS minimal media and in DMEM was confirmed by optical density (OD_{600}) readings, over time (Figure 3.1).

MAC-T cells. Bovine mammary epithelial (MAC-T) cells (151) are commonly used in studies of adherent and invasive *E. coli* (77, 80), and *E. coli* O157:H7 were previously shown to induce A/E lesions on this epithelial cell line (207). MAC-T cells were cultured in 75 cm^2 tissue flasks (Corning, Lowell MA)

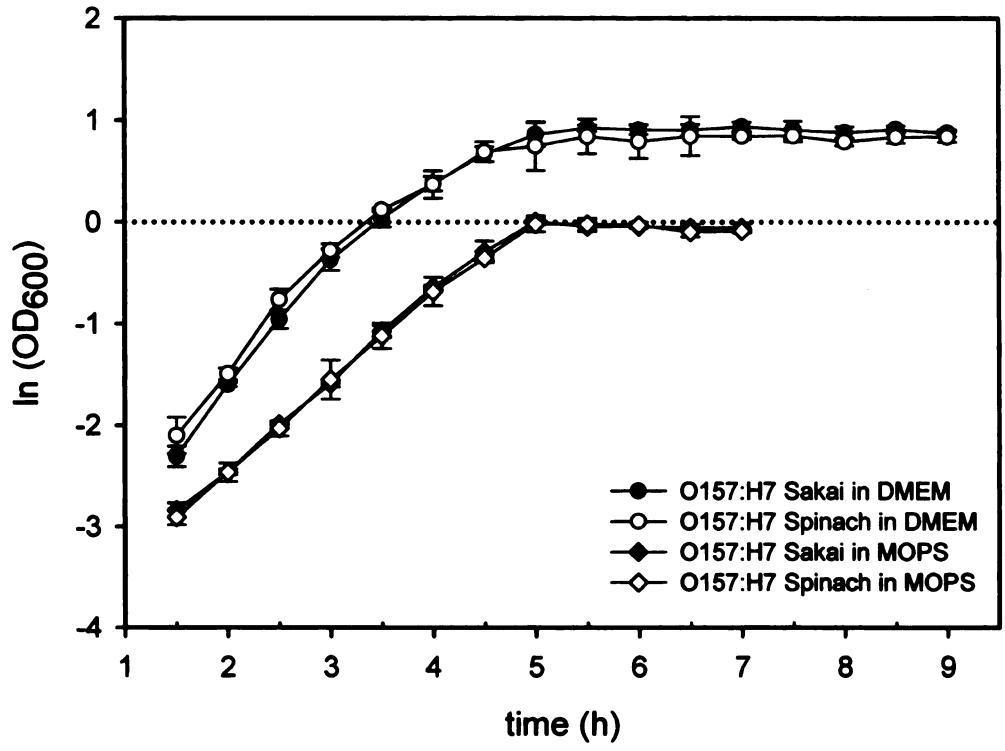

Figure 3.1. Average growth of E. coli O157:H7 strains Sakai and Spinach in DMEM and MOPS minimal medium. Growth is plotted as the increase in cell density, measured at OD_{600}, over time. Error bars represent the standard deviation of three independent cultures of each strain.

and maintained in DMEM supplemented with 10% fetal bovine serum (FBS) and 2% Antibiotic-Antimycotic solution (penicillin-streptomycin-amphotericin 100x, Invitrogen), at 37 °C with 5% CO_2. For microarray experiments, MAC-T cells were grown to confluence in 75 cm^2 flasks. Approximately 12 h before experiments, MAC-T cell monolayers were washed with fresh DMEM and the culture medium was replaced with fresh DMEM without antibiotics and 2% FBS. DMEM media was replaced again prior to experiments, with fresh DMEM without FBS.

Fluorescent microscopy. The ability of Sakai and Spinach strains to form A/E lesions on MAC-T cells was examined using the previously described fluorescent-actin staining (FAS) test (181, 282), with modification. Approximately 5×10^5 MAC-T cells/well were seeded into 24-well plates (Corning Inc., Lowell MA) containing one 12 mm glass coverslip (Fisher Scientific, Pittsburgh, PA) per well and were incubated overnight at 37 °C with 5% CO_2. The following day, MAC-T monolayers were infected with 100 µl of O157:H7 Sakai, Spinach, or K12 MG1655 culture in DMEM and incubated for 3 h at 37 °C with 5% CO_2. After incubation, wells were washed three times in excess PBS to remove non-adherent bacteria and cells were fixed and permeabilized with chilled acetone (-20 °C) for 2 min. Following three washes with PBS, a 30 min blocking step with 1% bovine serum albumin (BSA)/PBS was applied to inhibit non-specific staining. After washing in PBS, cells were stained with phalloidin conjugated to Alexa Fluor 488 (Molecular Probes, Carlsbad CA), according to the manufacturer's instructions, to detect filamentous actin. Cells were counterstained with

propidium iodide (Molecular Probes), which stains nucleic acids. Coverslips were mounted on microscope slides and samples were analyzed using a Zeiss 510 Meta ConfoCor3 LSM confocal laser scanning microscope with a 63× plan apochromat numerical aperture 1.4 objective, with oil immersion (Carl Zeiss MicroImaging Inc., Thornwood, N.Y.). Images were imported and handled with Zeiss LSM Image Browser Version 3.2.0.115; confocal slices were merged in Adobe Photoshop (version 6). The experiment was performed in triplicate for two independent cultures of each strain.

Association assays. Association assays, a measurement of adherence and invasion, were performed in 24-well plates by the method described previously (75), with modification. Confluent monolayers of MAC-T cells (~1×10^6 cells/well) were washed with DMEM and infected with 1 ml of Sakai or Spinach culture in DMEM at a multiplicity of infection (MOI), the ratio of bacteria to host cell, of 500; cell counts of O157:H7 inocula were $(5 \pm 0.4)\times10^8$ CFU/ml. After 30 min or 1 h of incubation at 37 °C with 5% CO_2, wells were washed with excess PBS and MAC-T were disrupted with 0.1 % Triton X-100 (Sigma-Aldrich, St. Louis MO) for 30 minutes. Serially diluted lysates were plated on LB agar with the Autoplate 4000 Spiral Plater (Spiral Biotech, Bethesda, MD) and enumerated following overnight incubation at 37 °C, using the Q-Count (Spiral Biotech). Each O157:H7 strain was assayed in quadruplicate and the experiment was repeated 3 times. The CFU/ml of Sakai and Spinach recovered from all wells of a biological replicate were normalized against the CFU/ml recovered from the first well of the corresponding biological replicate infected with Sakai. Normalized

data from 3 biological replications of the experiment were analyzed with a mixed ANOVA model (SAS v9.1, Cary Inst., NC), relative association = strain + replicate (strain) + error, where biological replicate was nested within the strain effect. The difference in association was expressed as the mean ± standard error of Spinach relative to Sakai.

Microarray experiments and RNA extraction. Monolayers of MAC-T cells, maintained in 75 cm^2 tissue culture flasks with 15 ml of DMEM, were infected with 3 ml, at a concentration of $(5 \pm 0.5)\times10^8$ CFU/ml, of O157:H7 Sakai or Spinach culture in DMEM. The co-culture was incubated for 30 min at 37 °C with 5% CO_2 and with gentle rocking at 1.5 rpm on a rocking platform (VWR International, West Chester PA) to mimic gut peristalsis. After incubation, 8 ml aliquots of non-adherent, suspended, bacteria were mixed with 1/10 volume of 10% phenol:ethanol buffer to stabilize the RNA (31), and centrifuged at 4 °C, 4500×*g* for 30 min to pellet cells. The supernatant was decanted and cell pellets were suspended in 5 ml of buffer (2 mM EDTA, 20 mM NaOAc, pH 5.2). Suspended cells were mixed with an equal volume of acid-phenol:chloroform at 65 °C, pH 4.5 (with isoamyl alcohol, 125:25:1) (Ambion, Austin, TX) and incubated at 65 °C for 10 min, with periodic vortexing, before centrifuging at 3200×*g* for 20 min. Supernatant was extracted again with an equal volume of acid-phenol chloroform and then with an equal volume of chloroform:isoamyl alcohol (24:1). RNA was precipitated overnight at -80 °C in 2.75 volumes 100% ethanol and 1/10 volume 3M sodium acetate, pH 5.2. RNA samples were purified and treated with DNase using the RNeasy kit (Qiagen). Integrity of RNA

populations was verified by visualization of the 23S and 16S rRNA bands after electrophoresis on formaldehyde-agarose gels. RNA isolation from O157:H7 Sakai and Spinach strains was performed from 5 biological replications of the experiment.

cDNA conversion. cDNA samples for microarray hybridization were generated by one-step aminoallyl-dUTP (Sigma) labeling of reverse transcribed RNA. Reactions containing 6 µg RNA, 2 µg random primers (Invitrogen, Carlsbad, CA), 1× first strand buffer (Invitrogen), 10 mM DTT, 400 U Superscript II (Invitrogen), 0.5 mM each dATP, dCTP, and dGTP, 0.3 mM dTTP, and 0.2 mM amino-allyl dUTP were incubated overnight at 42 °C. cDNAs were purified on QIAquick PCR purification columns (Qiagen), using PB binding buffer (Qiagen) and phosphate wash buffer (5 mM K_2HPO_4, pH 8.0, 80% ethanol) before elution with 60 µl of phosphate elution buffer (4 mM K_2HPO_4, pH 8.5). cDNA was dried and resuspended in 0.1 M sodium carbonate pH 9.3, and coupled with Cy3 or Cy5 dyes (Amersham Biosciences, Piscataway, N. J.), according to the manufacturer's instructions. Following another on-column purification to remove uncoupled Cy-dye, the concentration of cDNA and dye incorporation were measured for each sample using a Nanodrop spectrophotometer (model ND-1000) (Ambion). Dried cDNA samples were stored at -80 °C for no more than a week prior to hybridization.

Oligonucleotide microarray. The previously described microarray platform that probes for 5978 ORFs from E. coli strains O157:H7 Sakai and EDL 933, and K12 MG1655 (160), was upgraded to include additional 70-mer probes,

spotted in duplicate, which target 110 ORFs from the O157:H7 plasmid (pO157) (46).

Hybridization conditions and data collection. Microarray slides were prepared for hybridization by cross-linking (exposure to 6000 uJ of UV) and blocking in 1% SDS, 5× SSC, and 1 mg/mL BSA at 42 °C for 1 hour. After washing twice for 5 min in 0.1× SSC, twice for 5 min in 0.1× SSC and twice for 30 s in H2O, slides were dried and placed into hybridization cassettes (TeleChem International, Sunnyvale, Calif.). cDNA samples were resuspended in 10 mM EDTA, denatured for 5 min at 95 °C, mixed with 40 µl of SlideHyb buffer 1 (Ambion) and loaded under a coverslip onto the array slide. Each array slide was loaded with a pair of alternately Cy-dye coupled cDNA samples from the Sakai and Spinach strains. Dye-swap hybridizations were performed (e.g. Cy3-Sakai and Cy5-Spinach, and vice-versa) to account for dye incorporation bias. In total, 10 hybridizations, corresponding to 5 independent RNA extractions from each Sakai and Spinach strains, were carried out. After 18 h of hybridization at 47 °C, arrays were washed in 2× SSC, 0.5% SDS at 37 °C for 5 min, then twice for 5 min in 0.1× SSC, 0.1% SDS at 37 °C, and then twice for 2.5 min at room temperature 0.1× SSC. Microarrays were scanned with an Axon 4000B scanner (Molecular Devices, Sunnyvale, CA) and target intensities were retrieved with Genepix 6.0 software (Molecular Devices).

Analysis of microarray data. Microarray data were analyzed as described by Bergholz et al. (24). Lowess normalization (248) was applied to raw intensity values (median pixel intensities) for all probes on each array, using

the MAANOVA (version 0.98-8) package (249) in R software (version 2.2.1) (312). As all probes were printed in duplicate, signal intensities from probes were averaged prior to $\log_2$ transformation. Log transformed data were fitted to a mixed model ANOVA in R/MAANOVA ($y_{intensity}$ = Array + Dye + Strain + Sample (Sample = biological replicate)), which identifies fixed (Dye, Strain) and random (Array, Sample) sources of variation that influence microarray measurements of gene expression (63, 175). Differential expression of genes between Sakai and Spinach strains was determined with the Fs test, which does not assume equal variance between genes (64), using 1000 random permutations to generate p values. P values were corrected for multiple comparisons using the Benjamini-Hochberg step-up linear correction included in R/MAANOVA. Differences in gene expression with an adjusted p value < 0.05 were considered significant.

cDNA synthesis for quantitative real-time PCR (qRT-PCR). RNA was isolated from Sakai and Spinach strains following three independent replications of the host-pathogen challenge experiment, as described in Microarray experiments and RNA extraction. Reverse transcription of RNA was carried out using the iScript Select cDNA synthesis kit (BioRad, Hercules, Calif.) with the following protocol: 5 µl of RNA (200 ng/ul) was mixed with 2 µl of random primer (BioRad) and 8 µl of RNase-free water (BioRad), incubated for 5 min at 65 °C and chilled for 2 min on ice. Four microliters of reaction buffer (BioRad) and 1 µl of reverse transcriptase (BioRad) were added to the reaction mix, and reverse transcription was allowed to proceed in a thermal cycler (Applied Biosystems) at 42 °C for 30 min, and then at 85 °C for 5 min .

Validation of microarray data with qRT-PCR. Gene-specific oligonucleotide primer pairs were designed based on the published reference genome sequence of E.coli O157:H7 Sakai using the Primer3Plus free software (324), and synthesized commercially (Integrated DNA Technologies, Coralville, IA). Primer pairs were tested using Sakai and Spinach DNA, in a PCR across a 10 °C gradient of annealing temperatures to determine which temperature is optimal for amplification. Primer sequences and annealing temperatures are given in Table 3.1. The primers for the stx2B gene were specifically designed to discriminate between Stx2 and Stx2c variants of the B subunit gene. The forward primer is not specific whereas the reverse primer anneals to 103-120 bp downstream of the first nucleotide of the stx2B gene sequence; this is the variable region of stx2B between Stx2 and Stx2c variants. qRT-PCR reactions were performed in 25 µl reaction volumes containing 12.5 µl of SYBR Green Mastermix (BioRad), 0.63 µl of each primer (10 mM), 9.24 µl water and 2 µl cDNA template. cDNA amplification was carried out in the iCycler IQ5™ Multicolor Real-Time Detection System (BioRad) with the following conditions: 3 min at 95 °C, followed by 40 cycles 10 sec at 95 °C then 20 sec at specific annealing temperature. qRT-PCR reactions were performed with cDNA populations from 3 independent RNA extractions, from each O157:H7 strain, and each cDNA sample was tested in quadruplicate, across five-fold serial dilutions (1× to 0.008×). Relative expression of the 16S rRNA (rrsH) gene was used as an internal control for within-sample normalization of mRNA abundance (306).

Relative differences in transcript levels between Sakai and Spinach strains were determined with the Pfaffl method (244).

Table 3.1. Primer sequences and annealing temperatures used for qRT-PCR.

Primer	Sequence (5' to 3')	Annealing temperature
eae-F	GCCGGTAAAGCGACTGTTAG	55°C
eae-R	ATTAGGCAACTCGCCTCTGA	
tir-F	ACTTCCAGCCTTCGTTCAGA	57°C
tir-R	TTCTGGAACGCTTCTTTCGT	
espA-F	GCTGATGTTCAGAGTAGC	56°C
espA-R	ATCACCACTAAGATCACG	
espB-F	TCAGCATTGGGGATCTTAGG	57°C
espB-R	CTGCGACATCAGCAACACTT	
stx2A-F	TATATCAGTGCCCGGTGTGA	55°C
stx2A-R	TGACGACTGATTTGCATTCC	
stx2b-F	GAAGATGTTTATGGCGGT	55°C
stx2b-R	CACTGTAAATGTGTCATC	
flgE-F	CACGTTTAGCCTGAGCTTCC	60°C
flgE-R	CAACCGTACCGTCATCATTG	
cheB-F	CAAACCGCAACTGGGTATTC	60°C
cheB-R	CGACAATGGCTTATGTGCTG	

RESULTS

Interaction of O157:H7 with MAC-T cells. The fluorescent actin staining (FAS) test was carried out to ensure that MAC-T cells were an adequate epithelial cell line for mimicking EHEC O157:H7 interactions with the intestinal epithelium. Infection of MAC-T cells with both O157:H7 Spinach and Sakai strains induced marked cytoskeletal rearrangement, characterized by pedestals of filamentous actin emanating from MAC-T cells, which is typical of A/E lesions (Figure 3.2). Propidium iodide counter-staining of specimens allowed co-localization of actin pedestals and bacteria. The FAS test also indicated formation of densely packed bacterial micro-colonies on the surface of MAC-T cells, a colonization pattern known as localized adherence. A/E lesions were not observed on MAC-T cells following infection with E. coli K12.

Cell association assays were then used to quantify variation in the interaction of O157:H7 strains with epithelial cells. At the 30 min timepoint, no significant difference in association of Spinach and Sakai with MAC-T cells was detected ($p = 0.28$). At the 1 h timepoint, challenge of MAC-T cells with Spinach resulted in a significantly higher degree of association compared to Sakai ($p = 0.02$). Additionally, cell counts (CFU/ml) after 1 h of infection were 2.47 ± 0.27 fold higher in Spinach compared to Sakai (Figure 3.3). Since the growth rates of bacterial cultures were similar (Figure 3.1) and the CFU/ml of the starting O157:H7 inocula varied by less than 10%, differences in association counts were not merely a reflection of variation in growth phase or starting cell densities among O157:H7 strains.

Microarray expression profiling. Increased association of the O157:H7 Spinach strain with epithelial cells, compared to Sakai, implied that there is a difference in the expression of LEE, and potentially of other genes involved in O157:H7 pathogenesis, between the two outbreak strains. Since the expression of LEE genes in EHEC O157:H7 was previously shown to be downregulated following tight attachment to epithelial cells (23), we sought to compare transcriptomes of Spinach and Sakai prior to intimate adherence to MAC-T cells. Therefore, O157:H7 Spinach and Sakai were exposed to MAC-T monolayers for 30 min, and differences in gene expression were measured between non-adherent, planktonic, populations of Spinach and Sakai, using whole-genome microarrays. Transcriptional profiling at earlier timepoints was not justified, as differences in association between Spinach and Sakai were not significant at 30 min post-infection of MAC-T cells.

The Fs test found 914 genes to be significantly differentially expressed between Spinach and Sakai (adj. p value < 0.05), 41 of which were encoded on the pO157 plasmid (Figure 3.4). In the Spinach strain, 440 genes were downregulated, and 475 were upregulated, relative to Sakai. Of the 914 significant genes, 388 encode hypothetical proteins of unknown function. Relative differences in gene expression greater than 1.5 fold were detected in 206 of the 914 genes, 98 of which encode hypothetical proteins.

Differential expression of adhesion and motility associated genes. Of major interest were the expression ratios of 41 LEE genes, 36 of which were

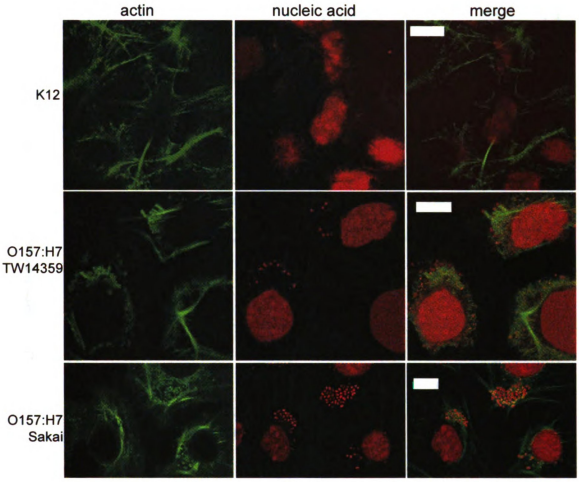

Figure 3.2. Fluorescence micrographs of MAC-T cells infected with E. coli K12, O157:H7 Spinach, and O157:H7 Sakai. Filamentous actin was stained green (Alexa Fluor 488), nucleid acid was stained red (propidium iodide). Merging the green and red fluorescence demonstrated co-localization of actin pedestals and bacteria. White scale bars in right column represent 10 um. Magnification, 63× with 2.7× scan zoom for K12 and Spinach, and 1.8× for Sakai.

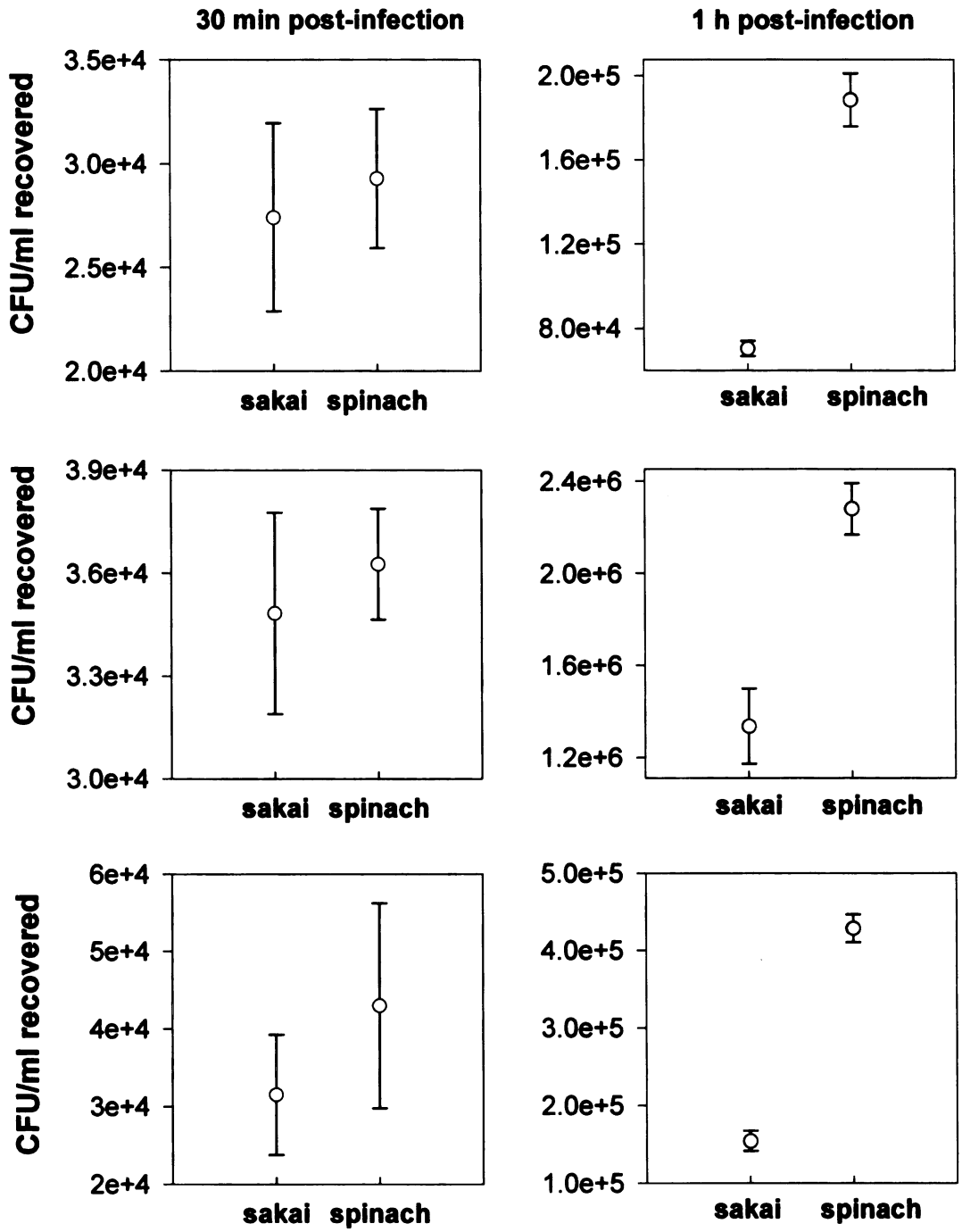

Figure 3.3. Association of O157:H7 Sakai and Spinach with MAC-T cells. Error bars indicate standard deviation of the average number of CFU/ml recovered from 4 wells. Each plot represents an independent experiment.

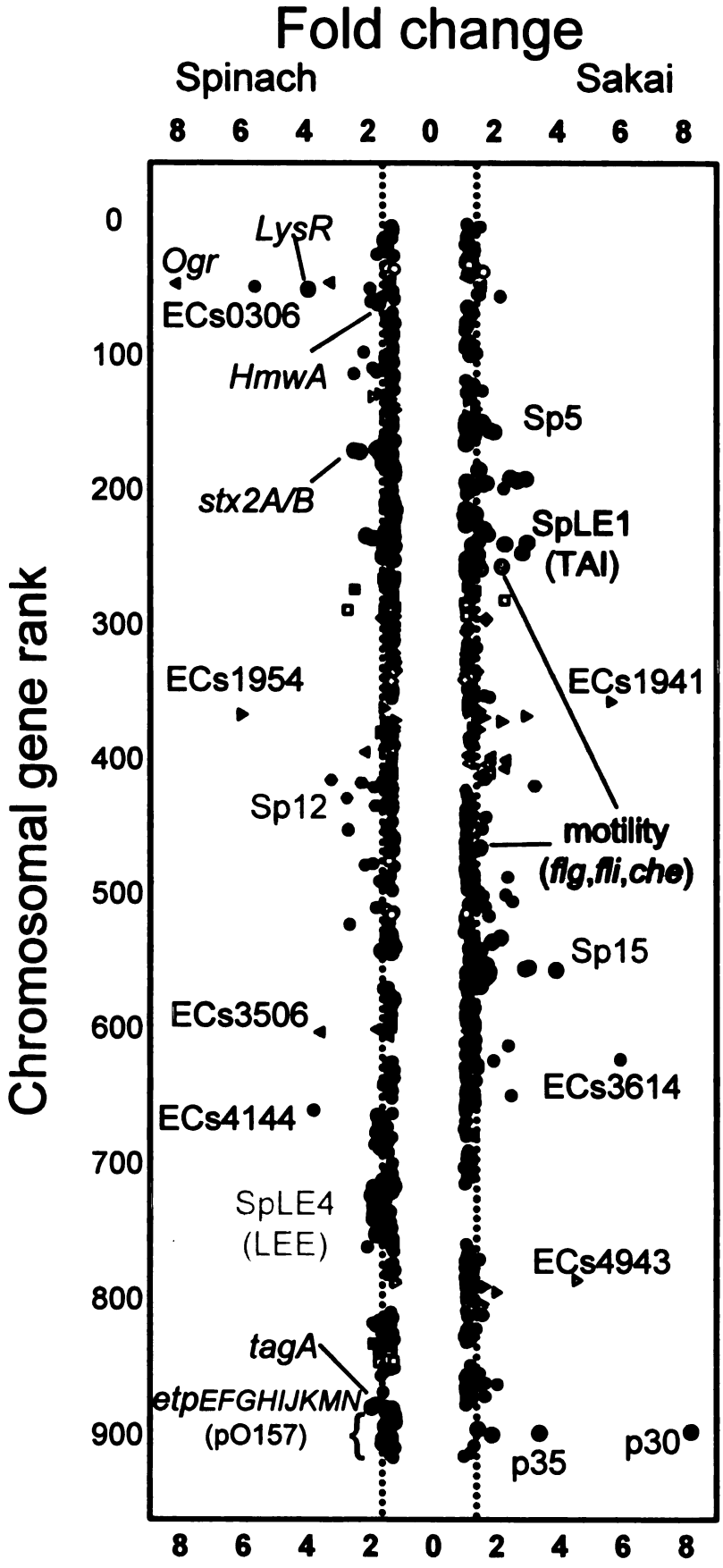

Figure 3.4. Significant differential expression of 914 genes between Spinach and Sakai. Genes were sorted according to chromosomal position (y axis) and differences in fold change are plotted on the x axis. The dotted line indicates a fold change of 1.5. Genes located on the same element (prophage, plasmid or backbone chromosome) are depicted by the same color or symbol. Annotations: ECs – O157:H7 Sakai gene number, Sp – Sakai prophage, SpLE – Sakai prophage like element, pO157 – plasmid genes.

upregulated in the Spinach strain (adj. p value < 0.05) (Table 3.2), including the positive regulators ler and grlA. LEE genes were almost uniformly upregulated from the LEE1 to the LEE4 operon (Figure 3.5), which encodes the EspADB needle complex that inserts into the host cell and allows translocation of effector proteins. The 5 LEE genes that did not have significantly elevated transcript levels in Spinach were escT and escU that encode inner membrane-bound constituents of the TTSS export structure, the negative LEE regulator grlR, and two genes of unknown function, orf1 and rorf3. Significant differences in gene expression ratios were validated for 5 LEE gene targets, with qRT-PCR (Table 3.5).

Together with the 7 LEE-encoded effector proteins (Tir, Map, EspF, EspG, EspH, EspB, and SepZ), the TTSS serves to export another 40 non-LEE encoded effectors (317). Genes coding for 24 of these effectors were found to differ in their expression between Spinach and Sakai. Specifically, 16 non-LEE effector genes were found to be upregulated in Spinach while 8 were upregulated in Sakai (Table 3.3).

Several genes relevant to adhesion, not associated with the TTSS, were found to be significantly differentially expressed (adj. p value < 0.05) (Table 3.2). The pO157 borne type II secretion system, encoded by the etpC-O polycistron, is represented by 12 probes on the microarray, 9 of which (etpEFGHIJKMN) indicated upregulation in the Spinach strain. The type II apparatus secretes several factors that influence colonization (270). The transcription of one such gene, *stcE/tagA*, which encodes a StcE metalloprotease that contributes to

Table 3.2. Significant differences in expression of LEE and other adhesion associated genes between Spinach and Sakai.

ECs #[a]	*gene*	function[b]	fold change[c]
ECs4550	*espF*	effector	1.60
ECs4551	*orf29*	unknown	1.23
ECs4552	*escF*	needle protein	1.70
ECs4553	*cesD2*	chaperone for EspD	1.73
ECs4554	*espB*	effector/translocator	1.83
ECs4555	*espD*	translocator	1.70
ECs4556	*espA*	translocator	1.70
ECs4557	*sepL*	TTSS	1.44
ECs4558	*escD*	TTSS	1.65
ECs4559	*eae*	intimin adherence protein	1.72
ECs4560	*cesT*	chaperone for Tir	1.64
ECs4561	*tir*	translocated intimin receptor	1.76
ECs4562	*map*	effector	1.54
ECs4563	*cesF*	chaperone for EspF	1.61
ECs4564	*espH*	effector	1.59
ECs4565	*sepQ*	TTSS	1.65
ECs4566	*orf16*	unknown	1.32
ECs4567	*orf15*	unknown	1.75
ECs4568	*escN*	TTSS	1.47
ECs4569	*escV*	TTSS	1.58

Table 3.2. continued

ECs #[a]	*gene*	function[b]	fold change[c]
ECs4570	*orf12*	unknown	1.55
ECs4571	*sepZ*	effector	1.77
ECs4572	*rorf8*	Unknown	1.72
ECs4573	*escJ*	TTSS	1.42
ECs4574	*sepD*	TTSS	1.31
ECs4575	*escC*	TTSS	1.41
ECs4576	*cesD*	chaperone for EspD	1.36
ECs4577	*grlA*	regulator, positive	1.42
ECs4582	*escS*	TTSS	1.28
ECs4583	*escR*	TTSS	1.35
ECs4584	*orf5(escL)*	binds to escN	1.50
ECs4585	*orf4*	unknown	1.51
ECs4586	*orf3*	unknown	1.69
ECs4587	*cesAB*	chaperone for EspA and EspB	1.68
ECs4588	*ler*	regulator, positive	1.48
ECs4590	*espG*	destruction of microtubules	1.38
pO157	*stcE/tagA*	StcE metalloprotease	1.83
ECs1772	*adfO*	putative colonization factor	1.22
pO157	*etpE*	type 2 secretion	1.20
pO157	*etpF*	type 2 secretion	1.20
pO157	*etpG*	type 2 secretion	1.19

Table 3.2. continued

ECs #[a]	*gene*	function[b]	fold change[c]
pO157	*etpH*	type 2 secretion	1.20
pO157	*etpI*	type 2 secretion	1.21
pO157	*etpJ*	type 2 secretion	1.14
pO157	*etpK*	type 2 secretion	1.15
pO157	*etpM*	type 2 secretion	1.14
pO157	*etpN*	type 2 secretion	1.17

a – ECs, O157:H7 Sakai chromosomal gene numbers, numbers ECs4550 through ECs4590 denote LEE genes; pO157, plasmid encoded genes.
b – LEE protein functions adopted from (65, 115, 235).
c – positive values were found to be upregulated in the Spinach strain; adj. p value < 0.05.

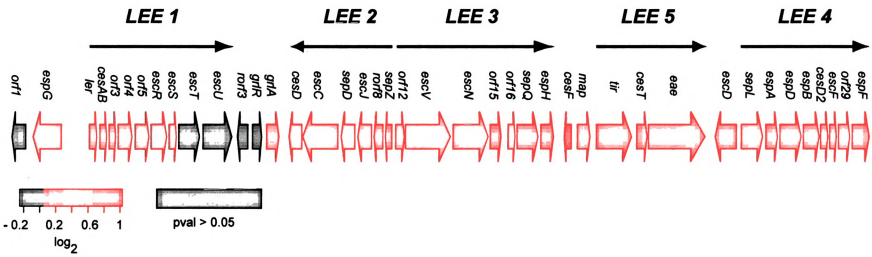

Figure 3.5. Heatmap of expression ratios of LEE genes between Spinach and Sakai. The heatmap was generated based on log_2 expression ratios of Spinach:Sakai, and imposed on a graphic representation of the genetic organization of the LEE island, adopted from (293).

intimate adherence (124), was elevated in the Spinach strain. Expression of adfO (ECs1772), which encodes another type II secretion substrate that was recently demonstrated to promote adherence of O157:H7 to epithelial cells (145), was also elevated in Spinach. Overall, these results indicate that the transcription of major and accessory colonization factors, preceding intimate adherence of O157:H7 to MAC-T epithelial cells, is higher in the O157:H7 Spinach strain relative to Sakai. This result is consistent with the increased ability of Spinach to associate with MAC-T cells.

An unexpected result was the significant increase in expression of genes related to motility in O157:H7 Sakai. Fourteen genes that mediate flagellar biosynthesis (flgCDEFGK, fliCDHL, and fhiA) and chemotaxis (cheB, tsr, and tar) were upregulated in the Sakai strain (Table 3.4). Relative expression differences were confirmed by qRT-PCR for 2 representative genes, flgE and cheB (Table 3.5).

Upregulation of Shiga toxin 2 in the O157:H7 Spinach strain. The Sakai strain is lysogenized with Stx1 and Stx2-converting phages (215), while the Spinach strain harbors Stx2 and Stx2c variants (205); the microarray used in this study contains probes for stxA and stxB subunits of Shiga toxin 1 and 2 genes, but not for the Shiga toxin 2c variant. As expected, the expression of genes encoding Shiga toxin 1, stx1a and stx1b, were found to be increased in Sakai by 36.4-fold and 29.7-fold, respectively. The transcription of Shiga toxin 2, which is shared by both strains, was increased in the Spinach strain, relative to Sakai, by 1.70-fold and 2.4-fold for stx2a and stx2b respectively; this result was

Table 3.3. Significant differential expression of non-LEE effector genes.

ECs #	effector [a]	fold change[b]
ECs0472	EspY3	-1.35
ECs1127	EspV'	1.45
ECs1567	EspO1-1	1.18
ECs1810/1	NleG2-1'	-1.26
ECs1812	NleA	-1.30
ECs1814	NleH1-2	1.30
ECs1824	NleG	1.23
ECs1994	NleG2-2	1.59
ECs1996	NleG5-1	1.46
ECs2154	NleG5-2	1.33
ECs2155	NleG6-2	1.36
ECs2156	NleG2-3	1.43
ECs2226	NleG7'	1.26
ECs2228	NleG3'	3.13
ECs2229	NleG2-4'	1.51
ECs2714	EspJ	-1.34
ECs2715	TccP	-1.40
ECs3485	EspM2	-1.48
ECs3487	EspW	1.20
ECs4642/3	EspL3'	1.17
ECs4653	EspY4	1.20

Table 3.3. continued

ECs #	effector[a]	fold change[b]
ECs4657	EspY5'	-1.25
ECs5048	EspX5	-1.20
ECs5295	EspX6	1.46

a – nomenclature adopted from (317).
b – positive values were found to be upregulated in the Spinach strain, negative values indicate upregulation in the Sakai strain; adj. *p* value < 0.05.

Table 3.4. Upregulation of flagellar genes in Sakai relative to Spinach.

ECs #	gene	function	fold change[a]
ECs0256	fhiA	flagellar, putative motility protein	1.13
ECs1452	flgC	flagellar, cell-proximal portion of basal-body rod	1.51
ECs1453	flgD	flagellar, initiation of hook assembly	1.16
ECs1454	flgE	flagellar, hook protein	2.27
ECs1455	flgF	flagellar, cell-proximal portion of basal-body rod	1.31
ECs1456	flgG	flagellar, cell-distal portion of basal-body rod	1.60
ECs1460	flgK	flagellar, hook-filament junction protein 1	1.15
ECs2662	fliC	flagellar; flagellin, filament structural protein	1.23
ECs2663	fliD	flagellar, capping protein for filament assembly	1.15
ECs2683	fliL	flagellar biosynthesis	1.32
ECs2679	fliH	flagellar, export of flagellar proteins	1.19
ECs2593	cheB	response regulator for chemotaxis (cheA sensor)	1.58
ECs2596	tar	methyl-accepting chemotaxis protein II	1.18
ECs5315	tsr	methyl-accepting chemotaxis protein I	1.74

a – positive values indicate upregulation in Sakai, adj. p value < 0.05.

Table 3.5. qRT-PCR validation of microarray data.

gene	fold change[a] Spinach : Sakai	E[b]
eae	1.94 ± 0.2	1.93
tir	2.08 ± 0.6	2.21
espA	2.13 ± 0.3	2.10
espB	2.04 ± 0.6	2.01
sepZ	1.80 ± 0.3	2.02
stx2A	4.86 ± 1.4	2.06
stx2B	4.3 ± 0.2	2.08
flgE	-8.33 ± 1.8	2.00
cheB	-3.41 ± 0.5	2.02

a – mean ± standard deviation of relative fold change differences in expression between Spinach and Sakai strains; negative sign indicates increased expression in Sakai.
b – average qRT-PCR reaction efficiency of both strains.

confirmed by qRT-PCR (Table 3.5). Interestingly, the q antiterminator (ECs1203) of stx2 was also found to be statistically significantly upregulated in the Spinach strain (1.27-fold). The phage borne q antiterminator, located upstream of stx2, is critical for antitermination of stx transcription that initiates at the pR' late promoter site (332). Given the significance of Stx2 in the development of HUS and the high frequency of this sequelae during the O157:H7 spinach outbreak, our results suggest that, in addition to an increased capacity to colonize the epithelium, the hyper-virulence of the Spinach strain is mediated, at least in part, by overexpression of this key EHEC cytotoxin.

DISCUSSION

The unprecedented increase in disease severity of the 2006 USA EHEC O157:H7 spinach outbreak has led us to examine the virulence properties of the Spinach strain and compare them to those of O157:H7 Sakai. Although O157:H7 Sakai is responsible for the largest outbreak of O157:H7 infection, this strain is associated with a low HUS frequency. The findings of this study indicate that during infection of epithelial cells, the Spinach strain is characterized by elevated levels of cell association, compared to Sakai, which was preceded by an increase in transcription of virulence determinants,.

It is well known that tight attachment of O157:H7 to epithelial cells occurs through binding of the adhesin intimin with the translocated intimin receptor Tir (115). This triggers actin rearrangements and the formation of pedestal structures, representative of A/E lesions. In this study, both O157:H7 strains showed similar localized adherence patterns as visualized by the FAS reaction, confirming that colonization of MAC-T cells is mediated through the intimin-Tir interaction. Similar observations have been made regarding the interaction of other O157:H7 strains with MAC-T cells (207), as well as several primary bovine epithelial cell lines (75). However, quantification of the interaction with MAC-T cells indicated that the Spinach strain associates with epithelial cells in significantly greater numbers, within 1 h post-challenge. Colonization of the host is a key initial step in the infection process, therefore early colonization of the epithelium is likely to increase the ability of the Spinach strain to repel clearance by host defenses and competitive exclusion by indigenous microbiota.

Transcriptional profiling was carried out under in vitro conditions that mimic the intestinal environment, including contact with epithelial cells (23) and physiologic bicarbonate ion availability (10), as these conditions are considered optimal for LEE expression. Also, gene expression was examined in bacteria that have not yet intimately adhered to epithelial cells, because this is the time when relevant virulence factors would be expected to be expressed. In support of the MAC-T association findings, transcription ratios of the LEE island indicate that the Spinach strain responds more efficiently to the presence of epithelial cells by overexpression of its key colonization factor, relative to Sakai.

Regulation of the LEE is complex, and is influenced by multiple environmental factors that act on several chromosomal regulators. In turn, these global regulators fine tune LEE expression through LEE-encoded regulators, Ler, GrlA, and GrlR (73, 289). Activation of Ler, the major LEE regulator, leads to induction of operons lee2, lee3, lee5, and lee4 (19, 130); however, GrlA can activate expression from lee2 and lee4 independently of Ler (265), and can stimulate Ler as well (73). Functional studies have shown that the promoter for the lee4 operon, which encodes the EspADB translocon, is also activated upon bacterial contact with the eukaryotic cell (23), further supporting the argument that its upregulation in the Spinach strain results in an enhanced interaction with the host cell compared to Sakai.

Non-LEE effectors were previously suggested to antagonize host immune defenses, including inhibition of host phagocytosis (55) and suppression of proinflammatory cytokine production (135). Additionally, the expression of

several of these factors was shown to be under the influence of the GrlA regulator (73, 289). Although the contribution of non-LEE effectors, which were differentially expressed in this study, to the pathogenesis of O157:H7 is not clear, their possible role in virulence warrants further investigation.

Increased adherence of the Spinach strain may have also been facilitated by upregulation of the type II secretion machinery. Mutation of etpC, the first gene in the etp operon, has been shown to result in a significant reduction of O157:H7 colonization in an infant rabbit model of disease (145). Two known effectors of type II secretion that are suggested to contribute to adherence, StcE (124), and AdfO (145), were upregulated in the Spinach strain. The StcE protease, the expression of which is positively influenced by Ler (194), is hypothesized to promote adherence by cleaving proteins in the glycocalyx and mucin layers atop the intestinal epithelium, allowing O157:H7 to come into close contact with the intestinal mucosa (124). The contribution of AdfO to adherence is not clear, as its mutation markedly decreases O157:H7 adherence to epithelial cells, in vitro, but it does not attenuate colonization following oral challenge of infant rabbits (145).

In Sakai, conversely, microarray measurements revealed the upregulation of motility genes of the flg and fli operons involved in flagellar biosynthesis, and of genes that encode chemotaxis proteins. In both enteropathogenic E. coli (EPEC) O127:H6 (118) and *Salmonella enteritidis* (12, 74), flagella were demonstrated to be important for initial contact with host cells. EPEC O127:H6 bacteria are flagellated in the early stages of adherence to epithelial cells, but

flagella are retracted after pedestal formation and intimate attachment of bacteria (343). Recently, Iyoda et al. have shown that GrlA inhibits cell motility by repressing flagellar gene expression in O157:H7 (152). Our finding of upregulation of grlA and LEE genes in Spinach, with concurrent downregulation of flagellar genes, is consistent with the study by Iyoda et al. Strict regulation of flagella and the TTSS is necessary for synchronized expression of motility and attachment; as simultaneous expression of both flagella and the TTSS might hinder efficient adhesion, and is energetically expensive. However, the reasons for discrepant expression of LEE and flagella between Spinach and Sakai cannot be explained by the transcriptional snapshot of O157:H7 described in this study. A time course investigation of gene expression could clarify whether this difference is merely a consequence of intrinsic overexpression of LEE in O157:H7 Spinach, or if there is a temporal lag characterized by an unsynchronized switch from flagellar to LEE expression between the two strains.

Shiga toxin is a key virulence factor of EHEC and can solely trigger HUS, which is evident from the fact that LEE-negative Shiga toxin-producing E. coli also cause HUS (129, 239). Stx2 has been associated with severe disease more frequently than Stx 1 (36, 91), and toxicity studies with mice have shown that Stx2 is 400 times more lethal than Stx1 (313). Therefore, an over 4-fold increase in Stx2 expression by the Spinach strain compared to Sakai, as detected by qRT-PCR, suggests that Stx 2 may be an important contributor to the increased frequency of severe disease in the 2006 spinach-associated outbreak of O157:H7.

CONLUSIONS

The results of this study support the hypothesis that the O157:H7 Spinach strain is characterized by higher pathogenic potential relative to O157:H7 Sakai. Increased ability of the O157:H7 Spinach strain to colonize the epithelium and express Shiga toxin indicates the capacity of this strain to mediate more fulminant disease. Thus, some of the basis for the striking increase in clinical burden of the 2006 outbreak of O157:H7 may be attributable to the hypervirulence of the Spinach strain. Intrinsic variation in the pathogenic potential of O157:H7 strains has been described before. A previous study of O157:H7 pathogenesis in germ-free mice, using several O157:H7 clinical strains, also indicated an increased ability of the Spinach strain to cause severe disease compared to Sakai (86). Furthermore, the variation in virulence of O157:H7 was recently correlated with the existence of distinct genetic lineages within the O157:H7 population (205). This study classified O157:H7 Sakai and Spinach strains into distinct lineages that dramatically differ in epidemiological characteristics. Functional genomic studies of a larger sample size will likely reveal that the variation in the pathogenicity of O157:H7 strains results from lineage-specific differences in the regulation of shared virulence genes.

ACKNOWLEDGMENTS

The authors thank Teresa Bergholz, James Riordan, Sivapriaya Kailasan Vanaja, Shannon Manning, Linda Mansfield, and Martha Mulks for critically reviewing earlier versions of the manuscript; and James Riordan for designing *stx2B* specific primers. This project was funded by the NIAID, NIH, DHHS, under NIH research contract N01-AI-30058 (TSW), which supports the STEC Center. This study will be submitted to the journal of BMC Microbiology.

CHAPTER 4

Hypervirulence of the Enterohemorrhagic *Escherichia coli* O157:H7 Clade 8 Subpopulation

SUMMARY

Outbreaks of enterohemorrhagic *Escherichia coli* O157:H7 infections are characterized by dramatic variation in severity of disease, ranging from diarrhea to hemorrhagic colitis and the multifactorial disorder termed hemolytic uremic syndrome. Phylogenetic analysis of clinical O157:H7 strains has correlated the variation in outbreak severity with the existence of genetically distinct lineages (clades 1-9) within O157:H7, of which clade 8 is indicated to be hyper-virulent. Using epithelial cell assays, we have quantified the association/invasion ability of 24 O157:H7 strains, from clade 8 and clade 2, and have examined whole-genome expression profiles of the 24 strains, following their exposure to epithelial cells. Adherence of 12 clade 8 strains with epithelial cells was found to be 2.3 ± 0.2 fold higher compared to 12 clade 2 strains. Transcriptional profiling, using multi-genome *E. coli* microarrays, detected significant differential expression in 604 genes, 186 of which had an increase in fold change > 1.5. Expression of major virulence factors, including the LEE island, Shiga toxin 2, and of several putative virulence factors was increased in clade 8 relative to clade 2. Differential expression of 3 regulators, *rpoS*, *grlA*, and *gadX*, is consistent with the upregulation of LEE in clade 8. Expression ratios of 13 virulence genes and 3 regulator genes were confirmed by qRT-PCR. Altogether, our data point to an increased pathogenic potential in the O157:H7 clade 8 subpopulation, in support of the hypothesis that this lineage of O157:H7 is hyper-virulent.

INTRODUCTION

Enterohemorrhagic *Escherichia coli* (EHEC) O157:H7 is the most prevalent EHEC serotype associated with outbreaks of food and waterborne disease in the US (212, 250). Clinical manifestations of O157:H7 infection include diarrhea, hemorrhagic colitis and the often fatal hemolytic uremic syndrome (HUS). Colonization of the intestinal mucosa via attaching and effacing (A/E) lesions, which are mediated by the type three secretion system (TTSS) encoded on the laterally acquired locus of enterocyte effacement (LEE), and destruction of the capillary wall due to secretion of phage borne Shiga toxins (Stx1, 2 and variants) are hallmarks of EHEC pathogenesis (164).

Interestingly, outbreaks of O157:H7 infection show remarkable variation in disease severity and HUS frequency (6, 211, 257, 305). Recently, epidemiological analysis of O157:H7 outbreaks and assessment of the genomic diversity of > 500 O157:H7 clinical strains, by means of single nucleotide polymorphism (SNP) genotyping of 96 loci, has correlated the discrepancy in the clinical burden of outbreaks with the existence of genetically distinct lineages (clades 1-9) within O157:H7 (205). The clade 8 subpopulation of O157:H7 strains was shown to have been associated with HUS at significantly higher rates compared to all other clades combined. Although the variation in virulence among strains of O157:H7 has been previously hypothesized to be attributable to different combinations of Stx genes (36, 156, 243), strains that belong to clade 8 do not possess a uniform Stx genotype. Furthermore, clade 2, which is also associated with severe sequelae, can either have a different complement of Stx

converting phages compared to clade 8, or share the same Stx2 variant (205). We have previously shown that O157:H7 outbreak strains differ in their capacity to colonize the epithelium and express virulence genes (Chapter 3), and in their ability to cause severe disease in germ-free mice (86). However, the variation in pathogenic potential among O157:H7 strains has not been investigated in the context of the SNP-inferred O157:H7 clade phylogeny. It is, therefore, necessary to determine the extent to which the outcome of O157:H7 infection is associated with intrinsic differences between O157:H7 clade subpopulations, other than variation of Stx type.

In this study, global gene expression patterns from 24 clinical clade 8 and clade 2 strains, which possess either identical or different Stx genes, exposed to MAC-T epithelial cells were analyzed. In addition, we assessed the ability of these strains to colonize the epithelium, *in vitro*. The results reveal a clade 8-specific upregulation of determinants that are central to EHEC pathogenesis as well as of ancillary virulence genes, under conditions that mimic the host-pathogen interaction. The superior virulence gene expression profile of clade 8 was complemented with the finding that clade 8 strains possess a significantly higher ability to adhere to epithelial cells, compared to clade 2. Altogether, the findings of this study support the hypothesis that the O157:H7 clade 8 subpopulation is hyper-virulent. Furthermore, our results shed light on the theme of alternative regulation of shared, horizontally acquired elements among distinct lineages of O157:H7, and highlight the importance of studying bacterial pathogenesis in a phylogenetic context.

MATERIALS AND METHODS

Bacterial strains and culture conditions. From a formerly characterized set of 528 clinically relevant EHEC O157:H7 strains (205), 24 were selected to equally represent clades 8 and 2, with an even distribution of respective Stx phages: 6 strains from clade 2 with Stx1 and 6 with Stx1, 2, and likewise, 6 strains from clade 8 with Stx2 and 6 with Stx2, 2c (Table 4.1). In addition, EHEC O157:H7 RIMD 0509952 (Sakai) (136) was used as a common denominator for MAC-T cell association and invasion assays. Upon revival of freezer stocks in LB broth (OD_{600} ~ 0.1 – 0.15), bacteria were physiologically normalized by growth to stationary phase, in morpholino-propanesulfonic acid (MOPS) buffered minimal media (223), containing 0.1 % glucose, pH 7.4; bacteria were grown in MOPS media twice as described in Chapter 3. Preceding exposure to MAC-T epithelial cells, for all experiments, bacteria were grown in Dulbecco's Modified Eagle's Medium (DMEM) (pH 7.4, without phenol-red, 0.45% glucose, 0.37% $NaHCO_3$) (Sigma, St. Louis MO) for 3 h. After 3 h of growth in DMEM, bacterial cell densities were $(5 \pm 1) \times 10^8$ colony forming units (CFU)/ml, based on enumeration of culture samples that were plated on LB agar media; the pH of DMEM bacterial cultures ranged from 7.09 to 7.20. For flow cytometry analysis of association/invasion assays, bacteria were grown in DMEM for 2.5 h. As bacteria multiply during fluorescent labeling, growing them for 2.5 h prior to labeling, instead of 3 h, ensured the same O157:H7 cell densities for flow cytometry as for the association/invasion and microarray experiments.

Table 4.1. Clade assignment and Stx profiles of O157:H7 strains used.

Strain	Clade[a]	*stx*[a]	Locale[b]	Date[c]	Clinical[d]	Source[e]
EK15	2	*1,2*	USA (WA)	6/2002	D	Tarr, P.
F6854	2	*1,2*	USA (PA)	7/2004	no data	Smole, S.
93111	2	*1,2*	USA (WA)	6/1993	D	Tarr, P.
MLVA-47	2	*1,2*	USA (CT)	7/2004	D	Smole, S.
96M1006	2	*1,2*	Austr. (Qld.)	8/2005	BD	Murphy, D.
DA-35	2	*1,2*	USA (OH)	3/2000	no data	Acheson, D.
MI02-57	2	*2*	USA (MI)	6/2005	no data	MDCH
MI02-1	2	*2*	USA (MI)	6/2005	no data	MDCH
05EN000757	2	*2*	USA (MI)	6/2005	no data	MDCH
MI02-68	2	*2*	USA (MI)	6/2005	no data	MDCH
MI04-43	2	*2*	USA (MI)	6/2005	no data	MDCH
MI01-29	2	*2*	USA (MI)	7/2005	no data	MDCH
MI06-63*	8	*2,2c*	USA (MI)	9/2006	no data	MDCH
E32511/O	8	*2,2c*	no data	6/1991	HUS	Cravioto, A.
EK27	8	*2,2c*	USA (WA)	6/2002	HUS	Tarr, P.
1:361	8	*2,2c*	USA (MI)	12/1997	D	Acheson, D.
MT#9	8	*2,2c*	USA(MT)	9/2000	no data	Tarr, P.
MI03-72	8	*2,2c*	USA (MI)	1/2004	no data	MDCH
MI02-55	8	*2*	USA (MI)	6/2005	no data	MDCH
EK1	8	*2*	USA (WA)	6/2002	D	Tarr, P.
EK2	8	*2*	USA (WA)	6/2002	D	Tarr, P.
DA-11	8	*2*	USA (MA)	3/2000	BD	Acheson, D.
MI03-35	8	*2*	USA (MI)	10/2003	no data	MDCH

Table 4.1. continued.

Strain	Clade[a]	*stx*[a]	Locale[b]	Date[c]	Clinical[d]	Source[e]
MI06-31	8	*2*	USA (MI)	7/2006	HUS	MDCH
Sakai	1	*1,2*	Japan			

* – O157:H7 TW14359 (Spinach) strain implicated in the 2006 spinach outbreak (205).

a – Clade assignment and *stx* gene profiles are based on the work of Manning *et al.* (205).

b – location of isolation.

c – date that O157:H7 isolate was deposited in the STEC Reference Center, Michigan State University.

d – D, diarrhea; BD, bloody diarrhea; HUS, hemolytic uremic syndrome

e – contributors of strains; MDCH, Michigan Department of Community Health – these strains were donated by Manning, S.

Association and invasion assays. Bovine mammary epithelial cells (MAC-T) (151) were maintained at 37 °C with 5% CO_2, using DMEM supplemented with 10% heat-inactivated fetal bovine serum (FBS) (Sigma, St. Louis MO). The ability of O157:H7 strains Spinach (clade 8) and 93111 (clade 2) to induce A/E lesions on MAC-T were observed using a modification of the fluorescent actin staining (FAS) method described by Shariff *et al.* (282); for a detailed protocol see Materials and Methods in Chapter 3. For the association assay, approximately 10^6 MAC-T cells/well were seeded into a 24-well plate (Corning Inc., Lowell MA) and maintained overnight in DMEM (2% FBS). The following day, MAC-T monolayers were washed with fresh DMEM and each well was inoculated with 1 ml of bacterial culture grown in DMEM, at a multiplicity of infection (MOI), ratio of bacteria to host cell, of 500:1. After 1 h of incubation at 37 °C with 5% CO_2, wells were washed with excess PBS and MAC-T cells were lysed with 0.1 % Triton X-100 (Sigma-Aldrich, St. Louis MO) for 30 minutes. Serially diluted lysates were plated on LB agar with the Autoplate 4000 Spiral Plater (Spiral Biotech, Bethesda, MD) and enumerated following overnight incubation at 37 °C, using the Q-Count instrument (Spiral Biotech). Each O157:H7 strain was assayed in triplicate and the experiment was repeated 3 times. In each assay, O157:H7 Sakai (clade 1) was used as a control and served as a common denominator to which other strains were compared. The mean CFU/ml of each strain recovered from three wells of a biological replicate was normalized against the mean CFU/ml of Sakai recovered from three wells of the corresponding biological replicate. Normalized data were analyzed with a

mixed ANOVA model, relative association = strain + replicate (strain) + error, where biological replicate was nested within the strain effect. Analysis was conducted using proc mixed in SAS version 9.1. Differences in association, the combination of adhesion and invasion (75), between clades was expressed as the mean ± standard error of clade 8 relative to clade 2. For invasion assays, following 1 h of incubation of O157:H7 with MAC-T, wells were washed with PBS and inoculated with fresh DMEM containing 200 µg/ml of gentamicin to kill extracellular bacteria. After 2 h of additional incubation at 37 °C with 5% CO_2, bacteria were enumerated as described above. Invasion assays were performed with 6 clade 8 and 6 clade 2 strains that yielded the highest association levels with MAC-T, and analyzed as described above.

Flow cytometry. Association assays using strains from clade 8 (n = 6) and from clade 2 (n = 6) that demonstrated the highest association levels with MAC-T cells, as determined by plate counting, were repeated and quantified using flow cytometry; the data from clade 8 and 2 strains were expressed relative to that of O157:H7 Sakai (clade 1). Bacteria were labeled using the Vybrant® CFDA SE Cell Tracer Kit (Invitrogen), following the manufacturer's recommendations. Briefly, 4 ml aliquots of O157:H7 culture in DMEM were centrifuged at 3200×*g*, 4 °C, for 10 min to pellet cells. The supernatants were decanted and pellets were suspended in 2 ml of fresh DMEM. Six microliters of 10 mM CFDA SE dye dissolved in dimethyl-sulfoxide was added to each suspended pellet, for a final dye concentration of 30 µM. Following 20 min of incubation in the dark at 37 °C, with gentle shaking, cultures were centrifuged at

3200×*g*, 4 °C, for 10 min to remove the excess dye. Pellets were resuspended in 4 ml of fresh DMEM and incubated for 30 min at 37 °C, with gentle shaking, to stabilize dye incorporation. After another step of centrifugation, pellets were suspended in 4 ml of fresh DMEM and used to infect MAC-T cells at a MOI of 500, as described above. After 1 h of incubation at 37 °C with 5% CO_2, MAC-T cells were washed twice with excess PBS and were detached from the wells by incubating with 0.5 ml of trypsin (Sigma) solution (50 mg trypsin and 1 ml of 62 mM EDTA in 99 ml of PBS) for 10 min. Trypsin was inhibited by addition of 0.5 ml of DMEM to each well and cell suspensions were centrifuged in polystyrene tubes (BD Biosciences, Bedford, MA) at 4 °C, 3200×*g* for 10 min. The supernatants were decanted, pellets were resuspended in 300 µl of flow cytometry staining buffer (PBS containing 0.1 % sodium-azide and 1 % FBS), and samples were analyzed with a FACS Vantage flow cytometer (BD Biosciences). From each sample, 15 000 viable MAC-T cells were analyzed after setting a live cell gate based on the forward and the side scatter profiles of uninfected MAC-T cells. Each strain was assayed in duplicate and the experiment was repeated twice. The mean fluorescence intensity (MFI) of test strain-infected MAC-T was normalized against the MFI of Sakai-infected MAC-T cells. The normalized MFI data were analyzed by the Student's *t*-test to determine statistically significant differences in association between clades.

MAC-T challenge experiments, microarray hybridization and analysis. Previously described oligo microarrays (24), which target 5978 genes from *E. coli* K12 MG1655 (35), O157:H7 Sakai (136) and O157:H7 EDL 933

(242), were upgraded with additional probes that detect expression of 100 ORFs from the Sakai pO157 plasmid. Three milliliters of individual O157:H7 cultures in DMEM were inoculated into 75 cm^2 tissue culture flasks containing confluent monolayers of MAC-T cells with 15 ml of DMEM. After a 30 minute incubation at 37 °C and 5% CO_2 with gentle rocking at 1.5 rpm on a rocking platform (VWR International, West Chester PA) to mimic gut peristalsis, 8 ml culture samples were taken from suspended, non-adherent O157:H7 populations and treated with 10% phenol:ethanol buffer to stabilize the RNA (31). Following centrifugation at 4500×*g* for 30 min, 4 °C, supernatants were decanted and cell pellets were suspended in 5 ml buffer (2 mM EDTA, 20 mM NaOAc, pH 5.2). RNA was extracted with hot phenol (pH 4.5, 65 °C) (Ambion, Austin TX) and purified using a RNeasy kit (Qiagen, Valencia CA). cDNA synthesis, dye-swap hybridization conditions and microarray scanning have been described (24). For the clade comparison, hybridizations were performed between 4 groups with 6 strains/group (Figure 4.1), where each strain was regarded as an independent biological replicate of its respective group. The microarray data were fitted to a 2-factor mixed ANOVA model (*intensity = Array + Dye + Clade + Stx + Clade:Stx + Sample; random effects = Array + Sample*) using the MAANOVA package (version 0.98-8) (249) in R software (version 2.2.1) (312). Subsequent to local Lowess normalization (248), significant differences in gene expression between groups of strains were inferred by the Fs statistic in R/MAANOVA and by pairwise contrast analysis of the 4 groups, which utilizes the *t*-test, as explained by Bergholz *et al.* (24). Expression estimates were considered significant if the *p*

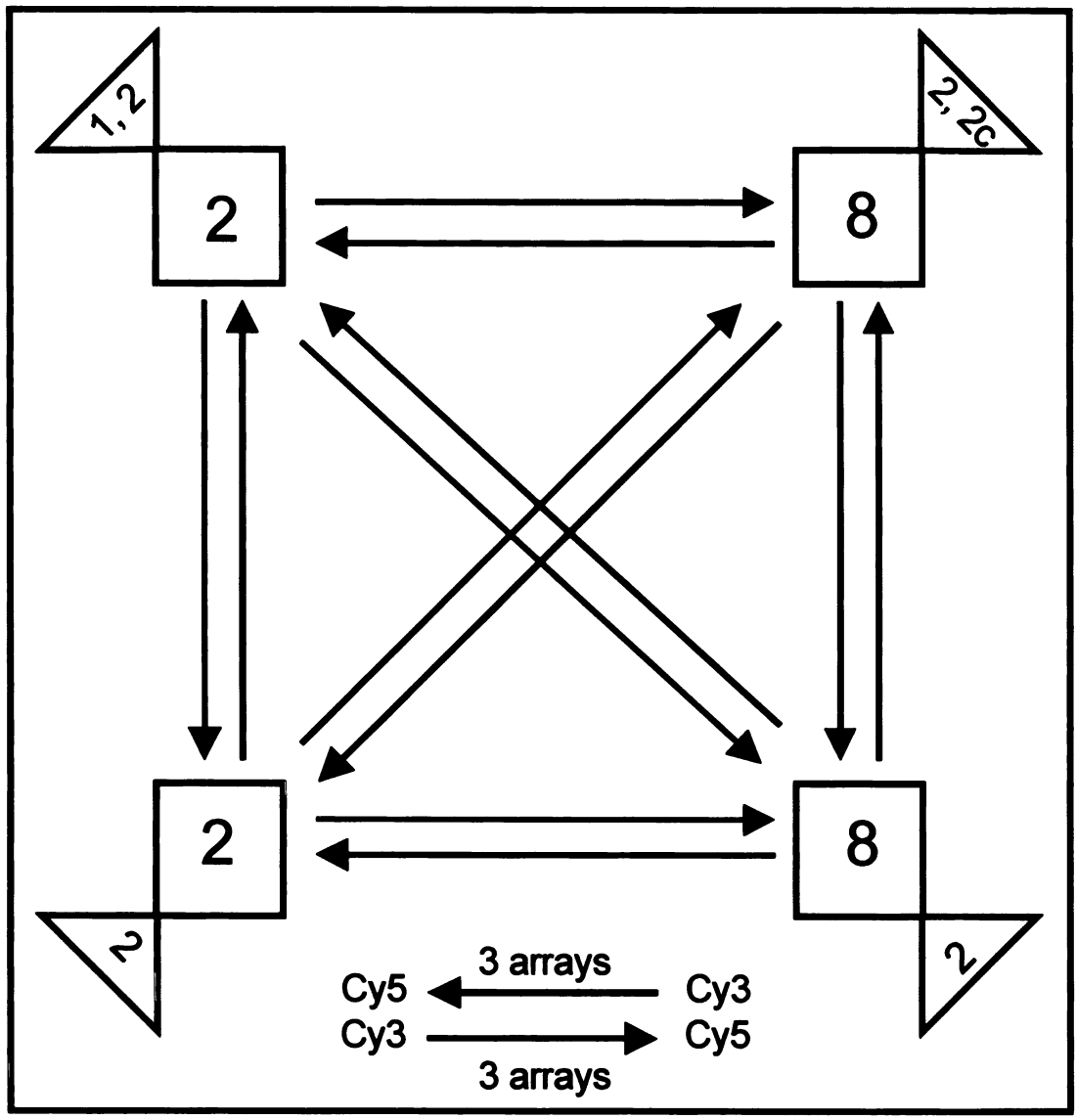

Figure 4.1. Microarray hybridization scheme. 24 O157:H7 strains were divided into 4 groups based on clade (squares) and Stx variant (triangles). The 6 strains of each group were considered as individual biological replicates of the particular group; expression estimates of 6 strains from the same group were analyzed as if they were 6 independent RNA extractions of the same strain. Randomized hybridizations were performed between groups so that all 6 strains from one group were compared to all 6 strains from another group, with dye-swaps. 6 hybridizations were performed between any 2 groups; RNAs from a different pair of strains were compared for each of the 6 hybridizations. In total, 36 hybridizations were performed.

value for the Fs statistic was < 0.05 after adjustment for multiple testing (24).

Quantitative Real-Time PCR. From the 24 strains, 12 were randomly selected, including 6 from clade 8 (3 with Stx2, and 3 with Stx2, 2c) and 6 from clade 2 (3 with Stx2, and 3 with Stx1, 2). Three independent MAC-T challenge experiments were carried out with these 12 strains, as described above, and three independent RNA populations were extracted from each of the 12 strains. Following reverse transcription using the iScript Select cDNA synthesis kit (BioRad, Hercules, Calif.), cDNA populations were subjected to SYBR Green (BioRad, Hercules, Calif) based qRT-PCR relative quantification of transcription, using the 16S *rrsH* gene for within sample normalization (24). Primer sequences are given in Table 4.2; the primers for the *stx2B* gene were specifically designed to discriminate between the B subunit of Stx2 and Stx2c variants and, the forward primer for the *q* gene is specific for the *q* antiterminator of the Stx2 phage. Each cDNA population was assayed in quadruplicate, with five-fold serial dilutions ranging from 1× to 0.008×. As there is no means to justify which clade 8 strain is compared with which clade 2 strain, gene expression for each clade was calculated as an individual data point, the mean ± standard deviation (S.D.) of 6 strains, and the relative differences were expressed as the ratio of clade 8/2, as explained by Schmittgen *et al.* (277).

Table 4.2. Primer sequences and annealing temperatures, used for qRT-PCR.

Primer	Sequence (5' to 3')	Annealing temperature
eae-F	GCCGGTAAAGCGACTGTTAG	55°C
eae-R	ATTAGGCAACTCGCCTCTGA	
tir-F	ACTTCCAGCCTTCGTTCAGA	57°C
tir-R	TTCTGGAACGCTTCTTTCGT	
espA-F	GCTGATGTTCAGAGTAGC	56°C
espA-R	ATCACCACTAAGATCACG	
espB-F	TCAGCATTGGGGATCTTAGG	57°C
espB-R	CTGCGACATCAGCAACACTT	
grlA-F	TAGAAAGTCCTGGAACAAC	56°C
grlA-R	AGACTGTCCCACAATACC	
ler-F	GACTGCGAGAGCAGGAAGTT	59°C
ler-R	CAGGTCTGCCCTTCTTCATT	
escN-F	GATGGCATAGGCAGACCAAT	55°C
escN-R	GCCCTGACGCCAAGTATAAA	
stx2A-F	TATATCAGTGCCCGGTGTGA	55°C
stx2A-R	TGACGACTGATTTGCATTCC	
stx2B-F	GAAGATGTTTATGGCGGT	55°C
stx2B-R	CACTGTAAATGTGTCATC	
q-F	CTATGAGGATGTTACATGG	56°C
q-R	CAACACGTAATAATCAACC	

Table 4.2. continued

Primer	Sequence (5' to 3')	Annealing temperature
stx2c-F	CTGAACAGAAAGTCACAGTYTTTA	57°C
stx2c-R	GGCCACTTTTACTGTGAATGTATC	
hlyA-F	CCAGGAGAAGAAGTTAGAG	56°C
hlyA-R	CAGACCATGTATCCTTACC	
toxB-F	AGAACTCCAACGCATCAGAGA	57°C
toxB-R	TGCAGGTATTCCTCCTATTGC	
tagA/stcE-F	CCAGAAGGACTTACCTATAC	56°C
tagA/stcE-R	GAAGGCTATATCCTGACC	
rpoS-F	TTATCGAAGAGGGCAACCTG	55°C
rpoS-R	GTTCAATCGTCTGGCGAATC	
gadX-F	TTACAACCGAACATGCGAAC	59°C
gadX-R	CAGACTTGGACTCATCAACAGC	
rrsH-F	CGATGCAACGCGAAGAACCT	55°C
rrsH-R	CCGGACCGCTGGCAACAAA	

RESULTS

Interaction of clade 8 and 2 strains with epithelial cells. The ability of clade 8 and 2 representatives to yield A/E lesions on bovine mammary epithelial cells (MAC-T) was confirmed by a positive FAS reaction (Figure 4.2), before differences in the capacity to associate with MAC-T cells were examined among clade 8 (n = 12) and clade 2 (n = 12) strains, by association and invasion assays. Following 1 h of incubation, all strains were associated with MAC-T monolayers. However, there were significant differences in association levels between clades (Figure 4.3); 10 of the 12 clade 8 strains associated with greater numbers than all clade 2 strains (CFU/ml counts are in Table 4.3). Clade 8 strains had a 2.3 ± 0.2 fold higher association with MAC-T cells relative to clade 2 (p val = 0.0001). Flow cytometric analyses of association assays, which were repeated with clade 8 (n = 6) and clade 2 (n = 6) strains that associated with greatest numbers, confirmed the significantly increased ability of clade 8 strains to associate with MAC-T cells (p value = 0.00001) (Figure 4.4). These twelve strains were then subjected to invasion assays to determine whether the increased association of clade 8 is attributable to differences in invasion or adherence, or both. All twelve strains invaded MAC-T cells with similar numbers (Figure 4.5), which was an order of magnitude lower than association, and no significant differences between clades were detected (p value = 0.22).

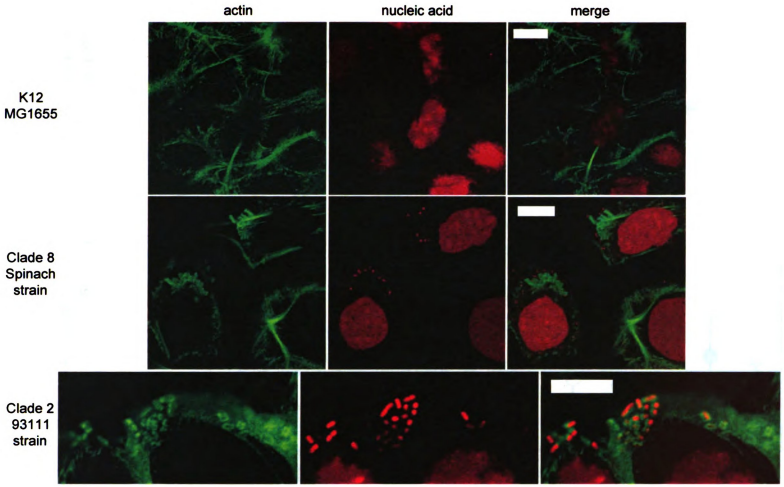

Figure 4.2. Fluorescence micrographs of MAC-T cells infected with *E. coli* K12, O157:H7 Spinach, and O157:H7 93111. Filamentous actin was stained green (Alexa Fluor 488), nucleic acid was stained red (propidium iodide). Merging the green and red fluorescence demonstrated complementarity of actin pedestals and bacterial location. White scale bar represents 10 μm. Magnification 63x with 2.7x scan zoom for K12 and Spinach, and 3.6x for 93111.

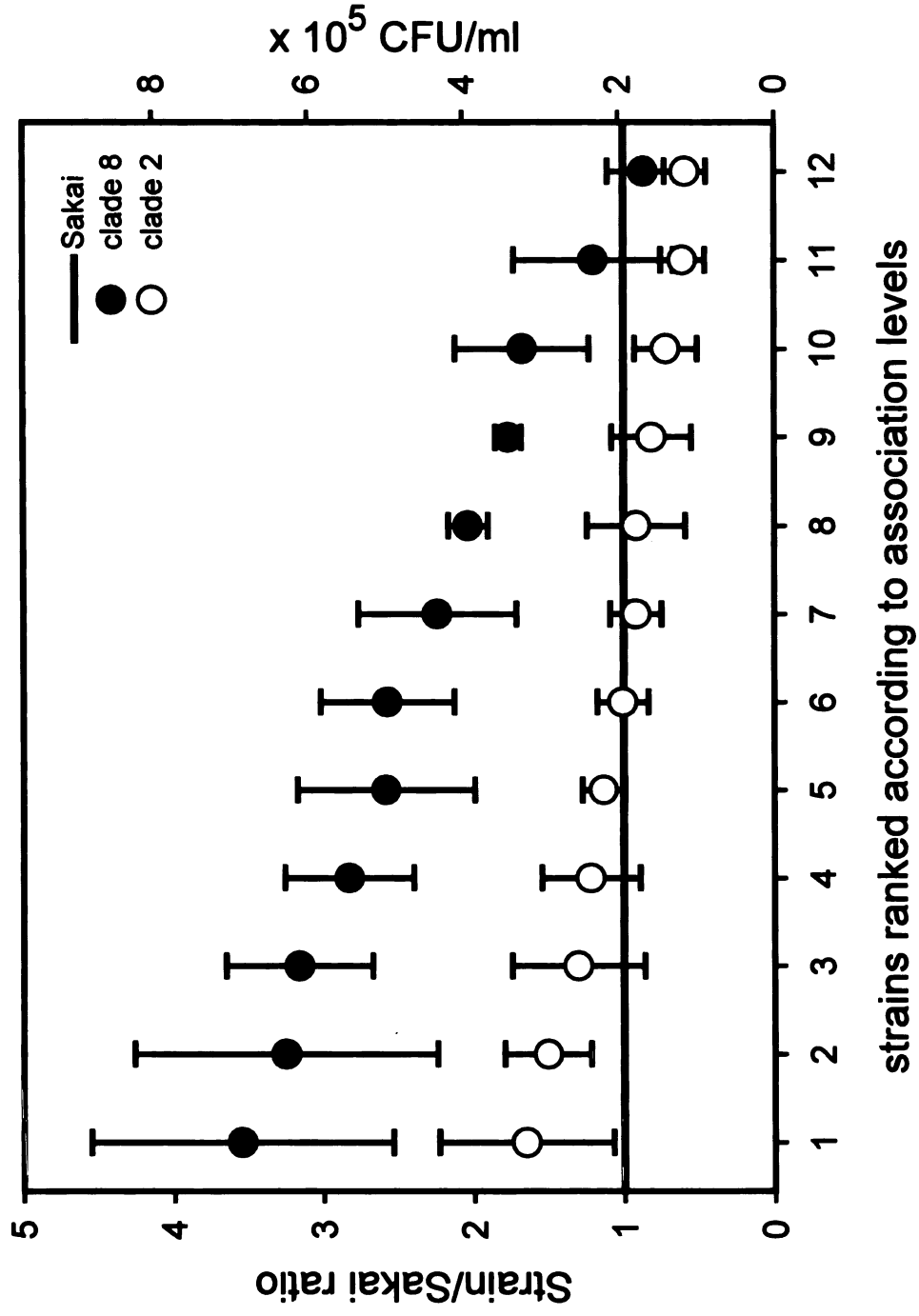

Figure 4.3. Association of 24 O157:H7 strains with MAC-T cells. Association levels of each strain were expressed relative to Sakai, which had an average of $1.9 \times 10^5 \pm 5.4 \times 10^4$ CFU/ml per well recovered from each assay. The symbols indicate the mean ± standard deviation of three separate experiments.

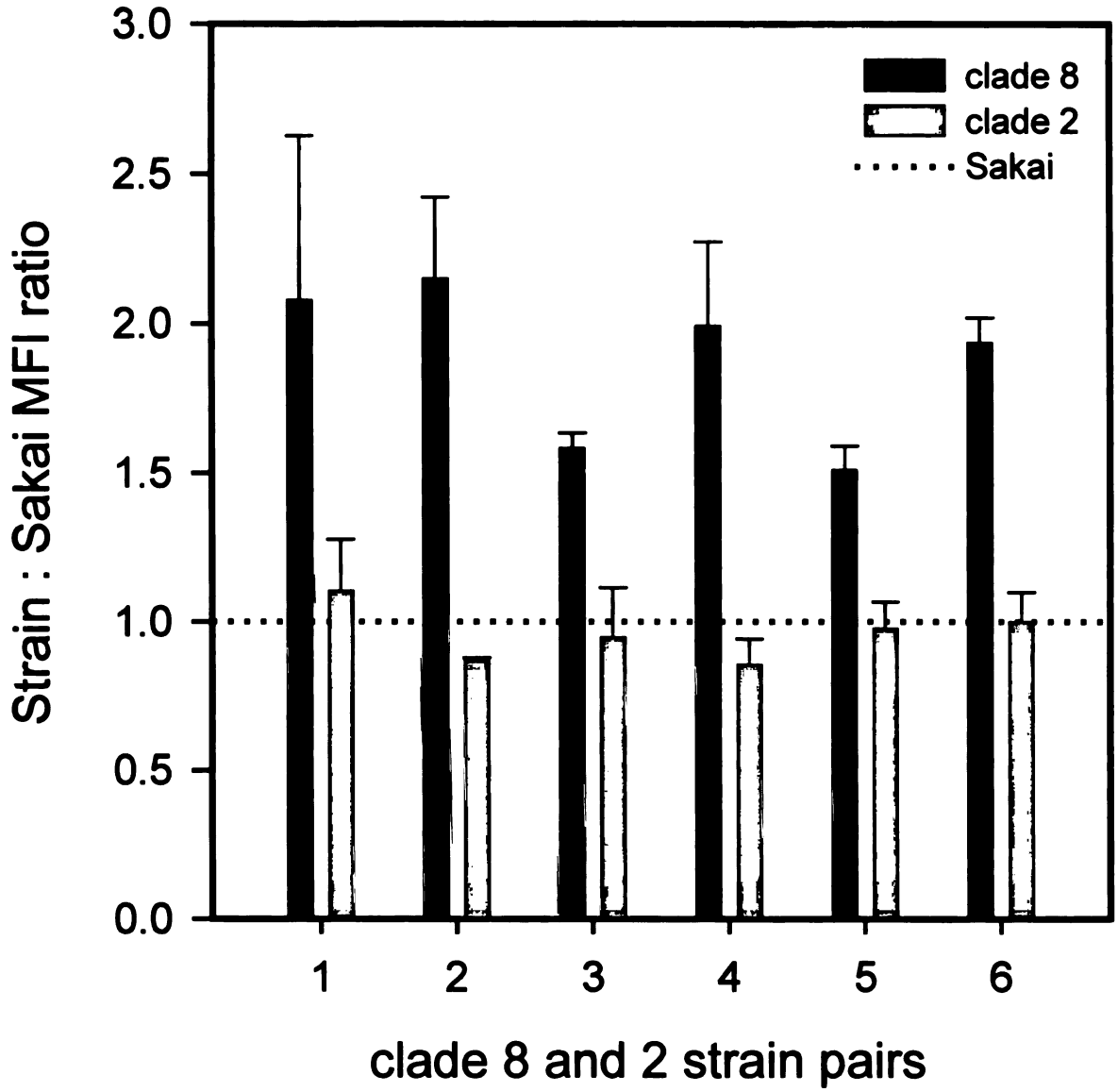

Figure 4.4. Association of 12 O157:H7 strains with MAC-T cells quantified by flow cytometry. Differences in association were expressed as the ratio of MFI of strain-infected MAC-T and the MFI of Sakai-infected MAC-T cells. Clade 8 (n = 6) and 2 (n = 6) strains with highest association levels, determined by plate counting, were ranked in the same order as in Figure 4.3. Bars represent the mean ± S. D. of two separate experiments.

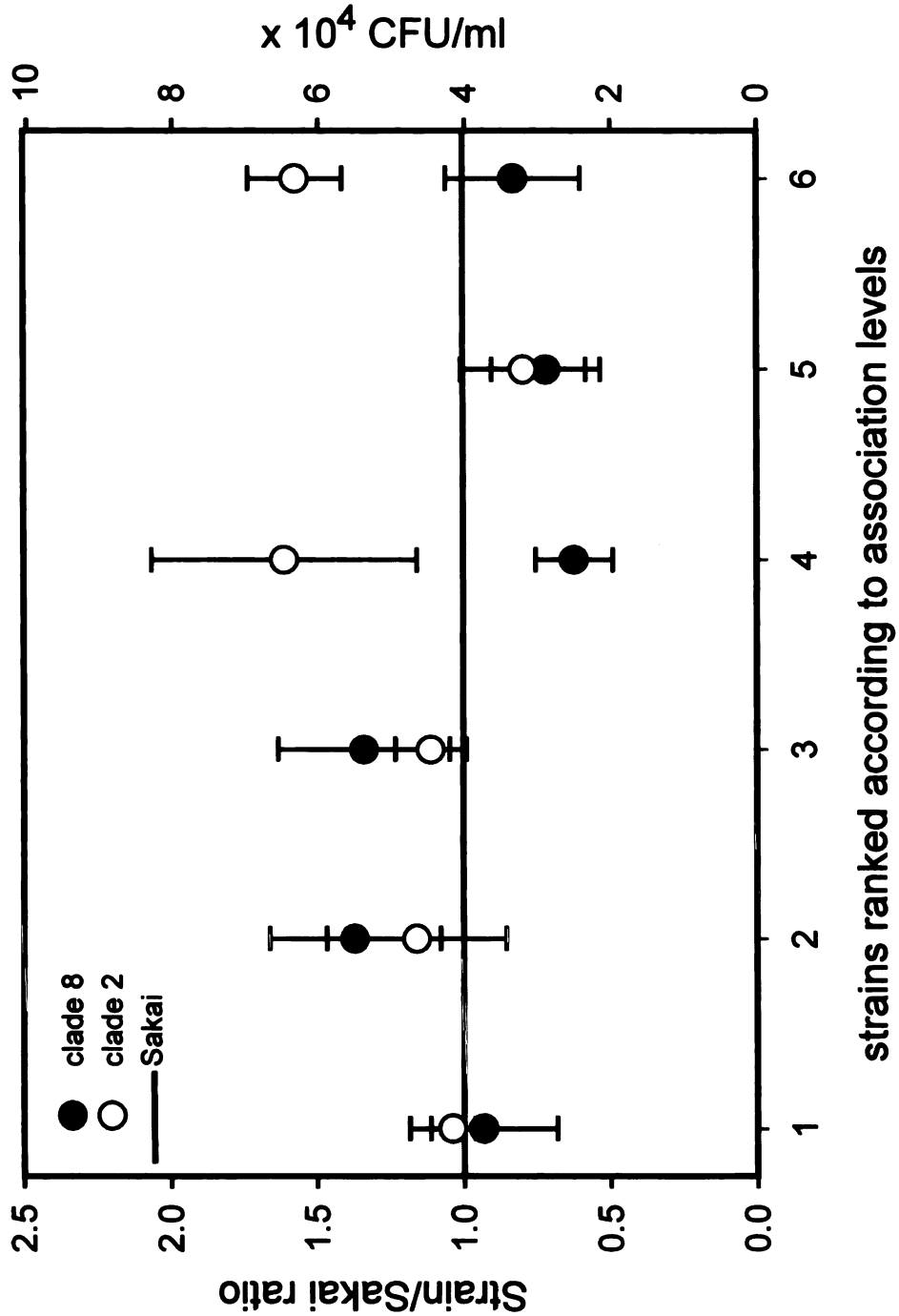

Figure 4.5. Invasion of MAC-T cells by 12 O157:H7 strains. Invasion levels of clade 8 (n = 6) and clade 2 (n = 6) strains, which associated with MAC-T cells with the highest numbers, were expressed relative to Sakai, which had an average of $4.0 \times 10^4 \pm 8.7 \times 10^3$ CFU/ml per well recovered from each assay. Clade 8 and 2 strains were ranked according to their association levels. The symbols indicate the mean ± standard deviation of three separate experiments.

Table 4.3. Colony counts recovered from association assays of 24 O157:H7 strains.

Strain	clade	*stx*	CFU/ml[a]		Ratio[b]
			average	S.D	(Strain/Sakai)
EK2	8	*2*	6.8×10^5	1.9×10^5	3.54
MI06-31	8	*2*	6.3×10^5	2.0×10^5	3.25
E32511/O	8	*2,2c*	6.1×10^5	9.5×10^4	3.16
MI03-35	8	*2*	5.5×10^5	8.3×10^4	2.83
MT#9	8	*2,2c*	5.0×10^5	1.1×10^5	2.58
EK1	8	*2*	5.0×10^5	8.6×10^4	2.57
MI03-72	8	*2,2c*	4.3×10^5	1.0×10^5	2.24
DA-11	8	*2*	3.9×10^5	2.5×10^4	2.04
MI06-63	8	*2,2c*	3.4×10^5	1.7×10^4	1.77
1:361	8	*2,2c*	3.2×10^5	8.6×10^4	1.68
EK27	8	*2,2c*	2.3×10^5	1.0×10^5	1.20
MI02-55	8	*2*	1.7×10^5	4.6×10^4	0.87
DA-35	2	*1,2*	3.2×10^5	1.1×10^5	1.65
EK15	2	*1,2*	2.9×10^5	5.6×10^4	1.51
MI02-57	2	*2*	2.5×10^5	8.5×10^4	1.30
96M1006	2	*1,2*	2.4×10^5	6.4×10^4	1.22
93111	2	*1,2*	2.2×10^5	2.8×10^4	1.13
F6854	2	*1,2*	2.0×10^5	3.3×10^4	1.01
MI01-29	2	*2*	1.8×10^5	3.3×10^4	0.92

Table 4.3. continued

Strain	clade	*stx*	CFU/ml[a]		Ratio[b]
			average	S.D	(Strain/Sakai)
MLVA-47	2	*1,2*	1.8×10^5	6.3×10^4	0.92
MI02-1	2	*2*	1.6×10^5	5.1×10^4	0.81
MI02-68	2	*2*	1.4×10^5	4.0×10^4	0.72
05EN000757	2	*2*	1.2×10^5	2.8×10^4	0.61
MI04-43	2	*2*	1.1×10^5	2.7×10^4	0.59

a – average and standard deviation (S. D.) of three experiments.
b – the average and S.D. CFU/ml of Sakai is $1.9 \times 10^5 \pm 5.4 \times 10^4$.

Gene expression analyses of O157:H7 subpopulations. To investigate O157:H7 transcriptional responses associated with the host-pathogen challenge, global gene expression analysis of O157:H7 upon a 30 min exposure to epithelial cells was performed. Secretion of LEE proteins (174), and the preceding expression of respective genes (23) was shown to be maximal under conditions that mimic the host-pathogen interaction. However, tight attachment of EHEC O157:H7 to the eukaryotic plasma membrane is followed by a decrease in expression of LEE genes (23, 65). Similarly, transcription of *Salmonella enterica* invasion genes is down-regulated following macrophage invasion (90). These reports suggest that potential differences in the transcription of colonization factors are more likely to be detected prior to bacterial colonization of the eukaryotic cell. Our previous investigation of O157:H7 gene expression following 30 min exposure to MAC-T cells, confirmed the feasibility of this timepoint (Chapter 3).

To analyze the effect of O157:H7 clade membership and Stx distribution on global gene expression upon exposure to MAC-T cells, we compared transcriptomes from 24 strains, classified into 4 groups based on clade and Stx profile, so that each hybridization examined a random pair of strains that differed by either clade or *stx* gene complement, or both (Figure 4.1). An overall Fs test found 363 genes to be significantly differentially expressed (p value = 0.05) among the 4 groups, and a dendrogram based on group column means clustered the groups according to clade (Figure 4.6). To determine which genes are differentially regulated between which groups, pairwise contrast analysis of

expression estimates from the 4 groups was applied. This analysis revealed a remarkable difference in expression between groups from different clades, whereas within clade differences were marginal (Figure 4.7). Only 4 genes were differentially expressed within clade 2, including *stx1A* and *stx1B*, a putative prophage repressor and an unknown gene from the Stx1 prophage (Sakai prophage (Sp) 15) (136); and 14 genes were differentially expressed within clade 8, most of which are unknown phage genes. Although the number of differentially expressed genes between clades 2 and 8 varied between groups with different Stx profiles, the 'Clade : Stx interaction effect' analysis of the 4 groups did not imply that the expression of any gene in either clade was influenced by the presence of a particular Stx complement.

The 'Clade effect' analysis, which utilized the Fs test to compare transcription profiles between clade 2 (n = 12) and 8 strains (n = 12), indicated a significant difference in expression of 604 genes, with a fold change difference in expression ≥ 1.5 in 186 genes; of the 604 genes, 265 code for hypothetical proteins of unknown function. Sequencing of the 2006 USA Spinach outbreak strain, MI06-63 (TW14359), has revealed that this strain and, by inference, clade 8, also differ in gene content of phage elements compared to sequenced O157:H7 strains Sakai (clade 1) and EDL-933 (clade 3) (205). We therefore performed BLASTN homology searches of 316 Sakai gene sequences, corresponding to phage borne genes that were found to be differentially expressed between clades, against a clade 8 (GenBank Acc. No. ABHL00000000) and a clade 2 (GenBank Acc. No. ABHT00000000) genome

sequence. Fifty-three ORFs in clade 8 and four ORFs in clade 2, which are located on prophages (Sp) 18, 10, 5, 7, and 15 in O157:H7 Sakai, revealed little to no homology with the clade 8 and 2 genome sequences, respectively, and were not further considered.

The 'Stx effect' analysis found only *stx1A* and *stx1B* to be differentially expressed within clade 2, while no gene was influenced by the Stx effect in clade 8; the microarrays we used, though, do not probe for the 75 predicted ORFs from the 2851 Stx2c-harboring phage (297). Collectively, these analyses indicated distinct transcriptional profiles within the O157:H7 population, under conditions that mimic the host-pathogen interaction. In particular, the relative difference in gene expression between O157:H7 strains was associated with the phylogenetic divergence within the O157:H7 population, predicted by the SNP-resolved clade phylogeny, and not with the carriage of different Stx phage combinations. We consider the relative differences in gene expression of virulence determinants between clades 8 and 2, as follows.

LEE Genes. Twenty-nine LEE genes were found to be upregulated in clade 8 relative to clade 2 (Table 4.4 and Figure 4.8), with a subtle decrease in fold change from the *lee* 4 operon to *lee 1*. Apart from *sepL*, transcription was highest in *lee4* genes (1.92 ± 0.13-fold); especially that of the *espADB* polycistron, which codes for the molecular syringae of the TTSS. The expression of *lee5* effectors and chaperones was slightly lower (1.72 ± 0.13-fold), followed by *lee3* (1.66 ± 0.14-fold) and *lee2* (1.50 ± 0.09-fold), which encode the membrane-bound TTSS components. Genes of the *lee1* operon, which code for

the Ler regulator, the CesAB chaperone, ORFs 3, 4, and 5, the EscRSTU inner membrane proteins of the TTSS, as well as *rorf1*, *grlR* and *orf29* were not significantly differentially expressed (*p* val > 0.05). To validate LEE gene expression differences, relative transcript levels of *lee* operon representatives *ler*, *sepZ*, *escN*, *espA*, *espB*, *tir*, and *eae* were measured by qRT-PCR (Table 4.6). Microarrays also detected significant expression of 13 non-LEE effector genes, 11 of which were upregulated in clade 8 (Table 4.5); these genes are located on various prophage elements that are dispersed throughout the O157:H7 genome and code for proteins that are exported by the TTSS (115, 317). Collectively, this transcriptional snapshot points to an enhanced expression of the LEE island in clade 8 strains, relative to clade 2.

Table 4.4. Differences in LEE gene expression between clades 8 and 2, as detected by microarrays.

ECs #[a]	*gene*	function[b]	fold change[c]
ECs4550	*espF*	effector	1.9
ECs4551	*orf29*	unknown	1.2*
ECs4552	*escF*	needle protein	1.7
ECs4553	*cesD2*	chaperone for EspD	2.0
ECs4554	*espB*	effector/translocator	2.0
ECs4555	*espD*	translocator	1.8
ECs4556	*espA*	translocator	2.0
ECs4557	*sepL*	TTSS	1.4
ECs4558	*escD*	TTSS	1.6
ECs4559	*eae*	intimin adherence protein	1.6
ECs4560	*cesT*	chaperone for Tir	1.8
ECs4561	*tir*	translocated intimin receptor	1.8
ECs4562	*map*	effector	1.5
ECs4563	*cesF*	chaperone for EspF	1.7
ECs4564	*espH*	effector	1.7
ECs4565	*sepQ*	TTSS	1.7
ECs4566	*orf16*	unknown	1.5
ECs4567	*orf15*	unknown	1.9
ECs4568	*escN*	TTSS	1.5
ECs4569	*escV*	TTSS	1.8

Table 4.4. continued

ECs #[a]	*gene*	function[b]	fold change[c]
ECs4570	*orf12*	unknown	1.6
ECs4571	*sepZ*	effector	1.4
ECs4572	*rorf8*	Unknown	1.5
ECs4573	*escJ*	TTSS	1.5
ECs4574	*sepD*	TTSS	1.5
ECs4575	*escC*	TTSS	1.7
ECs4576	*cesD*	chaperone for EspD	1.5
ECs4577	*grlA*	regulator	1.5
ECs4578	*grlR*	regulator	1.1*
ECs4579	*rorf3*	Unknown	-1.2
ECs4580	*escU*	TTSS	1.0*
ECs4581	*escT*	TTSS	1.3*
ECs4582	*escS*	TTSS	1.3*
ECs4583	*escR*	TTSS	1.3*
ECs4584	*orf5(escL)*	binds to escN	1.4*
ECs4585	*orf4*	unknown function	1.3*
ECs4586	*orf3*	unknown	1.3*
ECs4587	*cesAB*	chaperone for EspA and EspB	1.3*
ECs4588	*ler*	regulator	1.3*
ECs4590	*espG*	destruction of microtubules	1.6
ECs4591	*orf1*	unknown	1.1*

a – Sakai gene numbers, b – gene functions adopted from (115, 235), c – negative sign indicates increased expression in clade 2, * - adj *p* value > 0.05.

Shiga toxin genes. Stx1 genes (Sp15), *stx1A* and *stx1B*, were upregulated in the clade 2 strains that harbor the Stx1 converting phage (Table 4.5), which was expected as Stx1 are not present in clade 8 strains. However, microarrays also detected an increase in expression of *stx2A* and *stx2B* genes in clade 8; qRT-PCR revealed these differences to be greater (Tables 4.5 and 4.6), which was expected as microarray measurements are known to underestimate gene expression levels (49). qRT-PCR also detected a relative difference in mRNA abundance of *stx2* genes within clades, that is, transcription of *stx2A* and *stx2B* was found to be higher in clade 8 and clade 2 strains lysogenized with only the Stx2 converting phage, compared to super-infected strains that harbor both Stx2 and Stx2c, and Stx2 and Stx1 phages, respectively (Figure 4.9). Also found to be upregulated in clade 8 was the phage borne antitermination gene *q* (ECs1203), located upstream of *stx2* genes. qRT-PCR confirmed the increased expression of *q* in clade 8 (2.60 ± 0.16 fold), but it also detected higher *q* transcript levels, by almost 2 fold, in strains possessing both Stx variants relative to strains harboring only *stx2*, in both clades; this likely reflects sequence similarities of *q* anti-terminators among prophages that could not be resolved by sequence-specific primers. We then compared qRT-PCR expression estimates in *stx2*-only strains from clade 8 and 2, and detected that *q* is upregulated in clade 8 (Table 4.6).

Sequence divergence of the *q* anti-terminator has been associated with variation in transcription of *stx2* (182). Alignment of 2.5 Kb of sequence, encompassing the start of the *q* gene to the end of *stx2B*, from O157:H7 strains

Sakai (clade1), EDL 933 (clade 3), EC4115 (clade 8), and TW14588 (clade 2) revealed 100% identity in Sakai, EDL 933, and TW14588, and 4 polymorphisms were detected in EC4115. One SNP was detected in the *pS* tRNA promoter, a 2 bp deletion between *tRNA-Ile* and the first *tRNA-Arg*, one SNP in the first *tRNA-Arg*, and one SNP in the *stx2A* coding region. Sequences that are known to be relevant to *stx2* transcription efficiency (332), including those of the *q* antiterminator, *pR' stx2* promoter, *qut* site, *tR'1* and *tR'2* terminators, as well as the *stx2B* sequence showed 100% identity in all strains (data not shown), (GenBank Acc. No for clade 8 and 2 strains are CP001164 and ABKY00000000, respectively).

Plasmid borne virulence genes. Two adhesion-associated genes that were found to be upregulated in clade 8 are *toxB* and *tagA/StcE* (Table 4.5). The product of the pO157-borne *toxB* was demonstrated to postranscriptionally stimulate expression of LEE4 proteins and facilitate adhesion to epithelial cells (294, 307). The increase in transcription of the *tagA/StcE* protease, in clade 8, did not reach statistical significance (*p* value = 0.06), probably due to interstrain variation; qRT- PCR, however, detected an over 2-fold upregulation of *tagA/stcE* in clade 8 strains (Table 4.6). Differential expression of the *etp* plasmid-encoded type II secretion system that directs the export of StcE was not detected. Another pO157-borne virulence gene that was found to be significantly upregulated in clade 8 is *hlyA* (Table 4.5 and 4.6), which encodes the pore-forming RTX (repeats in toxin) EHEC hemolysin A (EHEC-HlyA).

Regulators. Three of the several genes that are known to directly or indirectly influence expression of the LEE island (289), *rpoS*, *grlA*, and *gadX*, were significantly differentially expressed between clade 8 and 2 (Tables 4.5 and 4.6). Upregulation of the sigma factor 38 (*rpoS*) in clade 2, with the concurrent down-regulation of LEE in clade 2, is in agreement with previous studies demonstrating the RpoS-dependent negative regulation of LEE genes (153, 318). Microarray measurements of gene expression pointed to a low, but statistically significant, increase in *gadX* transcription in clade 2 (Table 4.5). qRT-PCR validation indicated that the upregulation of *gadX* in clade 2 strains was indeed greater than estimated by microarrays, however, with a higher standard deviation, implying inter-strain variation within clade 2 (Table 4.6). In addition to controlling acid resistance, *gadX* has been shown to negatively influence transcription of virulence genes in enteropathogenic *E. coli* (284). The LEE-encoded positive regulator, *grlA*, was also upregulated in clade 8 strains. Apart from its stimulatory effect on LEE, *grlA* mediates expression of non-LEE encoded effectors (73) and was recently shown to positively regulate the expression of *hlyA* (269). These results are consistent with the assertion that clade 8 strains likely possess a distinct regulatory circuit allowing more efficient utilization of shared virulence determinants.

Figure 4.6. Heatmap of 363 genes that were significantly differentially expressed between 4 groups ($clade_{stx}$) of O157:H7, based on Fs test analysis of ANOVA gene expression estimates. Each column represents one of the 4 groups ($clade_{stx}$). Genes were sorted by chromosomal positions and the heat map was generated in R ('gplots' package version 2.3.2). Note that dendrogram, based on column means, clustered groups according to clade. Sp – Sakai prophage, SpLE – Sakai prophage-like element, pO157 – EHEC plasmid.

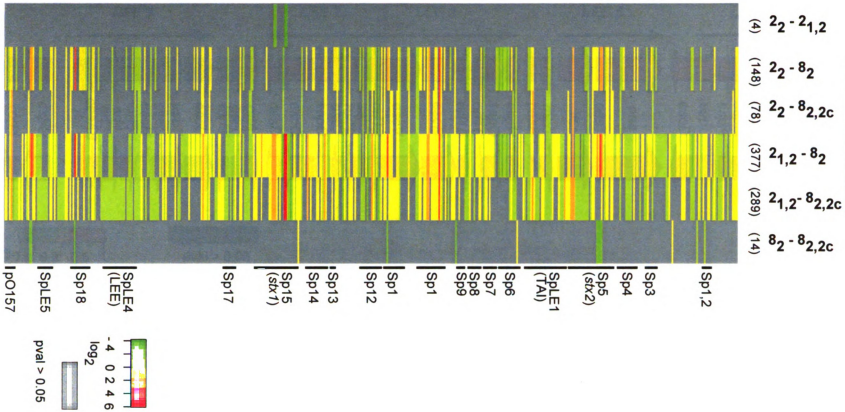

Figure 4.7. Heatmap of pairwise contrast analysis of ANOVA estimates of significantly differentially expressed genes between 4 groups of O157:H7 strains. Each column represents $\log_2$ differences in expression between 2 groups (clade$_{stx}$). In parenthesis atop each column is the number of genes indicated to be significantly differentially expressed between the 2 groups compared. Genes were sorted by chromosomal positions and the heat map was generated in R ('gplots' package version 2.3.2). Sp – Sakai prophage, SpLE – Sakai prophage-like element, pO157 – EHEC plasmid, TAI – Tellurite resistance and adherence conferring island.

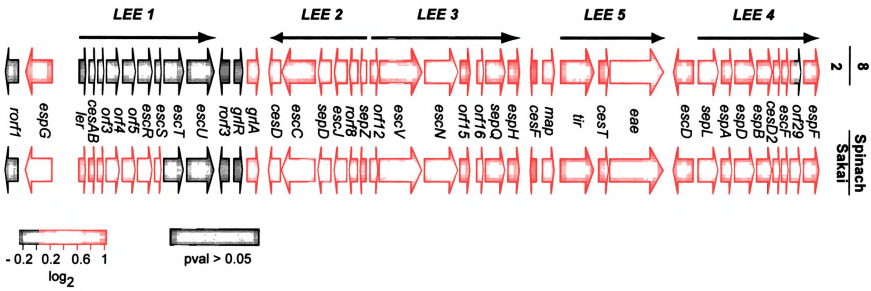

Figure 4.8. Heatmap of LEE expression differences between clades 8 and 2, and between Spinach and Sakai. For clade 8 to 2 ratios, expression data from the 'Clade effect' analysis was used to generate a heatmap in R ('gplots' package version 2.3.2) that was then fitted to a graphic representation of the genetic organization of the LEE island, adopted from (293). The Spinach-Sakai image was adopted from Chapter 3, for comparison. Arrows represent LEE operons, and between heatmaps are LEE gene names.

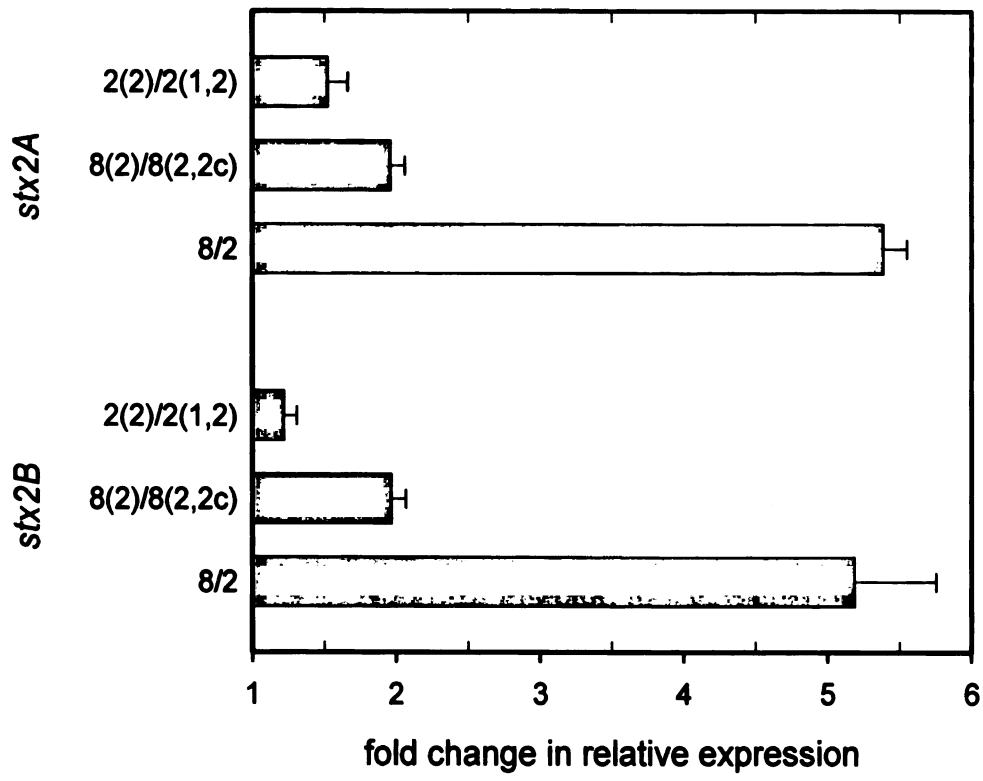

Figure 4.9. Differences in relative expression of Stx2 genes within and between clades, as determined by qRT-PCR. Labels on the ordinate represent clade and stx (in parenthesis) profiles of examined strains. Differences in expression are plotted as average fold change ratios, with standard deviations, of clade 8 (n = 6) to clade 2 (n = 6) strains; for within clade comparison, averages of 3 strains per group are compared.

Table 4.5. Relative differences in expression of genes associated with virulence, as detected by microarrays.

ECs#[a]	*gene*	Function[b]	Fold change (8/2) [c]
0848	*nleH1-1*	Non-LEE effector, function unknown	1.1
1127	*espV*	Non-LEE effector, function unknown	1.6
1814	*nleH1-2*	Non-LEE effector, function unknown	1.2
1825	*espM1*	Non-LEE effector, function unknown	-1.2
2226	*nleG7*	Non-LEE effector, function unknown	1.3
4653	*espY4*	Non-LEE effector, function unknown	1.4
1994	*nleG2-2*	Non-LEE effector, function unknown	1.7
1996	*nleG5-1*	Non-LEE effector, function unknown	1.5
2154	*nleG5-2*	Non-LEE effector, function unknown	1.4
2155	*nleG6-2*	Non-LEE effector, function unknown	1.4
2227	*nleG3.*	Non-LEE effector, function unknown	-1.4
2229	*nleG2-4*	Non-LEE effector, function unknown	1.4
1995	*nleG6-1*	Non-LEE effector, function unknown	1.2
0350	*hmwA*	HmwA-like adhesin	1.6
2973	*stx1B*	Shiga toxin I subunit B	-15.0
2974	*stx1A*	Shiga toxin I subunit A	-11.5
1205	*stx2A*	Shiga toxin II subunit A	1.8
1206	*stx2B*	Shiga toxin II subunit B	2.0
1203	*q*	Q anti-terminator of Stx2 phage	1.8

Table 4.5. continued

ECs#[a]	*gene*	Function[b]	Fold change (8/2)[c]
1161	-	Excisionase of Stx2 phage	-1.2
1189	*o*	Replication protein O of Stx2 phage	-1.5
1190	*p*	Replication protein P of Stx2 phage	-1.5
1190	*p*	Replication protein P of Stx2 phage	-1.5
pO157p58	*toxB*	Toxin B, adhesion-associated	1.3
pO157	*tagA/stcE*	StcE protease, adhesion-associated	1.5
pO157	*hlyA*	EHEC hemolysin A	1.5
3595	*rpoS*	Sigma factor RpoS, global regulator	-1.7
4577	*grlA*	GrlA, LEE- encoded positive regulator	1.5
4396	*gadX*	GadX regulator, acid resistance and LEE	-1.1
1351	*terZ*	Tellurite resistance	-1.7
1352	*terA*	Tellurite resistance	-1.4
1355	*terD*	Tellurite resistance	-1.3
1356	*terE*	Tellurite resistance	-1.3

a – Sakai O157:H7 gene numbers.
b – description of gene function was adopted from Qiagen annotation and (317).
c – fold change difference in expression based on microarray measurements; positive values were found to be upregulated in clade 8 negative sign indicates increased expression in clade 2.

Table 4.6. qRT-PCR validation of expression differences between clades.

gene	fold change[a] clade 8 : 2	E[b]
espA	5.90 ± 0.65	2.00
espB	3.55 ± 1.00	2.02
tir	2.43 ± 0.39	1.99
eae	2.07 ± 0.52	1.98
sepZ	1.72 ± 0.08	2.12
escN	2.06 ± 0.12	1.96
ler	1.09 ± 0.16	2.07
stx2A	5.19 ± 0.55	2.06
stx2B	5.39 ± 0.16	2.01
q[c]	2.90 ± 0.13	1.99
hlyA	5.04 ± 0.49	2.04
toxB	2.64 ± 0.27	1.96
tagA/stcE	2.34 ± 0.06	2.01
grlA	3.45 ± 0.11	2.02
rpoS	-2.99 ± 0.60	2.21
gadX	-4.70 ± 1.29	2.08

a – mean ± standard deviation of relative fold change differences in expression between clade 8 (n = 6) and clade 2 (n = 6) strains; negative sign denotes increased expression in clade 2.
b – mean reaction efficiencies of 12 O157:H7 strains.
c – relative difference in expression of the *q* antiterminator is based on clade 8 (n = 3) and 2 (n = 3) strains that carry only *stx2* genes.

DISCUSSION

EHEC O157:H7 utilize a shared set of pathogenicity determinants and yet the epidemiology of this pathogen is characterized by significant differences in the clinical burden between outbreaks of disease. Phylogenetic analysis of O157:H7 has explained some of the basis for the observed variation among strains, by resolving the O157:H7 population into distinct genetic lineages (205). Implications about clade 8 hyper-virulence, however, are based on epidemiological analyses of clinical strains isolated mostly from a single state, Michigan (205). To test the hypothesis that clade 8 is hyper-virulent regardless of geographic location, we compared the pathogenic potential of clade 8 and 2 strains that were isolated from multiple states. Our results indicate that the clade 8 subpopulation of O157:H7 is characterized by a superior capacity to colonize epithelial cells and by increased expression of shared virulence genes, upon exposure to the epithelium, relative to clade 2, the most abundant lineage of O157:H7.

Attachment to the gut mucosa is a key step in the pathogenesis of O157:H7 disease, therefore, cell assays were used to examine the ability of clade 8 and 2 strains to associate with MAC-T epithelial cells. MAC-T cells are commonly used to study pathogenesis of adherent/invasive *Escherichia* species (38, 39, 77, 81, 207), and their feasibility to mimic O157:H7 interactions with the mucosal epithelium was confirmed with a positive FAS test. Higher association levels of clade 8 strains with MAC-T cells suggest that this population has an increased ability to colonize and persist in the intestinal tract, compared to clade

2, the most frequent lineage of O157:H7. The capacity of O157:H7 strains to associate with epithelial cells was also examined in the context of Stx genotypes, as carriage and expression of Stx2 was implied to contribute to the adherence of O157:H7 to HEp-2 cells (263). No correlation was found between Stx genotypes and association levels, i. e. differences between strains were not influenced by any particular complement of Stx genes, but were instead clade-specific. Invasion assays demonstrate that the twelve strains with highest association levels, and, by inference, the other twelve O157:H7 strains used in this study, enter MAC-T cells at similar rates. This is consistent with a previous study about MAC-T invasion by O157:H7 (207), and indicates that the increase in association of clade 8 lies in the inherent ability of clade 8 strains to adhere to epithelial cells more efficiently. Although EHEC O157:H7 are regarded as non-invasive, they were shown to invade a number of primary bovine cell lines (75), as well as MAC-T cells and MDBK kidney epithelial cells (207).

Genome-wide gene expression analysis of O157:H7 strains revealed significant differences in the transcriptional response of clade 8 and 2, following their exposure to epithelial cells. Transcriptomes of 24 O157:H7 strains were interrogated using a microarray hybridization scheme that was designed to examine gene expression in the context of clade membership and Stx genotype, as well as the interaction (combined) effect of both, clade and Stx variation, on O157:H7 gene expression.

The LEE genes code for the central adhesion factor of O157:H7, therefore, the upregulation of this pathogenicity island in clade 8 is in agreement

with its increased adherence to epithelial cells. Although the DMEM media used in our experiments was not supplemented with mannose to account for type I fimbrial attachment, no significant increase in fimbrial gene transcription was detected. That differences in LEE expression between clades were not greater than observed is probably due to inter-strain variation within clade 8, which is consistent with the finding that some clade 8 strains associate with epithelial cells with greater numbers than other. In general, relative expression was highest in genes that code for the needle complex (NC) of the TTSS (EspADB) and in effector genes; transcription of genes that code for the basal membrane-bound secretion machinery was slightly lower or was not significantly differentially upregulated (*lee1* genes).

The finding that there was no difference in the expression of *lee1* genes, including *ler*, was unexpected. The Ler regulator directly activates transcription of *grlRA*, *lee2*, *lee3*, *lee5*, and *lee4*, which was demonstrated with electrophoretic mobility shift assays (19, 130, 265) and reporter gene transcriptional fusions (105). It is possible that our transcriptional snapshot was taken at the time when LEE transcription has proceeded past the *lee1* operon. The assembly of the TTSS is sequential, starting with the membrane-bound components, four of which are located on *lee1* (115) and, transcriptional analysis of O157:H7 adhering to the eukaryotic membrane indicates that polycistronic TTSS mRNAs are not degraded at the same rate (65).

The regulation of LEE revolves mostly around the expression of Ler, however, LEE operons can also be activated independently of Ler. Mutation of

grlA in *Citrobacter rodentium* was shown to considerably reduce expression of *lee2* and *lee5* genes (73). Russell *et al.* have recently reported that the O157:H7 GrlA regulator can be activated independently of Ler, by the QseA transcriptional factor acting through an unknown intermediate (265); GrlA in turn activates *lee2* and *lee4* (73, 265). Increased expression of the LEE in clade 8 relative to clade 2 may also be associated with the upregulation of the *rpoS* transcription factor in clade 2. Evidence about the contribution of this factor to LEE expression is conflicting, with studies indicating that it can both stimulate (188) and repress LEE activation (153). Our results agree with those of Iyoda *et al.*, which indicate that RpoS negatively influences LEE expression via a regulatory cascade that involves repression of *ler* activators *pchABC* by an unidentified factor (153). Lastly, upregulation of *gadX* in clade 2, which was shown to inhibit LEE expression through downregulation of the plasmid encoded Per regulator in enteropathogenic *E. coli* (284), can also contribute to the relative increase in LEE transcription in clade 8.

Interestingly, none of the other factors that have been implicated in the transcriptional control of LEE, including H-NS (47), Pch (154), SdiA (161), QseA (291), ClpXP (153), IHF (105), BipA (120), were significantly differentially expressed between clades 8 and 2. Although this may be ascribed to the transient stability of regulator mRNA, further investigation is necessary to identify the inherent differences in the complex regulatory circuits that govern LEE transcription in clade 8; it is tempting to speculate whether these differences are

attributable to point mutations that increase promoter efficiency, or may concern novel positive regulators of LEE in the clade 8 subpopulation of O157:H7.

The enhanced transcription of adherence genes in clade 8 is also reflected in the upregulation of two non-LEE adhesion associated genes, *toxB* and *tagA/stcE*. ToxB is encoded on the pO157 plasmid and is a partial homologue of LifA, lymphostatin, which is widely distributed in A/E Enterobacteria and is associated with the ability to inhibit lymphocyte activation through inhibition of IL-2 interleukin activation (178). Mutation of *lifA* in *C. rodentium* abolishes colonic inflammation in mice and leads to a significant reduction of murine intestinal colonization (177). ToxB is required for a full adherence phenotype in O157:H7, as mutation of *toxB* in O157:H7 results in decreased adhesion to Caco-2 cells and reduced secretion of LEE effector proteins, including EspA, EspB, EspD and Tir (294, 307). Similarly, deletion of *tagA/stcE* results in decreased adhesion of O157:H7 to HEp-2 cells (124). The TagA/StcE zinc metallo-protease is hypothesized to promote adherence by cleaving proteins in the glycocalyx and mucin layers atop the intestinal epithelium allowing O157:H7 to come into close contact with the intestinal mucosa (124).

The precise contribution of non-LEE effectors, which were detected in this study, to the pathogenesis of clade 8 strains is not known. Previous reports, however, indicate that non-LEE effectors play important roles in virulence of A/E pathogens, such as inhibition of host phagocytosis (55) and suppression of proinflammatory cytokine production (135). The non-LEE effector NleA/EspI, for example, plays a key, but unknown, role in virulence in a *C. rodentium* mouse

infection model (123), and is more commonly found in EHEC strains associated with severe disease, than in strains isolated from asymptomatic carriers (218). Upregulation of non-LEE effectors in clade 8 may be directed by GrlA, as Deng *et al.* have shown that overexpression of GrlA in *C. rodentium* increases expression of at least seven non-LEE effectors (73).

Epidemiological analyses indicate that the association between O157:H7 clade 8 and the most severe sequelae of EHEC infection, HUS, is seven times higher than that of all other clades combined (205). As Shiga toxin is the key virulence determinant in the development of HUS (164, 305), the finding of a > 5-fold higher transcription of Stx2, the most common Stx variant implicated in severe disease (36, 91), in clade 8 was of major interest. Transcription of Stx2 is connected to prophage induction, which is initiated through the bacterial SOS response pathway (141). Since no genes from the SOS regulon were determined as differentially expressed, increased activation of the *q* antiterminator and subsequent upregulation of *stx2* expression in clade 8 cannot be attributed to SOS-mediated amplification of lysogenic induction in clade 8. Upregulation of *stx2* in clade 8 is also not due to nucleotide polymorphisms in the upstream sequence between the *q* antiterminator and *stx2*. This phage region contains elements that influence RNA polymerase efficiency and that initiate transcription of *stx2* (332), and is conserved among clades.

Discrepant transcription and production of Stx2 in different seropathotypes of Shiga toxin-producing *E. coli* (67), as well as among two distinct lineages of O157:H7 (82) has been recently observed. Furthermore, De Sablet *et al.* imply

that increased transcription of Stx2 could be mediated independently of the SOS system, but instead, due to a high level of spontaneous phage induction (67). Alternatively, unknown bacterial host factors may stimulate *stx2* expression (67), which is a conceivable explanation of our results given the substantial genomic divergence of clade 8 compared to clade 2 (205).

Increased transcription of *stx2* in clade 8 and 2 strains harboring only the Stx2-phage, compared to strains that contain two Stx phages, is consistent with a recent study reported by Serra-Moreno et al. (280). By incorporating two Stx2 prophages into the K12 chromosome, the authors observed a decrease of Stx2 production compared to K12 strains infected with only one Stx2 prophage. This reduction is hypothesized to be mediated by the CI repressors of Stx-phages acting in trans, and ultimately leading to reduced pathogenicity of the host strain (280).

The biological significance of the EHEC-HlyA in the pathogenesis of O157:H7 is not clear (36), although it has been detected in sera from reconvalescent HUS patients (276). Aldick *et al.* have demonstrated a cytotoxic effect of the EHEC-HlyA to human endothelial cells, and suggest that this putative virulence factor contributes to severe disease by destruction of the microcirculatory endothelium (11), the primary tissue affected in HUS (305). Together with increased expression of Stx2, the key agent of endothelial cell damage, upregulation of EHEC-HlyA may, therefore, contribute to the pathogenicity of clade 8.

The present study provides novel evidence that lends support to the hypothesis that a phylogenetically distinct lineage of EHEC O157:H7 is hyper-virulent, based on the enhanced adherence to epithelial cells and elevated expression of virulence determinants. Further investigation is necessary to resolve the intrinsic differences in the finely tuned regulatory networks that confer more efficient adherence, as well as in the factors that determine increased expression of toxin genes in the clade 8 lineage of O157:H7. In conclusion, our findings invite questions that concern incongruent regulation of shared laterally acquired virulence genes, by bacterial host elements, between subpopulations of a highly specialized and adapted pathogen.

ACKNOWLEDGEMENTS

The authors wish to thank James Riordan, Sivapriya Kailasan Vanaja, and Shannon Manning for helpful scientific discussions; Martha Mulks for reading previous versions of the manuscript; and James Riordan for designing *stx2B* specific primers. This project was funded by the NIAID, NIH, DHHS, under NIH research contract N01-AI-30058 (TSW), which supports the STEC Center. This study will be submitted to the Journal of Molecular Microbiology.

CHAPTER 5

Whole genome expression profiles of *Esherichia coli* O157:H7 Sakai in response to treatment with preconditioned media

SUMMARY

Enterohemorrhagic Escherichia coli O157:H7 is responsible for numerous outbreaks of foodborne illness throughout the world, with clinical manifestations ranging from diarrhea, to hemorrhagic colitis and hemolytic uremic syndrome. The low infectious dose that is characteristic of O157:H7 infection is hypothesized to be mediated by quorum sensing of autoinducers (AI), which are secreted by indigenous microbiota that reside in the lower intestines as well as by host intestinal tissue. AI compounds stimulate expression of virulence factors, notably LEE genes that mediate intimate adherence of O157:H7 to the intestinal epithelium. In this study we examined the transcriptome of O157:H7, following its treatment with four different preconditioned (PC) media that were used to culture epithelial cells, or co-culture of epithelial cells infected with EHEC O157:H7, EHEC O26:H11, or the lab-derived K12. Microarray analysis detected 484 significantly differentially expressed genes, 211 of which are of unknown function and 273 are involved in various metabolic pathways. More genes were upregulated in O157:H7 following treatment with co-culture PC media compared to PC media from uninfected epithelial cells, but no significant difference was observed between treatment with the 3 co-culture PC media. No virulence genes were found to be differentially expressed between any of the treatments. Of interest was the upregulation of iron scavenging and genes that confer tellurite resistance and inhibition of phage infection in O157:H7 treated with co-culture PC media, opposed to epithelial cell PC media. Potential flaws of the experimental design that may have obscured our results are discussed.

INTRODUCTION

Enterohemorrhagic *Escherichia coli* (EHEC) O157:H7 is an important cause of food and water borne illness throughout the world. The most common clinical manifestations of O157:H7 infection range between uncomplicated diarrhea and pseudomembranous hemorrhagic colitis (HC) (220). In a proportion of patients (~15%) (305), HC is a prodromal stage that precedes development of the life-threatening hemolytic uremic syndrome (HUS) (246). Colonization of the intestinal mucosa via a type three secretion system (TTSS) and elaboration of cytotoxic Shiga toxins (Stx1, 2 and variants) are hallmarks of O157:H7 pathogenesis.

The ability of O157:H7 to colonize the mucosal epithelium is conferred by a pathogenicity island termed the locus of enterocyte effacement (LEE), which codes for a TTSS, effectors and chaperones, the adhesin intimin and its translocated receptor Tir. Through LEE-encoded colonization factors, O157:H7 intimately adheres to the epithelium, which yields the pathognomonic attaching and effacing (A/E) lesions (115).

Stx are phage-borne two-component toxins that enzymatically depurinate the 28S ribosomal RNA, which blocks protein synthesis and leads to eukaryotic cell death (89, 272). Expression and production of Stx is itself sufficient to mediate HUS, the most serious complication of O157:H7 infection (164, 305)

EHEC O157:H7 disease is characterized by an unusually low infectious dose, which is estimated to be under 100 bacterial cells (314); one outbreak of O157:H7 was estimated to have resulted from ingestion of fewer than 50

organisms (316). The ability of O157:H7 to cause overt human disease following ingestion of so few bacteria is hypothesized to result from bacterial quorum sensing (QS) of signals produced by non-pathogenic *E. coli* that reside in the digestive tract (290). Bacterial cell-to-cell signaling is mediated via autoinducer (AI) molecules that are produced by the *luxS* gene, which is conserved across Gram negative and positive bacteria, including *Escherichia coli*, *Salmonella typhimurium*, *Vibrio spp.*, *Enterococcus faecalis*, *Clostridium spp.*, and *Bacteroides spp.* (274, 300). These AI compounds inform bacterial populations of the cell density and the metabolic potential of the environment (299). It is suggested that QS serves to alert O157:H7 populations when it has reached the large intestine, the major site of EHEC-induced intestinal insult, which is abundant in microbiota that are capable of QS (291).

Through QS, AI molecules stimulate expression of LEE genes in O157:H7 and in enteropathogenic *E. coli* O127:H6, which was demonstrated by cultivation of these pathogens in media preconditioned by growth of luxS+ *E. coli* K12, prior to measurement of transcription and translation of LEE genes (290). The quorum sensing system of O157:H7 can also detect eukaryotic signals, such as the hormone epinephrine that was shown to increase LEE secretion through the QS system (291).

Here we report whole genome expression profiles of O157:H7 following its treatment with media that was used to sustain epithelial cells, or epithelial cells that were infected with EHEC O157:H7, EHEC O26:H11, or the lab-derived K12. The purpose of our study was to resolve whether the transcriptional response of

O157:H7 differs between treatment with media preconditioned with epithelial cells, a co-culture of epithelial cells and a pathogen, and a co-culture of epithelial cells and a non-pathogen.

MATERIALS AND METHODS

Bacterial strains. *Escherichia coli* strains O157:H7 Sakai (136), O26:H11 413/89-1 (72) and K12 MG1655 (35) were stored and cultured as described in Chapter 3.

Preconditioned media. Confluent monolayers of MAC-T bovine mammary epithelial cells (151) were sustained with DMEM media (without fetal bovine serum), for 24-48 h. The preconditioned (PC) DMEM media was collected and passed through a 0.22 µm filter (Millipore Corporation, Billerica, MA). The filtrate was supplemented with 20x DMEM to a final concentration of 0.5x and the pH adjusted to 7.4. PC media was kept frozen at -80 °C and thawed once prior to experiments. DMEM media was also preconditioned with co-cultures of MAC-T cells and *E. coli*. Confluent MAC-T monolayers in DMEM, which was not replaced for 24-48 h, were infected with DMEM cultures of O157:H7 Sakai, O26:H11 413/89-1 or K12 MG1655 in a 1:50 volume ratio and incubated for 3 h. The cell densities of DMEM bacterial cultures that were used to infect MAC-T monolayers were ~ 5×10^5 CFU/ml. After 3 h of co-culture, DMEM media was collected and processed as described above. Altogether, 4 different PC media were generated.

Induction conditions, and microarray hybridizations and analysis. Cultures of O157:H7 Sakai, which had been exponentially growing in 50 ml of DMEM for 2.5 h at 37 °C with shaking, were inoculated with 50 ml of warmed fresh DMEM (mock), or with one of the 4 PC DMEM media. Following additional 30 min of growth, 5 ml of Sakai culture were aliquoted for RNA harvesting, as

described in the Materials and Methods section of Chapter 3. RNA was collected from 5 independent biological replicates of each of the 5 induction experiments. cDNA conversion, Cy-dye labeling, microarray slides and hybridizations were described in Chapter 3. Hybridizations were performed according to the design in Figure 5.1, which allowed direct comparison of any 2 treatments. In total, 50 hybridizations were carried out. As described in Chapter 4, microarray data was fitted to a mixed model ANOVA in R software and the Fs test was used to infer differentially expressed genes among the 5 treatments. Pairwise contrast analysis was used to determine between which specific treatments were the genes differentially expressed, as described in Chapter 4. Quality threshold (QT) clustering of significantly differentially expressed genes, using the Pearson correlation, was performed with the TMEV software version 3.1 (267), with a diameter of 0.4 and minimum cluster size of 5.

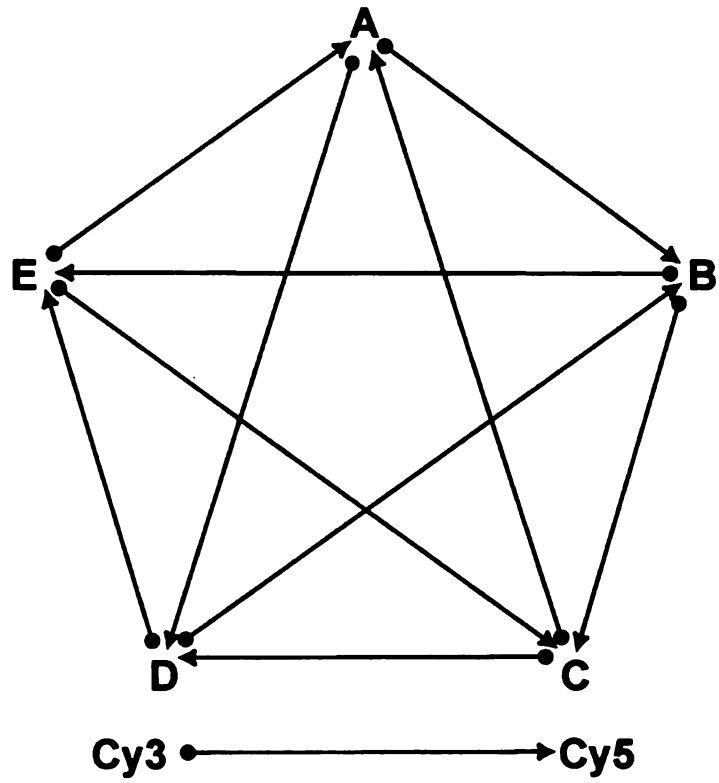

Figure 5.1. Connected double loop hybridization design. Letters A-E represent induction of O157:H7 Sakai with the following PC media: A - MAC-T (24-48h), B - MAC-T + K12 (24-48h + 3h), C - MAC-T + O157:H7 (24-48h + 3h), D - MAC-T + O26:H11 (24-48h + 3h), and E - Fresh DMEM (mock). Ten hybridizations per loop were carried out, with alternate Cy-dye labeling of samples among five biological replications of the experiments for each treatment. In total, 50 hybridizations were performed.

RESULTS

Analyses of expression ratios. Based on an overall Fs test, 484 genes were found to be significantly differentially expressed between O157:H7 Sakai cultures induced with the 5 treatments. Of these, 272 genes are shared between Sakai and K12, and 212 are specific to Sakai. The 484 genes were assigned to functional groups based on the O157:H7 gene function summary in the Qiagen annotation of microarray probes. Almost half of the 484 genes code for hypothetical proteins, whereas the other 273 genes code for proteins involved in various physiological and metabolic functions (Figure 5.2). The majority of differentially expressed genes with known functions are those that code for proteins involved in energy production, transport of carbohydrates, amino acids, ions, and transcription. To identify expression patterns of co-expressed genes, which are indicative of co-regulation in response to a stimuli, expression estimates of the 484 genes were subjected to QT clustering analysis. Most genes were clustered into 9 clusters, and only 19 genes were not classified into any cluster (Figure 5.3). In most clusters, genes upregulated in Sakai cultures treated with PC media from a co-culture of MAC-T with *E. coli* had the same direction of expression. This indicated that treatment with PC media from infected MAC-T cells leads to similar transcriptional responses in Sakai, as opposed to treatment with PC media from uninfected MAC-T monolayers or fresh DMEM.

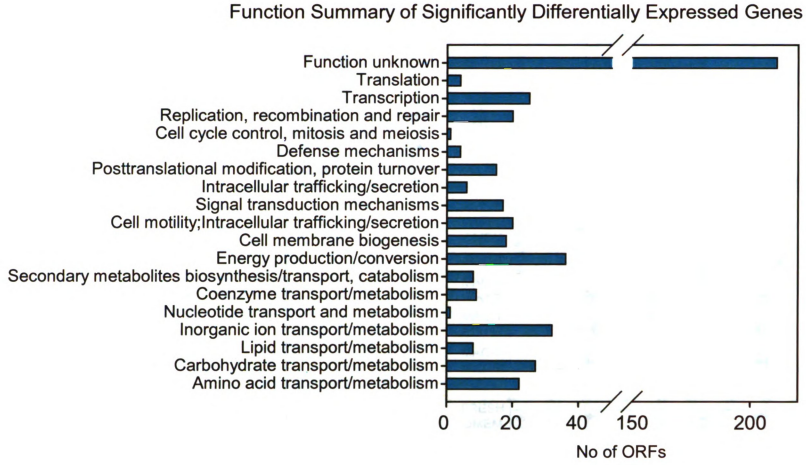

Figure 5.2. Function summary of the 484 significantly differentially expressed genes. Functional groups were based on Qiagen's annotation of the Sakai genome.

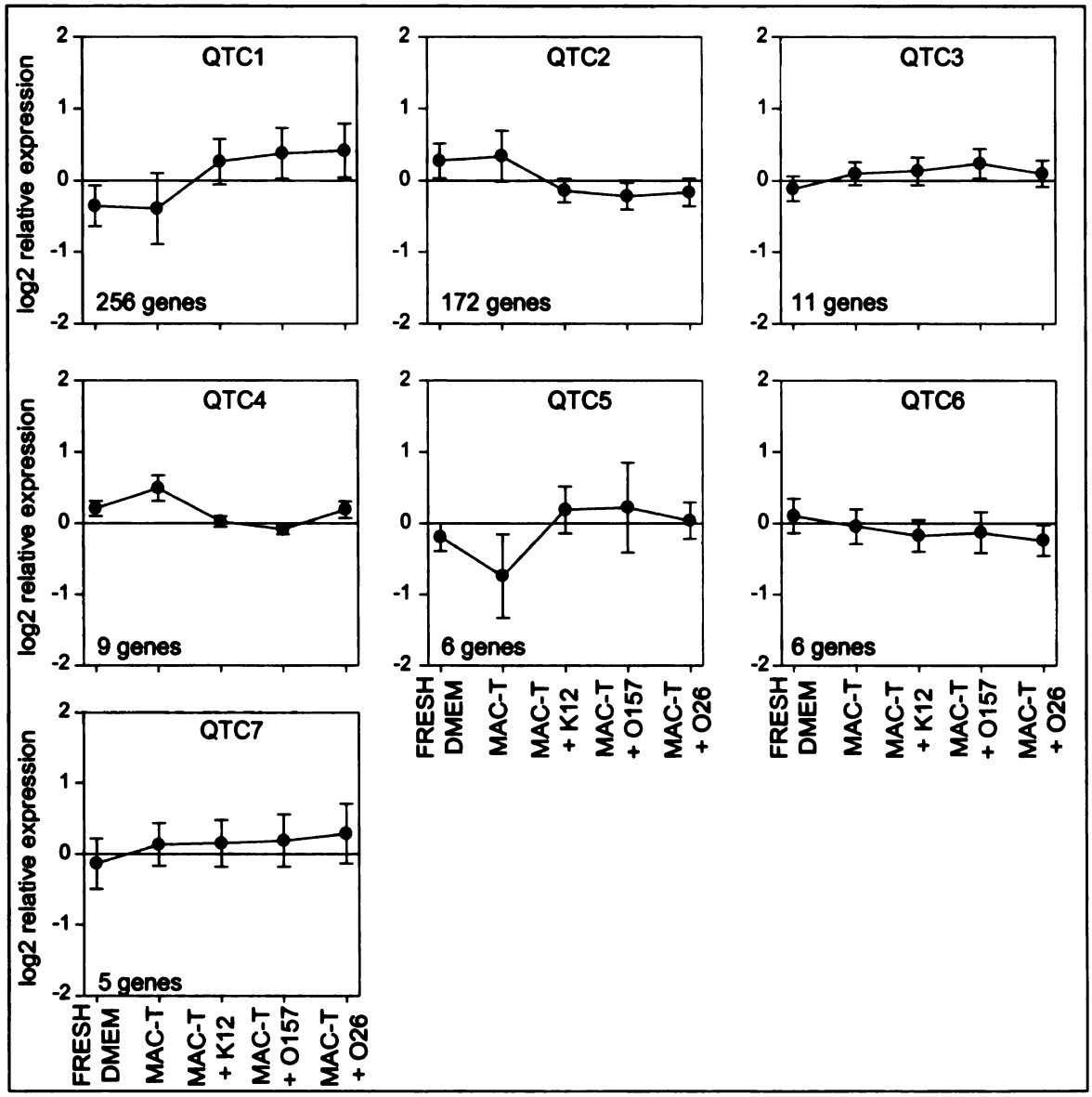

Figure 5.3. Expression profiles of 484 significantly differentially expressed genes classified by QT clustering using the Pearson correlation. In the bottom left corner of each graph is the number of genes belonging to a particular cluster. Of the 484 genes ($p<0.05$) 19 genes were not assigned to any cluster. The horizontal axis represents different preconditioned media treatments.

To determine specifically between which treatments were the genes differentially expressed, pairwise contrast analysis of the microarray data were performed. Table 5.1 summarizes the number of genes that were differentially expressed between the 5 treatments. As indicated by the QT clustering, there were considerable differences in gene expression of Sakai that was treated with PC media from infected compared to uninfected MAC-T cells. However, treatment of Sakai with the three co-culture PC media resulted in similar a number of expressed genes. Furthermore, there were no genes whose differential expression was specific to a particular comparison. Induction of Sakai with PC media from uninfected MAC-T cells was virtually indistinguishable from the mock treatment. Of the shared 50 genes that were found expressed in Sakai in following treatment with PC media from MAC-T cells infected with O157:H7 or O26:H11, 36 genes code for unknown proteins and 16 are metabolic genes. Similarly, of the 21 genes that were co-expressed in Sakai treated with PC media from MAC-T cells infected with O157:H7 or K12, 14 were unknown of which 7 are phage borne, and 7 code for metabolic enzymes.

None of the major virulence factors that mediate the pathogenesis of O157:H7 disease, including the LEE island and Shiga toxin genes, were found to be differentially expressed between any treatments. Differential expression was also not detected in any regulators, putative virulence genes, flagella, or quorum sensing genes (*qseABC*). Potentially interesting was the finding of upregulation of genes involved in iron metabolism in Sakai treated with co-culture PC media; including the *entABCDEF* operon that is involved for enterobactin synthesis,

Table 5.1. Number of genes differentially expressed in Sakai following PC media treatment.

PC media comparison	No. of genes differentially expressed			
	Total	Specific to comparison	MAC-T vs O157 and MAC-T vs O26 (absent in MAC-T vs K12)	MAC-T vs O157 and MAC-T vs K12 (absent in MAC-T vs O26)
DMEM vs K12	261	0		
DMEM vs MACT	6	0		
DMEM vs O157	384	0		
DMEM vs O26	370	0		
K12 vs MACT	202	0		21
K12 vs O157	0	0		
K12 vs O26	0	0		
MACT vs O157	295	0	50	21
MACT vs O26	266	0	50	
O157 vs O26	0	0		

the *fepACDE* operon that codes for enterobactin transport, *fhuA* encoding the ferrichrome receptor, and the *chuASTUWXY* operon that is involved in heme/hemoglobin metabolism. Interaction of O157:H7 or O26:H11 with MAC-T cells can lead to destruction of MAC-T cells, resulting in the release of iron compounds into the PC media which activate iron scavenging genes. This rationale, however, does not explain induction of said genes in Sakai by PC media from a co-culture of MAC-T cells and K12, as this lab-derived *E. coli* is not pathogenic.

The activation of tellurite resistance genes (*terWZADEF*) and the *iha* adhesin in Sakai, following co-culture PC media treatment, was another interesting finding (Figure 5.4). The *ter* operon is located on the tellurite resistance and adherence conferring island (TAI) in the Sakai prophage-like element 4 (SpLE 4). In the past, tellurium compounds have been used as antimicrobial chemotherapeuticals to treat tuberculosis, leprosy, skin, and eye infections, which may explain the evolution of tellurite resistance in bacteria (309). *ter* genes were, however, also shown to confer resistance to pore-forming colicins and bacteriophage infections, as well as protection from host cellular defenses (309). In *Listeria monocytogenes*, for example, a locus coding for tellurite resistance was shown to protect bacteria from reactive nitrogen and oxygen species produced by host phagocytes (21). Mutation of *lmo1967*, a *ter* homologue in *L. monocytogenes*, resulted in decreased virulence, as demonstrated by significant reduction in bacterial recovery from the murine

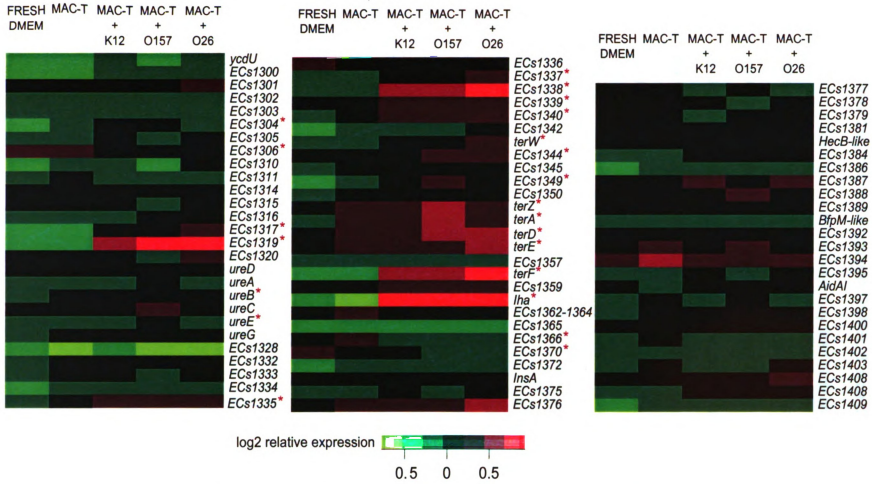

Figure 5.4. Heatmap of the Sakai prophage-like element 1 (SpLE1) that contains the tellurite resistance and adherence confering island (TAI). 22 genes from SpLE1, marked with an asterix, have been found to be significantly differentially expressed in at least one of the treatments. The heatmap was generated from ANOVA gene expression estimates in R sofware ('gplots' package version 2.3.2). ECs – O157:H7 Sakai gene numbers.

spleen and liver following challenge with C57/BL-6 mice (21). Therefore, interaction of the pathogen with the host may lead to secretion of innate host defense mechanisms in the PC media, which in turn activated the *ter* locus in Sakai. Alternatively, the host-pathogen challenge could have led to bacteriophage induction, and upregulation of *ter* genes may have been induced by bacteriophage surface structures in the PC media. The filtration of PC media through a 0.22 um membrane allows passage of small molecules such as phage surface structures into PC media, which may have activated *ter* genes in Sakai.

DISCUSSION

The present study is an attempt to identify O157:H7 virulence genes that are expressed in response to preconditioned cell culture medium, which was used to sustain epithelial cells or epithelial cells infected with *E. coli*. The idea for this experiment stems from the finding that quorum-sensing is a phenomenon that enables bacteria to modulate expression of virulence genes in response to chemical signals from other bacterial populations as well as from the intestinal tissue (291). We also sought to find whether O157:H7 responds differently between PC media from co-cultures of epithelial cells with pathogenic and non-pathogenic *E. coli*.

Our experiment did not yield expected results, which may have occurred due to a flawed experimental design. One of the likely reasons may have been insufficient stimulus from the PC media. PC media was collected from MAC-T cells infected with *E. coli* for 3 h, which may have not been enough time to elicit potent chemical secretion that would in turn induce quantifiable transcription of O157:H7 virulence genes. Also, O157:H7 Sakai cultures were only 'spiked' with PC medium that was not concentrated. Growing Sakai in concentrated PC medium may have induced a detectable difference in transcription of virulence determinants, between different PC media. Another possible flaw was the time of exposure of Sakai cultures to PC media; harvesting of Sakai RNA at a different time point may have revealed the expected differences in transcription of virulence genes.

Several findings did emerge from this research. Microarray measurements indicated that gene expression of O157:H7 differs in response to DMEM medium conditioned with uninfected epithelial cells, opposed to media conditioning with epithelial cells infected with *E. coli*. The majority of differentially expressed genes were unknown, but a considerable proportion of upregulated genes are involved in different metabolic pathways, most notably genes that code for iron scavenging mechanisms. In *Pseudomonas aeruginosa*, a syderophore termed pyoverdine was shown to act as a signaling molecule in regulating expression of major virulence genes, implicating iron uptake in bacterial cross-talk (191). Also of potential interest was the upregulation of the *ter* operon, which confers tellurite and colicin resistance, and inhibition of bacteriophage infection. Given the importance of iron scavenging in pathogenic bacteria, the conservation of *ter* genes across bacterial species (309, 310), and their co-activation by PC media conditioned with infected epithelial cell, the role of these genetic elements in EHEC pathogenesis warrants future investigation.

CHAPTER 6

Summary and Synthesis

The overall goals of the research described here were to assess the genomic composition of EHEC 2 lineages, and to characterize the virulence properties that are associated with the variation in severity of EHEC O157:H7 infections. The advantage of these studies is the use of multiple representatives of EHEC lineages, which allows conclusions to be drawn at a population level.

There are numerous STEC serotypes that have never been associated with illness. Even the LEE- and Stx2-positive O55:H7, the inferred O157:H7 progenitor, is seldom associated with disease and has never been implicated in an outbreak. Comparative genomic analysis of EHEC 2 serotypes that are most frequently associated with disease has advanced our knowledge about the cladogenesis of this clonal complex, and its relatedness to the EHEC 1 clone.

To probe the genome content of the EHEC 2 serotypes, genomic microarrays that target O157:H7 gene sequences were utilized. The hybridization data was used to compare the genetic similarity between O157:H7 and EHEC 2, as well as the inter-strain relatedness within EHEC 2. This assessment demonstrated a high level of similarity in genome composition between O157:H7 and EHEC 2, which may account for the ability of EHEC 2 and O157:H7 to cause similar disease in humans.

The O157:H7 'backbone' (shared with K12) genes are virtually fully conserved in EHEC 2, whereas the non-phage O157:H7 'specific' genes are found in significantly lower numbers in this population. The latter is likely a consequence of vertical transfer of genes that are specific to the EHEC 1 clone, which is consistent with the inference of parallel evolution of EHEC 1 and 2

clonal groups (255). The comparative genomic hybridization data also indicate that the EHEC 2 population is diverse. The distribution of O157:H7 phage borne genes was found to be heterogeneous among EHEC 2, implying that the plasticity of the EHEC 2 pan-genome is significantly influenced by the promiscuous exchange of foreign DNA.

Phylogenetic analysis of compatible genes, genes that are indicative of vertical transfer, demonstrates a serotype-specific homogeneity of O111:H8 and O118:H16 strains, whereas O26:H11 strains are considerably more diverse. Serotype O26:H11 is also characterized with the highest inter-strain variation in phage borne gene content, compared to the more uniform O111:H8 and O118:H16. This suggests that the genetic make-up of the O26:H11 lineage is such that it allows more frequent recombination of lateral elements, which can result in acquisition of novel fitness and virulence genes by O26:H11 more commonly than by other EHEC 2. For example, O26:H11 possess the *Yersinia spp.* high pathogenicity island (HPI) that encodes the iron-uptake siderophore yersiniabactin and its receptor, whereas other EHEC serotypes, including O157:H7, O111:H-, O103:H2, and O145:H-, do not have this HPI (165).

Ultimately, a hypervirulent subpopulation of EHEC 2 is more likely to evolve from O26:H11 rather than other EHEC 2 lineages. Researchers in Europe already warn of the emergence of a potentially highly pathogenic EHEC O26:H11 lineage, which is associated with multiple outbreaks, has distinct genotypic characteristics and, uncommonly for EHEC 2, produces only the Stx2 toxin (32).

Variation in virulence of O157:H7. The *in vitro* model of the host-pathogen interaction, which was used for transcriptional profiling of O157:H7, represents a controlled environment that provides optimal stimuli for inducing virulence gene expression in bacteria, such as contact with epithelial cells, ion and nutrient availability. Harvesting bacterial RNA following infection of epithelial cells with O157:H7, but prior to intimate adherence, allows investigation of the early events of the bacterial infection process, at the transcriptional level.

The comparison of adherence potential and virulence gene expression between the two O157:H7 outbreak strains has provided insight into the pathogenic mechanisms that underlie differences in the ability of O157:H7 strains to cause severe disease. Rapid adhesion of O157:H7 Spinach to the epithelium may facilitate more efficient colonization of the intestine and evasion of competitive exclusion by other intestinal microbiota, compared to Sakai. A 4-fold increase in Shiga toxin transcription in O157:H7 Spinach, coupled with a superior colonization phenotype, lends support to the inference that this O157:H7 strain is capable of mediating more fulminant disease than O157:H7 Sakai.

The advantage of studying bacterial pathogenesis in a phylogenetic context is that it helps identify common and unique strategies used by subpopulations of microbial pathogens to colonize the host and mediate disease. The work by Manning *et al.* has correlated the epidemiological variation in severity of O157:H7 illness with the existence of multiple distinct lineages of O157:H7 (clades 1-9) (205). Examination of the pathogenic potential of population samples of clade 8 (n = 12) and clade 2 (n = 12) is in agreement with

the epidemiological implications about the hypervirulence of O157:H7 clade 8. Furthermore, the findings of this study supported the inference that the difference in colonization capacity and virulence gene expression among O157:H7 strains is associated with lineage-specific differences between O157:H7 subpopulations.

Previously, variation in disease severity of O157:H7 infection was mainly attributed to the presence of different Shiga toxin variants (156, 233). The clade comparison study revealed a 5-fold increase in the expression of the shared Shiga toxin variant, Stx2, in clade 8 relative to clade 2. Although expression of Stx genes is linked to the bacterial SOS response to DNA damage, genes of the SOS regulon were not differentially expressed between clades. Clade 8 is also characterized by a greater ability to adhere to the host epithelium. These results imply incongruent regulation of shared, laterally acquired virulence traits by unknown intrinsic factors that are specific to particular lineages of O157:H7.

This is the first large scale, whole-genome study of differential expression of O157:H7 genes within a phylogenetic framework that represents the extant genetic diversity of the O157:H7 population. Appreciating the molecular basis of the hypervirulent potential of O157:H7 subpopulations is crucial for the development of preventative and therapeutic measures that aim to decrease the threat imposed by O157:H7 infection. As more data are collected, this study will contribute to the greater body of knowledge about the variation in virulence between subpopulations of bacterial species, which is ultimately a reflection of the 'relentless' evolution of microbial pathogens (262).

Future considerations. Several interesting questions concerning EHEC pathogenesis have emerged from this work. Comparative genomic assessment of the EHEC 2 clone implies that the LEE pathogenicity island has diverged between human and animal clinical EHEC 2 strains. An extension of that work could be to compare LEE nucleotide sequences between EHEC 2 associated with human and animal disease. This would help determine the extent to which host species adaptation influences the nucleotide diversity of EHEC genes involved in bacterial colonization of the host.

The inverse expression of LEE and flagellar genes in O157:H7 Spinach and Sakai strains, respectively, suggests that the expression of adhesion and motility genes between the two strains is not synchronized. More conclusive findings could be obtained by a longitudinal study of epithelial cell colonization, and expression of LEE and flagellar genes with the two O157:H7 strains. These data would resolve whether the observed discrepancy is a consequence of inherent over-expression of LEE in the Spinach strain, or whether there is an actual temporal lag in Sakai, relative to Spinach, that results in a delayed switch from flagellar to LEE expression. The latter inference is supported by the finding that 30 min post-infection the association levels of both strains are similar, following an increase in association of Spinach at the 1 h timepoint.

Differential expression of Stx2 between seropathotypes of STEC (67) and between distinct lineages of O157:H7 (82) has recently been implied. Overexpression of Shiga toxin 2 in the O157:H7 clade 8 lineage is in agreement with these observations. These data raise interesting questions about the effect

of divergent evolution on the regulation of laterally acquired elements by bacterial host factors. To reject the hypothesis that increased expression of Stx2 is solely due to polymorphisms in the Stx-converting phages between clades 8 and 2, it is necessary to test Stx2 expression in an identical bacterial host. One approach would be to transduce *E. coli* K12, or the O55:H7 progenitor of O157:H7, with Stx2-converting phages from clade 8 and 2. By modification of a previously described method (279, 280), the *stx2A* gene can be inactivated while the *stx2B* remains intact to avoid generation of pathogenic bacteria. Differential expression of Stx2 between recipients, which are transduced with either clade 8 and clade 2 Stx2-phages, would point to phage borne differences. Variation in Stx2 transcript levels between transductant and donor strains would imply a background effect.

E. coli are probably one of the most studied and utilized bacterial species. However, its extensive genomic diversity, relentless evolution, and dissemination into new niches offers ample opportunity to test new hypotheses regarding microbial pathogenesis, host specificity, and regulation of foreign DNA by chromosomal elements.

APPENDICES

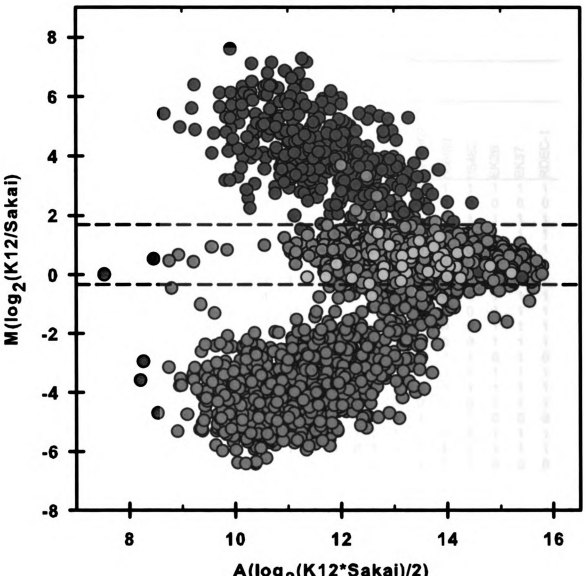

Figure A1. *M* versus *A* plot for two-color hybridization of O157:H7 Sakai and K-12 MG1655. Based on in silico analysis of single copy targets, 5222 probes (13 probes of the 5235 were excluded due to low intensity signal) were classified into 5 groups: grey, identical targets in both genomes (n=3585); red, Sakai-only targets (n=1002): green, K12-only targets (n=425); yellow, Sakai-like targets (n=41); cyan, K12-like targets (n=169). For Sakai-like and K12-like probes, homologous target sequences occur in both genomes but have diverged in sequence up to 20%. Dashed lines represent the GACK cutoffs of 0.1 for inferring absence or presence. Probes between the cutoffs have targets in both genomes; other probes are present in one strain only. Sakai-only (red) and K12-only (green) probes that fall between the GACK cutoffs reflect the false negative rate of CGH; probes with targets in both genomes (grey, cyan and yellow) that fall outside the GACK cutoffs reflect the false positive rate of CGH.

Table A1. Distribution of phylogenetically compatible genes in EHEC 2, determined with the clique program in the PHYLIP package.

ECs[a]	EHEC 2 strains[b]																							
	DEC9f	DEC10e	F5863	97-3250	413/89-1	DA-22	03-ST-296	CB7505	DEC8c	DEC8d	C408	BCL71	ML178190	W29104	EK34	EK35	RW2030	RW1302	666/89	05482	EK36	EK37	RDEC-1	02-3751
0182	0	0	0	0	1	1	1	1	1	1	1	1	1	1	0	0	1	1	1	1	1	1	1	1
0260	0	0	0	0	0	0	0	0	0	0	0	1	0	1	0	0	0	0	0	0	0	0	0	0
0261	0	0	0	0	1	1	1	1	1	1	1	0	1	0	1	1	1	1	1	1	1	1	1	1
0305	0	0	0	0	1	1	1	1	1	1	1	1	1	1	0	0	0	0	0	0	1	1	1	1
0313	0	0	0	0	1	1	1	1	1	1	1	1	1	1	0	0	0	0	0	0	1	1	1	1
0314	0	0	0	0	1	1	1	1	1	1	1	1	1	1	0	0	0	0	0	0	1	1	1	1
0319	0	0	0	0	1	1	1	1	1	1	1	1	1	1	0	0	0	0	0	0	1	1	1	1
0320	0	0	0	0	1	1	1	1	1	1	1	1	1	1	0	0	0	0	0	0	1	1	1	1
0323	0	0	0	0	1	1	1	1	1	1	1	1	1	1	0	0	0	0	0	0	1	1	1	1
0324	0	0	0	0	1	1	1	1	1	1	1	1	1	1	0	0	0	0	0	0	1	1	1	1
0500	0	0	0	0	1	1	1	1	1	1	1	1	1	1	1	1	0	0	0	0	1	1	1	1
0523	0	0	0	0	1	1	1	1	1	1	1	1	1	1	1	1	1	1	1	1	0	1	0	1
0870	0	0	0	0	1	1	1	1	1	1	1	0	1	0	1	1	1	1	1	1	1	1	1	1
1848	0	0	0	0	1	1	1	1	1	1	1	0	1	0	1	1	1	1	1	1	1	1	1	1
2118	0	0	0	0	1	1	1	1	1	1	1	1	1	1	0	0	0	0	0	0	1	1	1	1
2131	0	0	0	0	1	1	1	1	1	1	1	1	1	1	1	1	1	1	1	1	0	0	0	0
2343	0	0	0	0	1	1	1	1	1	1	1	0	1	0	1	1	1	1	1	1	1	1	1	1
2659	0	0	0	0	1	1	1	1	1	1	1	1	1	1	0	0	0	0	0	0	1	1	1	1
2705	0	0	0	0	1	1	1	1	1	1	1	1	1	1	1	1	1	1	1	1	0	0	0	0
2777	0	0	0	0	1	1	1	1	1	1	1	1	1	1	0	0	0	0	0	0	1	1	1	1
2811	0	0	0	0	1	1	1	1	1	1	1	1	1	1	1	1	1	1	1	1	1	0	1	0
2817	0	0	0	0	1	1	1	1	1	1	1	1	1	1	1	1	1	0	1	0	1	1	1	1
2822	0	0	0	0	1	1	1	1	1	1	1	1	1	1	0	0	0	0	0	0	1	1	1	1
2895	0	0	0	0	1	1	1	1	1	1	1	0	1	0	1	1	1	1	1	1	1	1	1	1
3159	0	0	0	0	1	1	1	1	1	1	1	0	1	0	1	1	1	1	1	1	1	1	1	1
3368	0	0	0	0	1	1	1	1	1	1	1	1	1	1	1	1	1	0	1	0	1	1	1	1
3414	0	0	0	0	1	1	1	1	1	1	1	0	1	0	1	1	1	1	1	1	1	1	1	1
4267	0	0	0	0	1	1	1	1	0	1	1	1	0	1	1	1	1	1	1	1	1	1	1	1
4422	0	0	0	0	1	1	1	1	1	1	1	1	1	1	1	1	1	0	1	0	1	1	1	1
4593	0	0	0	0	1	1	1	1	1	1	1	0	1	0	1	1	1	1	1	1	1	1	1	1
5111	0	0	0	0	1	1	1	1	1	1	1	1	1	1	0	0	0	0	0	0	1	1	1	1
5114	0	0	0	0	1	1	1	1	1	1	1	1	1	1	0	0	0	0	0	0	1	1	1	1
5235	0	0	0	0	1	1	1	1	1	1	1	1	1	1	1	1	0	0	0	0	1	1	1	1
5268	0	0	0	0	1	1	1	1	1	1	1	0	1	0	1	1	1	1	1	1	1	1	1	1
5269	0	0	0	0	1	1	1	1	1	1	1	0	1	0	1	1	1	1	1	1	1	1	1	1
5279	0	0	0	0	1	1	1	1	1	1	1	0	1	0	1	1	1	1	1	1	1	1	1	1
5336	0	0	0	0	1	1	1	1	1	1	1	0	1	0	1	1	1	1	1	1	1	1	1	1
5352	0	0	0	0	1	1	1	1	1	1	1	0	1	0	1	1	1	1	1	1	1	1	1	1
5358	0	0	0	0	0	1	1	1	1	1	1	1	1	1	1	1	1	1	1	1	1	1	1	1
1616	0	0	0	0	1	1	1	1	1	1	1	1	1	1	0	0	0	0	0	0	1	1	1	1
1617	0	0	0	0	1	1	1	1	1	1	1	1	1	1	0	0	0	0	0	0	1	1	1	1
1619	0	0	0	0	1	1	1	1	1	1	1	1	1	1	0	0	0	0	0	0	1	1	1	1
1627	0	0	0	0	1	0	0	1	0	0	1	0	0	0	0	0	0	0	0	0	0	0	0	0
1396	0	0	0	0	1	1	1	1	1	1	1	1	1	1	0	0	0	0	0	0	1	1	1	1

Appendix 1. continued

ECs[a]	EHEC 2 strains[b]																							
	DEC9f	DEC10e	F5863	97-3250	413/89-1	DA-22	03-ST-296	CB7505	DEC8c	DEC8d	C408	BCL71	ML178190	W29104	EK34	EK35	RW2030	RW1302	666/89	05482	EK36	EK37	RDEC-1	02-3751
2961	0	0	0	0	0	0	0	0	0	0	0	0	0	0	1	1	1	1	1	1	0	0	0	0
1626	0	0	0	0	1	0	0	1	0	0	1	0	0	0	0	0	0	0	0	0	0	0	0	0
1628	0	0	0	0	1	1	1	1	1	1	1	1	1	1	1	1	0	0	0	0	1	1	1	1
3484	0	0	0	0	1	1	1	1	1	1	1	1	1	1	1	1	0	0	0	0	1	1	1	1
1514	0	0	0	0	0	0	0	0	0	0	0	1	0	1	0	0	0	0	0	0	0	0	0	0
1400	0	0	0	0	0	1	1	1	1	1	1	1	1	1	1	1	1	1	1	1	1	1	1	1
0278	0	0	0	0	1	1	1	1	1	1	1	1	1	1	0	0	0	0	0	0	1	1	1	1
1612	0	0	0	0	1	1	1	1	1	1	1	1	1	1	0	0	0	0	0	0	1	1	1	1
1613	0	0	0	0	1	1	1	1	1	1	1	1	1	1	0	0	0	0	0	0	1	1	1	1
1620	0	0	0	0	0	0	0	0	0	0	0	1	0	1	0	0	0	0	0	0	0	0	0	0
1777	0	0	0	0	0	1	1	1	1	1	1	1	1	1	1	1	1	1	1	1	1	1	1	1
2191	0	0	0	0	0	1	1	1	1	1	1	1	1	1	1	1	1	1	1	1	1	1	1	1
2197	0	0	0	0	0	1	1	1	1	1	1	1	1	1	1	1	1	1	1	1	1	1	1	1
2729	0	0	0	0	0	1	1	1	1	1	1	1	1	1	1	1	1	1	1	1	1	1	1	1
2748	0	0	0	0	0	1	1	1	1	1	1	1	1	1	1	1	1	1	1	1	1	1	1	1
2755	0	0	0	0	0	1	1	0	0	1	0	1	0	1	0	0	0	0	0	0	0	0	0	0
2762	0	0	0	0	0	1	1	0	0	1	0	0	0	0	0	0	0	0	0	0	0	0	0	0
2763	0	0	0	0	0	1	1	0	0	1	0	0	0	0	0	0	0	0	0	0	0	0	0	0
2764	0	0	0	0	0	0	1	0	0	1	0	0	0	0	0	0	0	0	0	0	0	0	0	0
2999	0	0	0	0	1	1	1	1	1	1	1	1	1	1	0	0	0	0	0	0	1	1	1	1
3000	0	0	0	0	1	1	1	1	1	1	1	1	1	1	0	0	0	0	0	0	1	1	1	1
3001	0	0	0	0	1	1	1	1	1	1	1	1	1	1	0	0	0	0	0	0	1	1	1	1
2800	0	0	0	0	0	0	0	0	0	0	0	0	0	0	1	1	1	1	1	1	0	0	0	0
1188	0	0	0	0	0	0	0	0	0	0	0	0	0	0	1	1	1	1	1	1	0	0	0	0
1189	0	0	0	0	0	0	0	0	0	0	0	0	0	0	1	1	1	1	1	1	0	0	0	0
1644	0	0	0	0	1	1	1	1	1	1	1	1	1	1	0	0	0	0	0	0	1	1	1	1
1647	0	0	0	0	1	1	1	1	1	1	1	1	1	1	0	0	0	0	0	0	1	1	1	1
4551	0	0	0	0	1	1	1	1	1	1	1	0	1	0	1	1	1	1	1	1	1	1	1	1
4552	0	0	0	0	1	1	1	1	1	1	1	0	1	0	1	1	1	1	1	1	1	1	1	1
4565	0	0	0	0	0	0	0	0	0	0	0	0	0	0	0	0	1	1	1	1	0	0	0	0
4566	0	0	0	0	0	0	0	0	0	0	0	0	0	0	0	0	0	1	1	1	0	0	0	0
4574	0	0	0	0	0	0	0	0	0	0	0	0	0	0	0	0	1	1	1	1	0	0	0	0
4576	0	0	0	0	0	0	0	0	0	0	0	0	0	0	0	0	1	1	1	1	0	0	0	0
4591	0	0	0	0	0	0	0	0	0	0	0	0	0	0	0	0	0	1	1	1	0	0	0	0
3849	0	0	0	0	0	0	0	0	0	0	0	0	0	0	1	1	1	1	1	1	0	0	0	0
3850	0	0	0	0	0	0	0	0	0	0	0	0	0	0	1	1	1	1	1	1	0	0	0	0
3857	0	0	0	0	1	1	1	1	1	1	1	0	1	0	1	1	1	1	1	1	1	1	1	1
3859	0	0	0	0	1	1	1	1	1	1	1	0	1	0	1	1	1	1	1	1	1	1	1	1
3870	0	0	0	0	1	1	1	1	1	1	1	1	1	1	0	0	0	0	0	0	1	1	1	1
0140	0	0	0	0	0	0	0	0	0	0	0	1	0	1	0	0	0	0	0	0	0	0	0	0
0215	0	0	0	0	0	0	0	0	0	0	0	1	0	1	0	0	0	0	0	0	0	0	0	0
0225	0	0	0	0	1	1	1	1	1	1	1	0	1	0	1	1	1	1	1	1	1	1	1	1
0462	0	0	0	0	0	0	0	0	0	0	0	1	0	1	0	0	0	0	0	0	0	0	0	0
1287	0	0	0	0	0	0	0	0	0	0	0	1	0	1	0	0	0	0	0	0	0	0	0	0
1288	0	0	0	0	0	0	0	0	0	0	0	1	0	1	0	0	0	0	0	0	0	0	0	0
1296	0	0	0	0	0	0	0	0	0	0	0	1	0	1	0	0	0	0	0	0	0	0	0	0

Appendix 1. continued

ECs[a]	EHEC 2 strains[b]																						
	DEC9f	DEC10e	F5863	97-3250	413/89-1	DA-22	03-ST-296	CB7505	DEC8c	DEC8d	C408	BCL71	ML178190	W29104	EK34	EK35	RW2030	RW1302	866/89	05482	EK36	EK37	RDEC-1	02-3751
1908	0	0	0	0	1	1	1	1	1	1	1	0	1	0	1	1	1	1	1	1	1	1	1	1
2006	0	0	0	0	0	0	0	0	0	0	0	1	0	1	0	0	0	0	0	0	0	0	0	0
2017	0	0	0	0	0	0	0	0	0	0	0	1	0	1	0	0	0	0	0	0	0	0	0	0
2287	0	0	0	0	1	1	1	1	1	1	1	0	1	0	1	1	1	1	1	1	1	1	1	1
3591	0	0	0	0	1	1	1	1	1	1	1	0	1	0	1	1	1	1	1	1	1	1	1	1
3717	0	0	0	0	1	1	1	1	1	1	1	0	1	0	1	1	1	1	1	1	1	1	1	1
3723	0	0	0	0	1	1	1	1	1	1	1	0	1	0	1	1	1	1	1	1	1	1	1	1
3724	0	0	0	0	1	1	1	1	1	1	1	0	1	0	1	1	1	1	1	1	1	1	1	1
3725	0	0	0	0	1	1	1	1	1	1	1	0	1	0	1	1	1	1	1	1	1	1	1	1
3914	0	0	0	0	0	0	0	0	0	0	0	1	0	1	0	0	0	0	0	0	0	0	0	0
3916	0	0	0	0	0	0	0	0	0	0	0	1	0	1	0	0	0	0	0	0	0	0	0	0
3917	0	0	0	0	0	0	0	0	0	0	0	1	0	1	0	0	0	0	0	0	0	0	0	0
4501	0	0	0	0	1	1	1	1	1	1	1	0	1	0	1	1	1	1	1	1	1	1	1	1
4748	0	0	0	0	1	1	1	1	1	1	1	0	1	0	1	1	1	1	1	1	1	1	1	1
4827	0	0	0	0	0	0	0	0	0	0	0	1	0	1	0	0	0	0	0	0	0	0	0	0
0276	0	0	0	0	0	0	0	0	0	0	0	1	0	1	0	0	0	0	0	0	0	0	0	0
0825	0	0	0	0	1	0	0	1	0	0	1	0	0	0	0	0	0	0	0	0	0	0	0	0
0826	0	0	0	0	1	0	0	1	0	0	1	0	0	0	0	0	0	0	0	0	0	0	0	0
0828	0	0	0	0	1	0	0	1	0	0	1	0	0	0	0	0	0	0	0	0	0	0	0	0
0829	0	0	0	0	1	0	0	1	0	0	1	0	0	0	0	0	0	0	0	0	0	0	0	0
0832	0	0	0	0	1	0	0	1	0	0	1	0	0	0	0	0	0	0	0	0	0	0	0	0
0834	0	0	0	0	1	0	0	1	0	0	1	0	0	0	0	0	0	0	0	0	0	0	0	0
0835	0	0	0	0	1	0	0	1	0	0	1	0	0	0	0	0	0	0	0	0	0	0	0	0
0836	0	0	0	0	1	0	0	1	0	0	1	0	0	0	0	0	0	0	0	0	0	0	0	0
0837	0	0	0	0	1	0	0	1	0	0	1	0	0	0	0	0	0	0	0	0	0	0	0	0
0838	0	0	0	0	1	0	0	1	0	0	1	0	0	0	0	0	0	0	0	0	0	0	0	0
1167	0	0	0	0	0	0	0	0	0	0	0	0	0	0	1	1	1	1	1	1	0	0	0	0
1200	0	0	0	0	1	1	1	1	1	1	1	0	1	0	1	1	1	1	1	1	1	1	1	1
1515	0	0	0	0	0	0	0	0	0	0	0	1	0	1	0	0	0	0	0	0	0	0	0	0
1560	0	0	0	0	1	1	1	1	1	1	1	1	1	1	1	1	0	0	0	0	1	1	1	1
1568	0	0	0	0	0	1	1	1	1	1	1	1	1	1	1	1	1	1	1	1	1	1	1	1
1582	0	0	0	0	0	0	0	0	0	0	0	1	0	1	0	0	0	0	0	0	0	0	0	0
1584	0	0	0	0	0	0	0	0	0	0	0	1	0	1	0	0	0	0	0	0	0	0	0	0
1650	0	0	0	0	1	1	1	1	1	1	1	1	1	1	0	0	0	0	0	0	1	1	1	1
1654	0	0	0	0	0	0	0	0	0	0	0	1	0	1	0	0	0	0	0	0	0	0	0	0
1655	0	0	0	0	0	0	0	0	0	0	0	1	0	1	0	0	0	0	0	0	0	0	0	0
1758	0	0	0	0	1	1	1	1	1	1	1	0	1	0	1	1	1	1	1	1	1	1	1	1
1765	0	0	0	0	1	1	1	1	1	1	1	0	1	0	1	1	1	1	1	1	1	1	1	1
1766	0	0	0	0	1	1	1	1	1	1	1	0	1	0	1	1	1	1	1	1	1	1	1	1
1778	0	0	0	0	0	1	1	1	1	1	1	1	1	1	1	1	1	1	1	1	1	1	1	1
1779	0	0	0	0	0	1	1	1	1	1	1	1	1	1	1	1	1	1	1	1	1	1	1	1
1824	0	0	0	0	1	1	1	1	1	1	1	0	1	0	1	1	1	1	1	1	1	1	1	1
2196	0	0	0	0	0	1	1	1	1	1	1	1	1	1	1	1	1	1	1	1	1	1	1	1
2201	0	0	0	0	0	1	1	1	1	1	1	1	1	1	1	1	1	1	1	1	1	1	1	1
2208	0	0	0	0	1	0	0	0	0	0	0	0	0	0	0	0	0	0	0	0	0	0	0	0
2209	0	0	0	0	1	0	0	0	0	0	0	0	0	0	0	0	0	0	0	0	0	0	0	0
2211	0	0	0	0	0	1	1	1	1	1	1	1	1	1	1	1	1	1	1	1	1	1	1	1

Appendix 1. continued

ECs[a]	EHEC 2 strains[b]																									
	DEC9f	DEC10e	F5863	97-3250	413/89-1	DA-22	03-ST-296	CB7505	DEC8c	DEC8d	C408	BCL71	ML178190	W29104	EK34	EK35	RW2030	RW1302	666/89	05482	EK36	EK37	RDEC-1	02-3751
2225	0	0	0	0	1	1	1	1	1	1	1	1	1	1	0	0	0	0	0	0	1	1	1	1
2635	0	0	0	0	0	0	0	0	0	0	0	0	0	0	1	1	0	0	0	0	0	0	0	0
2757	0	0	0	0	0	1	1	0	0	1	0	0	0	0	0	0	0	0	0	0	0	0	0	0
2759	0	0	0	0	0	1	1	0	0	1	0	0	0	0	0	0	0	0	0	0	0	0	0	0
2761	0	0	0	0	0	1	1	0	0	1	0	0	0	0	0	0	0	0	0	0	0	0	0	0
2765	0	0	0	0	0	1	1	0	0	1	0	0	0	0	0	0	0	0	0	0	0	0	0	0
2766	0	0	0	0	0	1	1	0	0	1	0	0	0	0	0	0	0	0	0	0	0	0	0	0
2992	0	0	0	0	0	0	0	0	0	0	0	1	0	1	0	0	0	0	0	0	0	0	0	0
3009	0	0	0	0	0	0	0	0	0	0	0	0	0	0	1	1	1	1	1	1	0	0	0	0
3506	0	0	0	0	0	0	0	0	0	0	0	1	0	1	0	0	0	0	0	0	0	0	0	0

a – E. coli O157:H7 Sakai gene numbers

b – Conserved genes have a value of 1 and divergent/absent have a value of 0.

REFERENCES

REFERENCES

1. 1995. Community outbreak of hemolytic uremic syndrome attributable to *Escherichia coli* O111:NM--South Australia 1995. MMWR Morb Mortal Wkly Rep **44**:550-1, 557-8.

2. 2000. *Escherichia coli* O111:H8 outbreak among teenage campers--Texas, 1999. MMWR Morb Mortal Wkly Rep **49**:321-4.

3. 1995. *Escherichia coli* O157:H7 outbreak linked to commercially distributed dry-cured salami--Washington and California, 1994. MMWR Morb Mortal Wkly Rep **44**:157-60.

4. 2008. European Centre for Disease Prevention and Control: Annual Epidemiological Report on Communicable Diseases in Europe 2008. European Centre for Disease Prevention and Control.

5. 2004. FoodNet Surveillance Report for 2004 (Final Report). FoodNet Foodborne Diseases Active Surveillance Network CDC's Emerging Infections Program.

6. 2006. Ongoing multistate outbreak of *Escherichia coli* serotype O157:H7 infections associated with consumption of fresh spinach--United States, September 2006. MMWR Morb Mortal Wkly Rep **55**:1045-6.

7. 1995. Outbreak of acute gastroenteritis attributable to *Escherichia coli* serotype O104:H21--Helena, Montana, 1994. MMWR Morb Mortal Wkly Rep **44**:501-3.

8. 1993. Update: multistate outbreak of *Escherichia coli* O157:H7 infections from hamburgers--western United States, 1992-1993. MMWR Morb Mortal Wkly Rep **42**:258-63.

9. 1998. Presented at the Zoonotic non-O157 Shiga-toxin producing *Escherichia coli* (STEC) World Health Organization Scientific Working Group, 23-26 June, Berlin, Germany.

10. **Abe, H., I. Tatsuno, T. Tobe, A. Okutani, and C. Sasakawa.** 2002. Bicarbonate ion stimulates the expression of locus of enterocyte effacement-encoded genes in enterohemorrhagic *Escherichia coli* O157:H7. Infect Immun **70**:3500-9.

11. **Aldick, T., M. Bielaszewska, W. Zhang, J. Brockmeyer, H. Schmidt, A. W. Friedrich, K. S. Kim, M. A. Schmidt, and H. Karch.** 2007. Hemolysin from Shiga toxin-negative *Escherichia coli* O26 strains injures microvascular endothelium. Microbes Infect **9**:282-90.

12. **Allen-Vercoe, E., and M. J. Woodward.** 1999. The role of flagella, but not fimbriae, in the adherence of *Salmonella enterica* serotype Enteritidis to chick gut explant. J Med Microbiol **48:**771-80.

13. **Allerberger, F., A. W. Friedrich, K. Grif, M. P. Dierich, H. J. Dornbusch, C. J. Mache, E. Nachbaur, M. Freilinger, P. Rieck, M. Wagner, A. Caprioli, H. Karch, and L. B. Zimmerhackl.** 2003. Hemolytic-uremic syndrome associated with enterohemorrhagic *Escherichia coli* O26:H infection and consumption of unpasteurized cow's milk. Int J Infect Dis **7:**42-5.

14. **Altschul, S. F., W. Gish, W. Miller, E. W. Myers, and D. J. Lipman.** 1990. Basic local alignment search tool. J Mol Biol **215:**403-10.

15. **Andreoli, S. P., H. Trachtman, D. W. Acheson, R. L. Siegler, and T. G. Obrig.** 2002. Hemolytic uremic syndrome: epidemiology, pathophysiology, and therapy. Pediatr Nephrol **17:**293-8.

16. **Anjum, M. F., S. Lucchini, A. Thompson, J. C. Hinton, and M. J. Woodward.** 2003. Comparative genomic indexing reveals the phylogenomics of *Escherichia coli* pathogens. Infect Immun **71:**4674-83.

17. **Baker, D. R., Moxley, R.A., and Francis, D.H.** 1997. Variation in virulence in the gnotobiotic piglet model of O157:H7 *Escherichia coli* of bovine and human origin, p. 53-58. *In* Paul (ed.), Mechanisms in the pathogenesis of enteric diseases. Plenum Press, New York.

18. **Banatvala, N., M. M. Debeukelaer, P. M. Griffin, T. J. Barrett, K. D. Greene, J. H. Green, and J. G. Wells.** 1996. Shiga-like toxin-producing *Escherichia coli* O111 and associated hemolytic-uremic syndrome: a family outbreak. Pediatr Infect Dis J **15:**1008-11.

19. **Barba, J., V. H. Bustamante, M. A. Flores-Valdez, W. Deng, B. B. Finlay, and J. L. Puente.** 2005. A positive regulatory loop controls expression of the locus of enterocyte effacement-encoded regulators Ler and GrlA. J Bacteriol **187:**7918-30.

20. **Barkocy-Gallagher, G. A., T. M. Arthur, M. Rivera-Betancourt, X. Nou, S. D. Shackelford, T. L. Wheeler, and M. Koohmaraie.** 2003. Seasonal prevalence of Shiga toxin-producing *Escherichia coli*, including O157:H7 and non-O157 serotypes, and *Salmonella* in commercial beef processing plants. J Food Prot **66:**1978-86.

21. **Becker L. A., R. A. R., Velayudhan J., Fang F. C.** 2006. A Novel Tellurite Resistance Locus that Protects *Listeria monocytogenes* from Oxidative and Nitrosative Stress. 106th General meeting of the American Society for Microbiology; B-185; Orlando Florida; May 21-25, 2006, Washington DC.

22. **Begue, R. E., M. A. Neill, E. F. Papa, and P. H. Dennehy.** 1994. A prospective study of Shiga-like toxin-associated diarrhea in a pediatric population. J Pediatr Gastroenterol Nutr **19:**164-9.

23. **Beltrametti, F., A. U. Kresse, and C. A. Guzman.** 1999. Transcriptional regulation of the esp genes of enterohemorrhagic *Escherichia coli.* J Bacteriol **181:**3409-18.

24. **Bergholz, T. M., L. M. Wick, W. Qi, J. T. Riordan, L. M. Ouellette, and T. S. Whittam.** 2007. Global transcriptional response of *Escherichia coli* O157:H7 to growth transitions in glucose minimal medium. BMC Microbiol **7:**97.

25. **Bettelheim, K. A.** 2003. Non-O157 verotoxin-producing *Escherichia coli*: a problem, paradox, and paradigm. Exp Biol Med (Maywood) **228:**333-44.

26. **Beutin, L., M. Bulte, A. Weber, S. Zimmermann, and K. Gleier.** 2000. Investigation of human infections with verocytotoxin-producing strains of *Escherichia coli* (VTEC) belonging to serogroup O118 with evidence for zoonotic transmission. Epidemiol Infect **125:**47-54.

27. **Beutin, L., D. Geier, H. Steinruck, S. Zimmermann, and F. Scheutz.** 1993. Prevalence and some properties of verotoxin (Shiga-like toxin)-producing *Escherichia coli* in seven different species of healthy domestic animals. J Clin Microbiol **31:**2483-8.

28. **Beutin, L., D. Geier, S. Zimmermann, S. Aleksic, H. A. Gillespie, and T. S. Whittam.** 1997. Epidemiological relatedness and clonal types of natural populations of *Escherichia coli* strains producing Shiga toxins in separate populations of cattle and sheep. Appl Environ Microbiol **63:**2175-80.

29. **Beutin, L., G. Krause, S. Zimmermann, S. Kaulfuss, and K. Gleier.** 2004. Characterization of Shiga toxin-producing *Escherichia coli* strains isolated from human patients in Germany over a 3-year period. J Clin Microbiol **42:**1099-108.

30. **Beutin, L., S. Zimmermann, and K. Gleier.** 1998. Human infections with Shiga toxin-producing *Escherichia coli* other than serogroup O157 in Germany. Emerg Infect Dis **4:**635-9.

31. **Bhagwat, A. A., R. P. Phadke, D. Wheeler, S. Kalantre, M. Gudipati, and M. Bhagwat.** 2003. Computational methods and evaluation of RNA stabilization reagents for genome-wide expression studies. J Microbiol Methods **55:**399-409.

32. **Bielaszewska, M., W. Zhang, A. Mellmann, and H. Karch.** 2007. Enterohaemorrhagic *Escherichia coli* O26:H11/H-: a human pathogen in emergence. Berl Munch Tierarztl Wochenschr **120:**279-87.

33. **Blanco, J. E., M. Blanco, M. P. Alonso, A. Mora, G. Dahbi, M. A. Coira, and J. Blanco.** 2004. Serotypes, virulence genes, and intimin types of Shiga toxin (verotoxin)-producing *Escherichia coli* isolates from human patients: prevalence in Lugo, Spain, from 1992 through 1999. J Clin Microbiol **42:**311-9.

34. **Blanco, M., J. E. Blanco, A. Mora, G. Dahbi, M. P. Alonso, E. A. Gonzalez, M. I. Bernardez, and J. Blanco.** 2004. Serotypes, virulence genes, and intimin types of Shiga toxin (verotoxin)-producing *Escherichia coli* isolates from cattle in Spain and identification of a new intimin variant gene (eae-xi). J Clin Microbiol **42:**645-51.

35. **Blattner, F. R., G. Plunkett, 3rd, C. A. Bloch, N. T. Perna, V. Burland, M. Riley, J. Collado-Vides, J. D. Glasner, C. K. Rode, G. F. Mayhew, J. Gregor, N. W. Davis, H. A. Kirkpatrick, M. A. Goeden, D. J. Rose, B. Mau, and Y. Shao.** 1997. The complete genome sequence of *Escherichia coli* K-12. Science **277:**1453-74.

36. **Boerlin, P., S. A. McEwen, F. Boerlin-Petzold, J. B. Wilson, R. P. Johnson, and C. L. Gyles.** 1999. Associations between virulence factors of Shiga toxin-producing *Escherichia coli* and disease in humans. J Clin Microbiol **37:**497-503.

37. **Bokete, T. N., C. M. O'Callahan, C. R. Clausen, N. M. Tang, N. Tran, S. L. Moseley, T. R. Fritsche, and P. I. Tarr.** 1993. Shiga-like toxin-producing *Escherichia coli* in Seattle children: a prospective study. Gastroenterology **105:**1724-31.

38. **Boudjellab, N., H. S. Chan-Tang, X. Li, and X. Zhao.** 1998. Interleukin 8 response by bovine mammary epithelial cells to lipopolysaccharide stimulation. Am J Vet Res **59:**1563-7.

39. **Boudjellab, N., H. S. Chan-Tang, and X. Zhao.** 2000. Bovine interleukin-1 expression by cultured mammary epithelial cells (MAC-T) and its involvement in the release of MAC-T derived interleukin-8. Comp Biochem Physiol A Mol Integr Physiol **127:**191-9.

40. **Boyd, B., and C. Lingwood.** 1989. Verotoxin receptor glycolipid in human renal tissue. Nephron **51:**207-10.

41. **Brooks, J. T., D. Bergmire-Sweat, M. Kennedy, K. Hendricks, M. Garcia, L. Marengo, J. Wells, M. Ying, W. Bibb, P. M. Griffin, R. M. Hoekstra, and C. R. Friedman.** 2004. Outbreak of Shiga toxin-producing

Escherichia coli O111:H8 infections among attendees of a high school cheerleading camp. Clin Infect Dis **38:**190-8.

42. **Brooks, J. T., E. G. Sowers, J. G. Wells, K. D. Greene, P. M. Griffin, R. M. Hoekstra, and N. A. Strockbine.** 2005. Non-O157 Shiga toxin-producing *Escherichia coli* infections in the United States, 1983-2002. J Infect Dis **192:**1422-9.

43. **Brown, C. A., B. G. Harmon, T. Zhao, and M. P. Doyle.** 1997. Experimental *Escherichia coli* O157:H7 carriage in calves. Appl Environ Microbiol **63:**27-32.

44. **Bruen, T. C., H. Philippe, and D. Bryant.** 2006. A simple and robust statistical test for detecting the presence of recombination. Genetics **172:**2665-81.

45. **Brussow, H., C. Canchaya, and W. D. Hardt.** 2004. Phages and the evolution of bacterial pathogens: from genomic rearrangements to lysogenic conversion. Microbiol Mol Biol Rev **68:**560-602.

46. **Burland, V., Y. Shao, N. T. Perna, G. Plunkett, H. J. Sofia, and F. R. Blattner.** 1998. The complete DNA sequence and analysis of the large virulence plasmid of *Escherichia coli* O157:H7. Nucleic Acids Res **26:**4196-204.

47. **Bustamante, V. H., F. J. Santana, E. Calva, and J. L. Puente.** 2001. Transcriptional regulation of type III secretion genes in enteropathogenic *Escherichia coli*: Ler antagonizes H-NS-dependent repression. Mol Microbiol **39:**664-78.

48. **Campos, L. C., T. S. Whittam, T. A. Gomes, J. R. Andrade, and L. R. Trabulsi.** 1994. *Escherichia coli* serogroup O111 includes several clones of diarrheagenic strains with different virulence properties. Infect Immun **62:**3282-8.

49. **Canales, R. D., Y. Luo, J. C. Willey, B. Austermiller, C. C. Barbacioru, C. Boysen, K. Hunkapiller, R. V. Jensen, C. R. Knight, K. Y. Lee, Y. Ma, B. Maqsodi, A. Papallo, E. H. Peters, K. Poulter, P. L. Ruppel, R. R. Samaha, L. Shi, W. Yang, L. Zhang, and F. M. Goodsaid.** 2006. Evaluation of DNA microarray results with quantitative gene expression platforms. Nat Biotechnol **24:**1115-22.

50. **Caprioli, A., I. Luzzi, F. Rosmini, C. Resti, A. Edefonti, F. Perfumo, C. Farina, A. Goglio, A. Gianviti, and G. Rizzoni.** 1994. Community-wide outbreak of hemolytic-uremic syndrome associated with non-O157 verocytotoxin-producing *Escherichia coli*. J Infect Dis **169:**208-11.

51. **Caprioli, A., Tozzi, A E.** 1998. Epidemiology of Shiga toxin-producing *Escherichia coli* infections in continental Europe, p. 38-48. *In* J. B. Kaper, O'Brien, A D (ed.), *Escherichia coli* O157:H7 and other Shiga toxin-producing *Escherichia coli* strains. American Society for Microbiology, Washington.

52. **Carlson, C.** 2002. Investigation of an *Escherichia coli* O111:NM outbreak in a daycare in South Dakota [abstract: session 28, board 80], International Conference on Emerging Infectious Diseases 2002. Centers for Disease Control and Prevention, Atlanta.

53. **Carter, A. O., A. A. Borczyk, J. A. Carlson, B. Harvey, J. C. Hockin, M. A. Karmali, C. Krishnan, D. A. Korn, and H. Lior.** 1987. A severe outbreak of *Escherichia coli* O157:H7--associated hemorrhagic colitis in a nursing home. N Engl J Med **317:**1496-500.

54. **Castillo, A., L. E. Eguiarte, and V. Souza.** 2005. A genomic population genetics analysis of the pathogenic enterocyte effacement island in *Escherichia coli*: the search for the unit of selection. Proc Natl Acad Sci U S A **102:**1542-7.

55. **Celli, J., M. Olivier, and B. B. Finlay.** 2001. Enteropathogenic *Escherichia coli* mediates antiphagocytosis through the inhibition of PI 3-kinase-dependent pathways. Embo J **20:**1245-58.

56. **Chong, Y., R. Fitzhenry, R. Heuschkel, F. Torrente, G. Frankel, and A. D. Phillips.** 2007. Human intestinal tissue tropism in *Escherichia coli* O157 : H7--initial colonization of terminal ileum and Peyer's patches and minimal colonic adhesion ex vivo. Microbiology **153:**794-802.

57. **Cobbold, R., and P. Desmarchelier.** 2000. A longitudinal study of Shiga-toxigenic *Escherichia coli* (STEC) prevalence in three Australian diary herds. Vet Microbiol **71:**125-37.

58. **Cobbold, R. N., and P. M. Desmarchelier.** 2004. In vitro studies on the colonization of bovine colonic mucosa by Shiga-toxigenic *Escherichia coli* (STEC). Epidemiol Infect **132:**87-94.

59. **Colpoys, W. E., B. H. Cochran, T. M. Carducci, and C. M. Thorpe.** 2005. Shiga toxins activate translational regulation pathways in intestinal epithelial cells. Cell Signal **17:**891-9.

60. **Conradi, H.** 1903. Uber losliche, durch aseptische Autolyste erhatlene Giftstoffe von Ruhr- und typhus-bazillen. Dtsch. Med. Wochenschr.:26-28.

61. **Creuzburg, K., B. Kohler, H. Hempel, P. Schreier, E. Jacobs, and H. Schmidt.** 2005. Genetic structure and chromosomal integration site of the

cryptic prophage CP-1639 encoding Shiga toxin 1. Microbiology **151:**941-50.

62. **Creuzburg, K., J. Recktenwald, V. Kuhle, S. Herold, M. Hensel, and H. Schmidt.** 2005. The Shiga toxin 1-converting bacteriophage BP-4795 encodes an NleA-like type III effector protein. J Bacteriol **187:**8494-8.

63. **Cui, X., and G. A. Churchill.** 2003. Statistical tests for differential expression in cDNA microarray experiments. Genome Biol **4:**210.

64. **Cui, X., J. T. Hwang, J. Qiu, N. J. Blades, and G. A. Churchill.** 2005. Improved statistical tests for differential gene expression by shrinking variance components estimates. Biostatistics **6:**59-75.

65. **Dahan, S., S. Knutton, R. K. Shaw, V. F. Crepin, G. Dougan, and G. Frankel.** 2004. Transcriptome of enterohemorrhagic *Escherichia coli* O157 adhering to eukaryotic plasma membranes. Infect Immun **72:**5452-9.

66. **Darfeuille-Michaud, A., J. Boudeau, P. Bulois, C. Neut, A. L. Glasser, N. Barnich, M. A. Bringer, A. Swidsinski, L. Beaugerie, and J. F. Colombel.** 2004. High prevalence of adherent-invasive *Escherichia coli* associated with ileal mucosa in Crohn's disease. Gastroenterology **127:**412-21.

67. **de Sablet, T., Y. Bertin, M. Vareille, J. P. Girardeau, A. Garrivier, A. P. Gobert, and C. Martin.** 2008. Differential expression of stx2 variants in Shiga toxin-producing *Escherichia coli* belonging to seropathotypes A and C. Microbiology **154:**176-86.

68. **Dean, P., M. Maresca, S. Schuller, A. D. Phillips, and B. Kenny.** 2006. Potent diarrheagenic mechanism mediated by the cooperative action of three enteropathogenic *Escherichia coli*-injected effector proteins. Proc Natl Acad Sci U S A **103:**1876-81.

69. **Dean-Nystrom, E. A., B. T. Bosworth, W. C. Cray, Jr., and H. W. Moon.** 1997. Pathogenicity of *Escherichia coli* O157:H7 in the intestines of neonatal calves. Infect Immun **65:**1842-8.

70. **Dean-Nystrom, E. A., B. T. Bosworth, and H. W. Moon.** 1997. Pathogenesis of O157:H7 *Escherichia coli* infection in neonatal calves. Adv Exp Med Biol **412:**47-51.

71. **Dean-Nystrom, E. A., B. T. Bosworth, H. W. Moon, and A. D. O'Brien.** 1998. *Escherichia coli* O157:H7 requires intimin for enteropathogenicity in calves. Infect Immun **66:**4560-3.

72. **Deibel, C., S. Kramer, T. Chakraborty, and F. Ebel.** 1998. EspE, a novel secreted protein of attaching and effacing bacteria, is directly translocated into infected host cells, where it appears as a tyrosine-phosphorylated 90 kDa protein. Mol Microbiol **28:**463-74.

73. **Deng, W., J. L. Puente, S. Gruenheid, Y. Li, B. A. Vallance, A. Vazquez, J. Barba, J. A. Ibarra, P. O'Donnell, P. Metalnikov, K. Ashman, S. Lee, D. Goode, T. Pawson, and B. B. Finlay.** 2004. Dissecting virulence: systematic and functional analyses of a pathogenicity island. Proc Natl Acad Sci U S A **101:**3597-602.

74. **Dibb-Fuller, M. P., E. Allen-Vercoe, C. J. Thorns, and M. J. Woodward.** 1999. Fimbriae- and flagella-mediated association with and invasion of cultured epithelial cells by *Salmonella* enteritidis. Microbiology **145 (Pt 5):**1023-31.

75. **Dibb-Fuller, M. P., A. Best, D. A. Stagg, W. A. Cooley, and M. J. Woodward.** 2001. An in-vitro model for studying the interaction of *Escherichia coli* O157:H7 and other enteropathogens with bovine primary cell cultures. J Med Microbiol **50:**759-69.

76. **Dobrindt, U., F. Agerer, K. Michaelis, A. Janka, C. Buchrieser, M. Samuelson, C. Svanborg, G. Gottschalk, H. Karch, and J. Hacker.** 2003. Analysis of genome plasticity in pathogenic and commensal *Escherichia coli* isolates by use of DNA arrays. J Bacteriol **185:**1831-40.

77. **Dogan, B., S. Klaessig, M. Rishniw, R. A. Almeida, S. P. Oliver, K. Simpson, and Y. H. Schukken.** 2006. Adherent and invasive *Escherichia coli* are associated with persistent bovine mastitis. Vet Microbiol **116:**270-82.

78. **Donnenberg, M. S.** 2002. Introduction, p. xxi-xxv. *In* M. Donnenberg (ed.), *Escherichia coli*, Virulence Mechanisms of a Versatile Pathogen. Academic Press.

79. **Donnenberg, M. S., and T. S. Whittam.** 2001. Pathogenesis and evolution of virulence in enteropathogenic and enterohemorrhagic *Escherichia coli*. J Clin Invest **107:**539-48.

80. **Dopfer, D., R. A. Almeida, T. J. Lam, H. Nederbragt, S. P. Oliver, and W. Gaastra.** 2000. Adhesion and invasion of *Escherichia coli* from single and recurrent clinical cases of bovine mastitis in vitro. Vet Microbiol **74:**331-43.

81. **Dopfer, D., H. Nederbragt, R. A. Almeida, and W. Gaastra.** 2001. Studies about the mechanism of internalization by mammary epithelial cells of *Escherichia coli* isolated from persistent bovine mastitis. Vet Microbiol **80:**285-96.

82. **Dowd, S. E., and J. B. Williams.** 2008. Comparison of Shiga-like toxin II expression between two genetically diverse lineages of *Escherichia coli* O157:H7. J Food Prot **71**:1673-8.

83. **Drasar, B. S., and M. J. Hill.** 1974. Human intestinal flora, p. 36-43. Academic Press, Ltd., London, United Kingdom.

84. **Durso, L. M., J. L. Bono, and J. E. Keen.** 2005. Molecular serotyping of *Escherichia coli* O26:H11. Appl Environ Microbiol **71**:4941-4.

85. **Dziva, F., P. M. van Diemen, M. P. Stevens, A. J. Smith, and T. S. Wallis.** 2004. Identification of *Escherichia coli* O157 : H7 genes influencing colonization of the bovine gastrointestinal tract using signature-tagged mutagenesis. Microbiology **150**:3631-45.

86. **Eaton, K. A., D. I. Friedman, G. J. Francis, J. S. Tyler, V. B. Young, J. Haeger, G. Abu-Ali, and T. S. Whittam.** 2008. Pathogenesis of renal disease due to enterohemorrhagic *Escherichia coli* in germ-free mice. Infect Immun **76**:3054-63.

87. **Eklund, M., F. Scheutz, and A. Siitonen.** 2001. Clinical isolates of non-O157 Shiga toxin-producing *Escherichia coli*: serotypes, virulence characteristics, and molecular profiles of strains of the same serotype. J Clin Microbiol **39**:2829-34.

88. **Elliott, E. J., R. M. Robins-Browne, E. V. O'Loughlin, V. Bennett-Wood, J. Bourke, P. Henning, G. G. Hogg, J. Knight, H. Powell, and D. Redmond.** 2001. Nationwide study of haemolytic uraemic syndrome: clinical, microbiological, and epidemiological features. Arch Dis Child **85**:125-31.

89. **Endo, Y., K. Tsurugi, T. Yutsudo, Y. Takeda, T. Ogasawara, and K. Igarashi.** 1988. Site of action of a Vero toxin (VT2) from *Escherichia coli* O157:H7 and of Shiga toxin on eukaryotic ribosomes. RNA N-glycosidase activity of the toxins. Eur J Biochem **171**:45-50.

90. **Eriksson, S., S. Lucchini, A. Thompson, M. Rhen, and J. C. Hinton.** 2003. Unravelling the biology of macrophage infection by gene expression profiling of intracellular *Salmonella enterica*. Mol Microbiol **47**:103-18.

91. **Ethelberg, S., K. E. Olsen, F. Scheutz, C. Jensen, P. Schiellerup, J. Enberg, A. M. Petersen, B. Olesen, P. Gerner-Smidt, and K. Molbak.** 2004. Virulence factors for hemolytic uremic syndrome, Denmark. Emerg Infect Dis **10**:842-7.

92. **FDA** 2006, posting date. Nationwide *E. coli* O157:H7 Outbreak: Questions & Answers (Food and Drug Administration, Rockville, MD),

www.cfsan.fda.gov/~dms/spinacqa.html#howmany, accessed 2009. [Online.]

93. **Feil, E. J.** 2004. Small change: keeping pace with microevolution. Nat Rev Microbiol **2:**483-95.

94. **Felsenstein, J.** 1989. PHYLIP - Phylogeny Inference Package (Version 3.2). Cladistics **5:**164-166.

95. **Feng, P., K. A. Lampel, H. Karch, and T. S. Whittam.** 1998. Genotypic and phenotypic changes in the emergence of *Escherichia coli* O157:H7. J Infect Dis **177:**1750-3.

96. **Fey, P. D., R. S. Wickert, M. E. Rupp, T. J. Safranek, and S. H. Hinrichs.** 2000. Prevalence of non-O157:H7 shiga toxin-producing *Escherichia coli* in diarrheal stool samples from Nebraska. Emerg Infect Dis **6:**530-3.

97. **Fitzhenry, R. J., D. J. Pickard, E. L. Hartland, S. Reece, G. Dougan, A. D. Phillips, and G. Frankel.** 2002. Intimin type influences the site of human intestinal mucosal colonisation by enterohaemorrhagic *Escherichia coli* O157:H7. Gut **50:**180-5.

98. **Fitzhenry, R. J., S. Reece, L. R. Trabulsi, R. Heuschkel, S. Murch, M. Thomson, G. Frankel, and A. D. Phillips.** 2002. Tissue tropism of enteropathogenic *Escherichia coli* strains belonging to the O55 serogroup. Infect Immun **70:**4362-8.

99. **Fitzhenry, R. J., M. P. Stevens, C. Jenkins, T. S. Wallis, R. Heuschkel, S. Murch, M. Thomson, G. Frankel, and A. D. Phillips.** 2003. Human intestinal tissue tropism of intimin epsilon O103 *Escherichia coli*. FEMS Microbiol Lett **218:**311-6.

100. **Fletcher, J. N., H. E. Embaye, B. Getty, R. M. Batt, C. A. Hart, and J. R. Saunders.** 1992. Novel invasion determinant of enteropathogenic *Escherichia coli* plasmid pLV501 encodes the ability to invade intestinal epithelial cells and HEp-2 cells. Infect Immun **60:**2229-36.

101. **Flexner, S.** 1900. On the etiology of tropical dysentery. Bull. Johns Hopkins Hosp.:231-242.

102. **Frankel, G., O. Lider, R. Hershkoviz, A. P. Mould, S. G. Kachalsky, D. C. Candy, L. Cahalon, M. J. Humphries, and G. Dougan.** 1996. The cell-binding domain of intimin from enteropathogenic *Escherichia coli* binds to beta1 integrins. J Biol Chem **271:**20359-64.

103. **Frankel, G., A. D. Phillips, I. Rosenshine, G. Dougan, J. B. Kaper, and S. Knutton.** 1998. Enteropathogenic and enterohaemorrhagic *Escherichia coli*: more subversive elements. Mol Microbiol **30:**911-21.

104. **Frankel, G., A. D. Phillips, L. R. Trabulsi, S. Knutton, G. Dougan, and S. Matthews.** 2001. Intimin and the host cell--is it bound to end in Tir(s)? Trends Microbiol **9:**214-8.

105. **Friedberg, D., T. Umanski, Y. Fang, and I. Rosenshine.** 1999. Hierarchy in the expression of the locus of enterocyte effacement genes of enteropathogenic *Escherichia coli*. Mol Microbiol **34:**941-52.

106. **Friedrich, A. W., M. Bielaszewska, W. L. Zhang, M. Pulz, T. Kuczius, A. Ammon, and H. Karch.** 2002. *Escherichia coli* harboring Shiga toxin 2 gene variants: frequency and association with clinical symptoms. J Infect Dis **185:**74-84.

107. **Fukiya, S., H. Mizoguchi, T. Tobe, and H. Mori.** 2004. Extensive genomic diversity in pathogenic *Escherichia coli* and Shigella Strains revealed by comparative genomic hybridization microarray. J Bacteriol **186:**3911-21.

108. **Fukushima, H., T. Hashizume, Y. Morita, J. Tanaka, K. Azuma, Y. Mizumoto, M. Kaneno, M. Matsuura, K. Konma, and T. Kitani.** 1999. Clinical experiences in Sakai City Hospital during the massive outbreak of enterohemorrhagic *Escherichia coli* O157 infections in Sakai City, 1996. Pediatr Int **41:**213-7.

109. **Gamage, S. D., A. K. Patton, J. F. Hanson, and A. A. Weiss.** 2004. Diversity and host range of Shiga toxin-encoding phage. Infect Immun **72:**7131-9.

110. **Gansheroff, L. J., and A. D. O'Brien.** 2000. *Escherichia coli* O157:H7 in beef cattle presented for slaughter in the U.S.: higher prevalence rates than previously estimated. Proc Natl Acad Sci U S A **97:**2959-61.

111. **Gansheroff, L. J., M. R. Wachtel, and A. D. O'Brien.** 1999. Decreased adherence of enterohemorrhagic *Escherichia coli* to HEp-2 cells in the presence of antibodies that recognize the C-terminal region of intimin. Infect Immun **67:**6409-17.

112. **Garcia, A., C. J. Bosques, J. S. Wishnok, Y. Feng, B. J. Karalius, J. R. Butterton, D. B. Schauer, A. B. Rogers, and J. G. Fox.** 2006. Renal injury is a consistent finding in Dutch belted rabbits experimentally infected with enterohemorrhagic *Escherichia coli*. Journal of Infectious Diseases **193:**1125-1134.

113. **Garcia, A., R. P. Marini, Y. Feng, A. Vitsky, K. A. Knox, N. S. Taylor, D. B. Schauer, and J. G. Fox.** 2002. A naturally occurring rabbit model of enterohemorrhagic *Escherichia coli*-induced disease. J Infect Dis **186:**1682-6.

114. **Garmendia, J., and G. Frankel.** 2005. Operon structure and gene expression of the espJ--tccP locus of enterohaemorrhagic *Escherichia coli* O157:H7. FEMS Microbiol Lett **247:**137-45.

115. **Garmendia, J., G. Frankel, and V. F. Crepin.** 2005. Enteropathogenic and enterohemorrhagic *Escherichia coli* infections: translocation, translocation, translocation. Infect Immun **73:**2573-85.

116. **Gasser, C., E. Gautier, A. Steck, R. E. Siebenmann, and R. Oechslin.** 1955. [Hemolytic-uremic syndrome: bilateral necrosis of the renal cortex in acute acquired hemolytic anemia]. Schweiz Med Wochenschr **85:**905-9.

117. **Gerber, A., H. Karch, F. Allerberger, H. M. Verweyen, and L. B. Zimmerhackl.** 2002. Clinical course and the role of shiga toxin-producing *Escherichia coli* infection in the hemolytic-uremic syndrome in pediatric patients, 1997-2000, in Germany and Austria: a prospective study. J Infect Dis **186:**493-500.

118. **Giron, J. A., A. G. Torres, E. Freer, and J. B. Kaper.** 2002. The flagella of enteropathogenic *Escherichia coli* mediate adherence to epithelial cells. Mol Microbiol **44:**361-79.

119. **Gomez, D., E. Miliwebsky, A. Silva, N. Deza, C. Zotta, O. Cotella, E. Martinez Espinosa, I. Chinen, C. Fernandez Pascua, and M. Rivas.** 2005. [Isolation of Shiga-toxin-producing *Escherichia coli* strains during a gastrointestinal outbreak at a day care center in Mar del Plata City]. Rev Argent Microbiol **37:**176-83.

120. **Grant, A. J., M. Farris, P. Alefounder, P. H. Williams, M. J. Woodward, and C. D. O'Connor.** 2003. Co-ordination of pathogenicity island expression by the BipA GTPase in enteropathogenic *Escherichia coli* (EPEC). Mol Microbiol **48:**507-21.

121. **Griffin, P. M., L. C. Olmstead, and R. E. Petras.** 1990. *Escherichia coli* O157:H7-associated colitis. A clinical and histological study of 11 cases. Gastroenterology **99:**142-9.

122. **Griffin, P. M., and R. V. Tauxe.** 1991. The epidemiology of infections caused by *Escherichia coli* O157:H7, other enterohemorrhagic *E. coli*, and the associated hemolytic uremic syndrome. Epidemiol Rev **13:**60-98.

123. **Gruenheid, S., I. Sekirov, N. A. Thomas, W. Deng, P. O'Donnell, D. Goode, Y. Li, E. A. Frey, N. F. Brown, P. Metalnikov, T. Pawson, K.**

Ashman, and B. B. Finlay. 2004. Identification and characterization of NleA, a non-LEE-encoded type III translocated virulence factor of enterohaemorrhagic *Escherichia coli* O157:H7. Mol Microbiol **51:**1233-49.

124. **Grys, T. E., M. B. Siegel, W. W. Lathem, and R. A. Welch.** 2005. The StcE protease contributes to intimate adherence of enterohemorrhagic *Escherichia coli* O157:H7 to host cells. Infect Immun **73:**1295-303.

125. **Grys, T. E., L. L. Walters, and R. A. Welch.** 2006. Characterization of the StcE protease activity of *Escherichia coli* O157:H7. J Bacteriol **188:**4646-53.

126. **Gunning, R. F., A. D. Wales, G. R. Pearson, E. Done, A. L. Cookson, and M. J. Woodward.** 2001. Attaching and effacing lesions in the intestines of two calves associated with natural infection with *Escherichia coli* O26:H11. Vet Rec **148:**780-2.

127. **Gunzer, F., I. Hennig-Pauka, K. H. Waldmann, R. Sandhoff, H. J. Grone, H. H. Kreipe, A. Matussek, and M. Mengel.** 2002. Gnotobiotic piglets develop thrombotic microangiopathy after oral infection with enterohemorrhagic *Escherichia coli*. Am J Clin Pathol **118:**364-75.

128. **Guttman, D. S., and D. E. Dykhuizen.** 1994. Clonal Divergence in Escherichia-Coli as a Result of Recombination, Not Mutation. Science **266:**1380-1383.

129. **Gyles, C. L.** 2007. Shiga toxin-producing *Escherichia coli*: an overview. J Anim Sci **85:**E45-62.

130. **Haack, K. R., C. L. Robinson, K. J. Miller, J. W. Fowlkes, and J. L. Mellies.** 2003. Interaction of Ler at the LEE5 (tir) operon of enteropathogenic *Escherichia coli*. Infect Immun **71:**384-92.

131. **Hacker, J., and J. B. Kaper.** 2000. Pathogenicity islands and the evolution of microbes. Annu Rev Microbiol **54:**641-79.

132. **Hall, G. A., C. R. Dorn, N. Chanter, S. M. Scotland, H. R. Smith, and B. Rowe.** 1990. Attaching and effacing lesions in vivo and adhesion to tissue culture cells of Vero-cytotoxin-producing *Escherichia coli* belonging to serogroups O5 and O103. J Gen Microbiol **136:**779-86.

133. **Hartland, E. L., R. M. Robins-Browne, A. D. Philips, and G. Frankel.** 2005. Tissue Tropism in Intestinal Colonization, p. 237-251. *In* J. P. Nataro, P. S. Cohen, H. L. T. Mobley, and J. N. Weiser (ed.), Colonization of Mucosal Surfaces. American Society for Microbiology, Washington DC.

134. **Hashimoto, H., K. Mizukoshi, M. Nishi, T. Kawakita, S. Hasui, Y. Kato, Y. Ueno, R. Takeya, N. Okuda, and T. Takeda.** 1999. Epidemic of

gastrointestinal tract infection including hemorrhagic colitis attributable to Shiga toxin 1-producing *Escherichia coli* O118:H2 at a junior high school in Japan. Pediatrics **103**:E2.

135. **Hauf, N., and T. Chakraborty.** 2003. Suppression of NF-kappa B activation and proinflammatory cytokine expression by Shiga toxin-producing *Escherichia coli*. J Immunol **170**:2074-82.

136. **Hayashi, T., K. Makino, M. Ohnishi, K. Kurokawa, K. Ishii, K. Yokoyama, C. G. Han, E. Ohtsubo, K. Nakayama, T. Murata, M. Tanaka, T. Tobe, T. Iida, H. Takami, T. Honda, C. Sasakawa, N. Ogasawara, T. Yasunaga, S. Kuhara, T. Shiba, M. Hattori, and H. Shinagawa.** 2001. Complete genome sequence of enterohemorrhagic *Escherichia coli* O157:H7 and genomic comparison with a laboratory strain K-12. DNA Res **8**:11-22.

137. **Hayward, R. D., R. J. Cain, E. J. McGhie, N. Phillips, M. J. Garner, and V. Koronakis.** 2005. Cholesterol binding by the bacterial type III translocon is essential for virulence effector delivery into mammalian cells. Mol Microbiol **56**:590-603.

138. **Hendrix, R. W., G. F. Hatfull, and M. C. Smith.** 2003. Bacteriophages with tails: chasing their origins and evolution. Res Microbiol **154**:253-7.

139. **Hendrix, R. W., M. C. Smith, R. N. Burns, M. E. Ford, and G. F. Hatfull.** 1999. Evolutionary relationships among diverse bacteriophages and prophages: all the world's a phage. Proc Natl Acad Sci U S A **96**:2192-7.

140. **Herbelin, C. J., S. C. Chirillo, K. A. Melnick, and T. S. Whittam.** 2000. Gene conservation and loss in the mutS-rpoS genomic region of pathogenic *Escherichia coli*. J Bacteriol **182**:5381-90.

141. **Herold, S., H. Karch, and H. Schmidt.** 2004. Shiga toxin-encoding bacteriophages--genomes in motion. Int J Med Microbiol **294**:115-21.

142. **Higami, S., K. Nishimoto, T. Kawamura, T. Tsuruhara, G. Isshiki, and A. Ookita.** 1998. [Retrospective analysis of the relationship between HUS incidence and antibiotics among patients with *Escherichia coli* O157 enterocolitis in the Sakai outbreak]. Kansenshogaku Zasshi **72**:266-72.

143. **Hilborn, E. D., J. H. Mermin, P. A. Mshar, J. L. Hadler, A. Voetsch, C. Wojtkunski, M. Swartz, R. Mshar, M. A. Lambert-Fair, J. A. Farrar, M. K. Glynn, and L. Slutsker.** 1999. A multistate outbreak of *Escherichia coli* O157:H7 infections associated with consumption of mesclun lettuce. Arch Intern Med **159**:1758-64.

144. **Hiruta, N., T. Murase, and N. Okamura.** 2001. An outbreak of diarrhoea due to multiple antimicrobial-resistant Shiga toxin-producing *Escherichia coli* O26:H11 in a nursery. Epidemiol Infect **127:**221-7.

145. **Ho, T. D., B. M. Davis, J. M. Ritchie, and M. K. Waldor.** 2008. Type 2 secretion promotes enterohemorrhagic *Escherichia coli* adherence and intestinal colonization. Infect Immun **76:**1858-65.

146. **Hoey, D. E., C. Currie, R. W. Else, A. Nutikka, C. A. Lingwood, D. L. Gally, and D. G. Smith.** 2002. Expression of receptors for verotoxin 1 from *Escherichia coli* O157 on bovine intestinal epithelium. J Med Microbiol **51:**143-9.

147. **Hogan, M. C., J. M. Gloor, J. R. Uhl, F. R. Cockerill, and D. S. Milliner.** 2001. Two cases of non-O157:H7 *Escherichia coli* hemolytic uremic syndrome caused by urinary tract infection. Am J Kidney Dis **38:**E22.

148. **Hurley, B. P., C. M. Thorpe, and D. W. Acheson.** 2001. Shiga toxin translocation across intestinal epithelial cells is enhanced by neutrophil transmigration. Infect Immun **69:**6148-55.

149. **Huson, D. H., and D. Bryant.** 2006. Application of phylogenetic networks in evolutionary studies. Mol Biol Evol **23:**254-67.

150. **Hussein, H. S., B. H. Thran, M. R. Hall, W. G. Kvasnicka, and R. C. Torell.** 2003. Verotoxin-producing *Escherichia coli* in culled beef cows grazing rangeland forages. Exp Biol Med (Maywood) **228:**352-7.

151. **Huynh, H. T., G. Robitaille, and J. D. Turner.** 1991. Establishment of bovine mammary epithelial cells (MAC-T): an in vitro model for bovine lactation. Exp Cell Res **197:**191-9.

152. **Iyoda, S., N. Koizumi, H. Satou, Y. Lu, T. Saitoh, M. Ohnishi, and H. Watanabe.** 2006. The GrlR-GrlA regulatory system coordinately controls the expression of flagellar and LEE-encoded type III protein secretion systems in enterohemorrhagic *Escherichia coli.* J Bacteriol **188:**5682-92.

153. **Iyoda, S., and H. Watanabe.** 2005. ClpXP protease controls expression of the type III protein secretion system through regulation of RpoS and GrlR levels in enterohemorrhagic *Escherichia coli.* J Bacteriol **187:**4086-94.

154. **Iyoda, S., and H. Watanabe.** 2004. Positive effects of multiple pch genes on expression of the locus of enterocyte effacement genes and adherence of enterohaemorrhagic *Escherichia coli* O157 : H7 to HEp-2 cells. Microbiology **150:**2357-571.

155. **Jacewicz, M. S., D. W. Acheson, D. G. Binion, G. A. West, L. L. Lincicome, C. Fiocchi, and G. T. Keusch.** 1999. Responses of human intestinal microvascular endothelial cells to Shiga toxins 1 and 2 and pathogenesis of hemorrhagic colitis. Infect Immun **67:**1439-44.

156. **Jelacic, J. K., T. Damrow, G. S. Chen, S. Jelacic, M. Bielaszewska, M. Ciol, H. M. Carvalho, A. R. Melton-Celsa, A. D. O'Brien, and P. I. Tarr.** 2003. Shiga toxin-producing *Escherichia coli* in Montana: bacterial genotypes and clinical profiles. J Infect Dis **188:**719-29.

157. **Jeter, C., and A. G. Matthysse.** 2005. Characterization of the binding of diarrheagenic strains of *E. coli* to plant surfaces and the role of curli in the interaction of the bacteria with alfalfa sprouts. Mol Plant Microbe Interact **18:**1235-42.

158. **Johnson, J. R.** 2002. Evolution of Pathogenic *Escherichia coli*, p. 55-77. *In* M. S. Donnenberg (ed.), *Escherichia coli*: Virulence Mechanisms of a Versatile Pathogen. Academic Press.

159. **Jores, J., L. Rumer, S. Kiessling, J. B. Kaper, and L. H. Wieler.** 2001. A novel locus of enterocyte effacement (LEE) pathogenicity island inserted at pheV in bovine Shiga toxin-producing *Escherichia coli* strain O103:H2. FEMS Microbiol Lett **204:**75-9.

160. **Kailasan Vanaja, S., T. M. Bergholz, and T. S. Whittam.** 2008. Characterization of the *Escherichia coli* O157:H7 Sakai GadE regulon. J Bacteriol.

161. **Kanamaru, K., I. Tatsuno, T. Tobe, and C. Sasakawa.** 2000. SdiA, an *Escherichia coli* homologue of quorum-sensing regulators, controls the expression of virulence factors in enterohaemorrhagic *Escherichia coli* O157:H7. Mol Microbiol **38:**805-16.

162. **Kaper, J. B., and O. G. Gomez-Duarte.** 1997. The per regulator of enteropathogenic *Escherichia coli*. Mol Microbiol **23:**179-81.

163. **Kaper, J. B., and M. A. Karmali.** 2008. The continuing evolution of a bacterial pathogen. Proc Natl Acad Sci U S A **105:**4535-6.

164. **Kaper, J. B., J. P. Nataro, and H. L. Mobley.** 2004. Pathogenic *Escherichia coli*. Nat Rev Microbiol **2:**123-40.

165. **Karch, H., S. Schubert, D. Zhang, W. Zhang, H. Schmidt, T. Olschlager, and J. Hacker.** 1999. A genomic island, termed high-pathogenicity island, is present in certain non-O157 Shiga toxin-producing *Escherichia coli* clonal lineages. Infect Immun **67:**5994-6001.

166. **Karch, H. H., Hans-Iko; Bockemühl, Jochen; Schmidt, Herbert; Schwarzkopf, Andreas; Lissner, Reinhard.** 1997. Shiga Toxin-Producing *Escherichia coli* Infections in Germany. Journal of Food Protection **60**:1454-1457.

167. **Karmali, M. A.** 1989. Infection by verocytotoxin-producing *Escherichia coli*. Clin Microbiol Rev **2**:15-38.

168. **Karmali, M. A., M. Petric, C. Lim, P. C. Fleming, and B. T. Steele.** 1983. *Escherichia coli* cytotoxin, haemolytic-uraemic syndrome, and haemorrhagic colitis. Lancet **2**:1299-1300.

169. **Karmali, M. A., B. T. Steele, M. Petric, and C. Lim.** 1983. Sporadic cases of haemolytic-uraemic syndrome associated with faecal cytotoxin and cytotoxin-producing *Escherichia coli* in stools. Lancet **1**:619-20.

170. **Karpman, D., Z. D. Bekassy, A. C. Sjogren, M. S. Dubois, M. A. Karmali, M. Mascarenhas, K. G. Jarvis, L. J. Gansheroff, A. D. O'Brien, G. S. Arbus, and J. B. Kaper.** 2002. Antibodies to intimin and *Escherichia coli* secreted proteins A and B in patients with enterohemorrhagic *Escherichia coli* infections. Pediatr Nephrol **17**:201-11.

171. **Karpman, D., H. Connell, M. Svensson, F. Scheutz, P. Alm, and C. Svanborg.** 1997. The role of lipopolysaccharide and Shiga-like toxin in a mouse model of *Escherichia coli* O157:H7 infection. J Infect Dis **175**:611-20.

172. **Karpman, D., A. Hakansson, M. T. Perez, C. Isaksson, E. Carlemalm, A. Caprioli, and C. Svanborg.** 1998. Apoptosis of renal cortical cells in the hemolytic-uremic syndrome: in vivo and in vitro studies. Infect Immun **66**:636-44.

173. **Karpman, D., D. Papadopoulou, K. Nilsson, A. C. Sjogren, C. Mikaelsson, and S. Lethagen.** 2001. Platelet activation by Shiga toxin and circulatory factors as a pathogenetic mechanism in the hemolytic uremic syndrome. Blood **97**:3100-8.

174. **Kenny, B., A. Abe, M. Stein, and B. B. Finlay.** 1997. Enteropathogenic *Escherichia coli* protein secretion is induced in response to conditions similar to those in the gastrointestinal tract. Infect Immun **65**:2606-12.

175. **Kerr, M. K.** 2003. Linear models for microarray data analysis: hidden similarities and differences. J Comput Biol **10**:891-901.

176. **Kim, C. C., E. A. Joyce, K. Chan, and S. Falkow.** 2002. Improved analytical methods for microarray-based genome-composition analysis. Genome Biol **3**:RESEARCH0065.

177. **Klapproth, J. M., M. Sasaki, M. Sherman, B. Babbin, M. S. Donnenberg, P. J. Fernandes, I. C. Scaletsky, D. Kalman, A. Nusrat, and I. R. Williams.** 2005. *Citrobacter rodentium* lifA/efa1 is essential for colonic colonization and crypt cell hyperplasia in vivo. Infect Immun **73:**1441-51.

178. **Klapproth, J. M., I. C. Scaletsky, B. P. McNamara, L. C. Lai, C. Malstrom, S. P. James, and M. S. Donnenberg.** 2000. A large toxin from pathogenic *Escherichia coli* strains that inhibits lymphocyte activation. Infect Immun **68:**2148-55.

179. **Kleanthous, H., H. R. Smith, S. M. Scotland, R. J. Gross, B. Rowe, C. M. Taylor, and D. V. Milford.** 1990. Haemolytic uraemic syndromes in the British Isles, 1985-8: association with verocytotoxin producing *Escherichia coli*. Part 2: Microbiological aspects. Arch Dis Child **65:**722-7.

180. **Klein, E. J., J. R. Stapp, C. R. Clausen, D. R. Boster, J. G. Wells, X. Qin, D. L. Swerdlow, and P. I. Tarr.** 2002. Shiga toxin-producing *Escherichia coli* in children with diarrhea: a prospective point-of-care study. J Pediatr **141:**172-7.

181. **Knutton, S., T. Baldwin, P. H. Williams, and A. S. McNeish.** 1989. Actin accumulation at sites of bacterial adhesion to tissue culture cells: basis of a new diagnostic test for enteropathogenic and enterohemorrhagic *Escherichia coli*. Infect Immun **57:**1290-8.

182. **Koitabashi, T., V. Vuddhakul, S. Radu, T. Morigaki, N. Asai, Y. Nakaguchi, and M. Nishibuchi.** 2006. Genetic characterization of *Escherichia coli* O157: H7/- strains carrying the stx2 gene but not producing Shiga toxin 2. Microbiol Immunol **50:**135-48.

183. **Konowalchuk, J., N. Dickie, S. Stavric, and J. I. Speirs.** 1978. Comparative studies of five heat-labile toxic products of *Escherichia coli*. Infect Immun **22:**644-8.

184. **Konowalchuk, J., J. I. Speirs, and S. Stavric.** 1977. Vero response to a cytotoxin of *Escherichia coli*. Infect Immun **18:**775-9.

185. **Koster, F., J. Levin, L. Walker, K. S. Tung, R. H. Gilman, M. M. Rahaman, M. A. Majid, S. Islam, and R. C. Williams, Jr.** 1978. Hemolytic-uremic syndrome after shigellosis. Relation to endotoxemia and circulating immune complexes. N Engl J Med **298:**927-33.

186. **Kudva, I. T., P. G. Hatfield, and C. J. Hovde.** 1997. Characterization of *Escherichia coli* O157:H7 and other Shiga toxin-producing *E. coli* serotypes isolated from sheep. J Clin Microbiol **35:**892-9.

187. **Kumar, S., K. Tamura, and M. Nei.** 2004. MEGA3: Integrated software for Molecular Evolutionary Genetics Analysis and sequence alignment. Brief Bioinform **5:**150-63.

188. **Laaberki, M. H., N. Janabi, E. Oswald, and F. Repoila.** 2006. Concert of regulators to switch on LEE expression in enterohemorrhagic *Escherichia coli* O157:H7: interplay between Ler, GrlA, HNS and RpoS. Int J Med Microbiol **296:**197-210.

189. **Lacher, D. W., H. Steinsland, T. E. Blank, M. S. Donnenberg, and T. S. Whittam.** 2007. Molecular evolution of typical enteropathogenic *Escherichia coli*: clonal analysis by multilocus sequence typing and virulence gene allelic profiling. J Bacteriol **189:**342-50.

190. **Lacher, D. W., H. Steinsland, and T. S. Whittam.** 2006. Allelic subtyping of the intimin locus (eae) of pathogenic *Escherichia coli* by fluorescent RFLP. FEMS Microbiol Lett **261:**80-7.

191. **Lamont, I. L., P. A. Beare, U. Ochsner, A. I. Vasil, and M. L. Vasil.** 2002. Siderophore-mediated signaling regulates virulence factor production in Pseudomonasaeruginosa. Proc Natl Acad Sci U S A **99:**7072-7.

192. **Lan, R., and P. R. Reeves.** 2000. Intraspecies variation in bacterial genomes: the need for a species genome concept. Trends Microbiol **8:**396-401.

193. **Lan, R., Reeves, P. R.** 2006. Evolution of Enteric Pathogens, p. 273-299. *In* H. S. D. Seifert, V. J. (ed.), Evolution of Microbial Pathogens. ASM Press, Washington, D. C.

194. **Lathem, W. W., T. E. Grys, S. E. Witowski, A. G. Torres, J. B. Kaper, P. I. Tarr, and R. A. Welch.** 2002. StcE, a metalloprotease secreted by *Escherichia coli* O157:H7, specifically cleaves C1 esterase inhibitor. Mol Microbiol **45:**277-88.

195. **Leomil, L., L. Aidar-Ugrinovich, B. E. Guth, K. Irino, M. P. Vettorato, D. L. Onuma, and A. F. de Castro.** 2003. Frequency of Shiga toxin-producing *Escherichia coli* (STEC) isolates among diarrheic and non-diarrheic calves in Brazil. Vet Microbiol **97:**103-9.

196. **Leomil, L., A. F. Pestana de Castro, G. Krause, H. Schmidt, and L. Beutin.** 2005. Characterization of two major groups of diarrheagenic *Escherichia coli* O26 strains which are globally spread in human patients and domestic animals of different species. FEMS Microbiol Lett **249:**335-42.

197. **Levine, M. M.** 1987. *Escherichia coli* that cause diarrhea: enterotoxigenic, enteropathogenic, enteroinvasive, enterohemorrhagic, and enteroadherent. J Infect Dis **155:**377-89.

198. **Levine, M. M., J. G. Xu, J. B. Kaper, H. Lior, V. Prado, B. Tall, J. Nataro, H. Karch, and K. Wachsmuth.** 1987. A DNA probe to identify enterohemorrhagic *Escherichia coli* of O157:H7 and other serotypes that cause hemorrhagic colitis and hemolytic uremic syndrome. J Infect Dis **156:**175-82.

199. **Lingwood, C. A.** 1994. Verotoxin-binding in human renal sections. Nephron **66:**21-8.

200. **Liptakova, A., L. Siegfried, M. Kmetova, E. Birosova, D. Kotulova, A. Bencatova, M. Kosecka, and P. Banovcin.** 2005. Hemolytic uremic syndrome caused by verotoxin-producing *Escherichia coli* O26. Case report. Folia Microbiol (Praha) **50:**95-8.

201. **Louise, C. B., and T. G. Obrig.** 1995. Specific interaction of *Escherichia coli* O157:H7-derived Shiga-like toxin II with human renal endothelial cells. J Infect Dis **172:**1397-401.

202. **Mainil, J. G., and G. Daube.** 2005. Verotoxigenic *Escherichia coli* from animals, humans and foods: who's who? J Appl Microbiol **98:**1332-44.

203. **Mainil, J. G., C. J. Duchesnes, S. C. Whipp, L. R. Marques, A. D. O'Brien, T. A. Casey, and H. W. Moon.** 1987. Shiga-like toxin production and attaching effacing activity of *Escherichia coli* associated with calf diarrhea. Am J Vet Res **48:**743-8.

204. **Manning, S. D., R. T. Madera, W. Schneider, S. E. Dietrich, W. Khalife, W. Brown, T. S. Whittam, P. Somsel, and J. T. Rudrik.** 2007. Surveillance for Shiga toxin-producing *Escherichia coli*, Michigan, 2001-2005. Emerg Infect Dis **13:**318-21.

205. **Manning, S. D., A. S. Motiwala, A. C. Springman, W. Qi, D. W. Lacher, L. M. Ouellette, J. M. Mladonicky, P. Somsel, J. T. Rudrik, S. E. Dietrich, W. Zhang, B. Swaminathan, D. Alland, and T. S. Whittam.** 2008. Variation in virulence among clades of *Escherichia coli* O157:H7 associated with disease outbreaks. Proc Natl Acad Sci U S A **105:**4868-73.

206. **Marches, O., T. N. Ledger, M. Boury, M. Ohara, X. Tu, F. Goffaux, J. Mainil, I. Rosenshine, M. Sugai, J. De Rycke, and E. Oswald.** 2003. Enteropathogenic and enterohaemorrhagic *Escherichia coli* deliver a novel effector called Cif, which blocks cell cycle G2/M transition. Mol Microbiol **50:**1553-67.

207. **Matthews, K. R., P. A. Murdough, and A. J. Bramley.** 1997. Invasion of bovine epithelial cells by verocytotoxin-producing *Escherichia coli* O157:H7. J Appl Microbiol **82:**197-203.

208. **McCarthy, T. A., N. L. Barrett, J. L. Hadler, B. Salsbury, R. T. Howard, D. W. Dingman, C. D. Brinkman, W. F. Bibb, and M. L. Cartter.** 2001. Hemolytic-Uremic Syndrome and *Escherichia coli* O121 at a Lake in Connecticut, 1999. Pediatrics **108:**E59.

209. **McDaniel, T. K., K. G. Jarvis, M. S. Donnenberg, and J. B. Kaper.** 1995. A genetic locus of enterocyte effacement conserved among diverse enterobacterial pathogens. Proc Natl Acad Sci U S A **92:**1664-8.

210. **McGraw, E. A., J. Li, R. K. Selander, and T. S. Whittam.** 1999. Molecular evolution and mosaic structure of alpha, beta, and gamma intimins of pathogenic *Escherichia coli.* Mol Biol Evol **16:**12-22.

211. **Mead, P. S., and P. M. Griffin.** 1998. *Escherichia coli* O157:H7. Lancet **352:**1207-12.

212. **Mead, P. S., L. Slutsker, V. Dietz, L. F. McCaig, J. S. Bresee, C. Shapiro, P. M. Griffin, and R. V. Tauxe.** 1999. Food-related illness and death in the United States. Emerg Infect Dis **5:**607-25.

213. **Melton-Celsa, A. R., J. F. Kokai-Kun, and A. D. O'Brien.** 2002. Activation of Shiga toxin type 2d (Stx2d) by elastase involves cleavage of the C-terminal two amino acids of the A2 peptide in the context of the appropriate B pentamer. Mol Microbiol **43:**207-15.

214. **Mercado, E. C., A. Gioffre, S. M. Rodriguez, A. Cataldi, K. Irino, A. M. Elizondo, A. L. Cipolla, M. I. Romano, R. Malena, and M. A. Mendez.** 2004. Non-O157 Shiga toxin-producing *Escherichia coli* isolated from diarrhoeic calves in Argentina. J Vet Med B Infect Dis Vet Public Health **51:**82-8.

215. **Michino, H., K. Araki, S. Minami, S. Takaya, N. Sakai, M. Miyazaki, A. Ono, and H. Yanagawa.** 1999. Massive outbreak of *Escherichia coli* O157:H7 infection in schoolchildren in Sakai City, Japan, associated with consumption of white radish sprouts. Am J Epidemiol **150:**787-96.

216. **Misselwitz, J., H. Karch, M. Bielazewska, U. John, F. Ringelmann, G. Ronnefarth, and L. Patzer.** 2003. Cluster of hemolytic-uremic syndrome caused by Shiga toxin-producing *Escherichia coli* O26:H11. Pediatr Infect Dis J **22:**349-54.

217. **Moxley, R. A., and D. H. Francis.** 1986. Natural and experimental infection with an attaching and effacing strain of *Escherichia coli* in calves. Infect Immun **53:**339-46.

218. **Mundy, R., C. Jenkins, J. Yu, H. Smith, and G. Frankel.** 2004. Distribution of espI among clinical enterohaemorrhagic and enteropathogenic *Escherichia coli* isolates. J Med Microbiol **53:**1145-9.

219. **Muniesa, M., M. A. Schembri, N. Hauf, and T. Chakraborty.** 2006. Active genetic elements present in the locus of enterocyte effacement in *Escherichia coli* O26 and their role in mobility. Infect Immun **74:**4190-9.

220. **Nataro, J. P., and J. B. Kaper.** 1998. Diarrheagenic *Escherichia coli.* Clin Microbiol Rev **11:**142-201.

221. **Naylor, S. W., D. L. Gally, and J. C. Low.** 2005. Enterohaemorrhagic *E. coli* in veterinary medicine. Int J Med Microbiol **295:**419-41.

222. **Naylor, S. W., J. C. Low, T. E. Besser, A. Mahajan, G. J. Gunn, M. C. Pearce, I. J. McKendrick, D. G. Smith, and D. L. Gally.** 2003. Lymphoid follicle-dense mucosa at the terminal rectum is the principal site of colonization of enterohemorrhagic *Escherichia coli* O157:H7 in the bovine host. Infect Immun **71:**1505-12.

223. **Neidhardt, F. C., P. L. Bloch, and D. F. Smith.** 1974. Culture medium for enterobacteria. J Bacteriol **119:**736-47.

224. **Nielsen E. M., Jensen C., and D. L. Baggesen.** 2005. Evidence of transmission of verocytotoxin-producing *E. coli* O111 from a cattle stable to a child. Clin Microbiol Infect **11:**767-770.

225. **Nielsen, E. M., F. Scheutz, and M. Torpdahl.** 2006. Continuous surveillance of Shiga toxin-producing *Escherichia coli* infections by pulsed-field gel electrophoresis shows that most infections are sporadic. Foodborne Pathog Dis **3:**81-7.

226. **Nims Linda J., D. S. H., Larry L. Buck, Stephan A. Young, John L. Golobic, Katherine D. Greene, Evangeline G. Sowers.** 2001. Isolation of Shiga Toxin-producing *Escherichia coli* in New Mexico [abstract C-165], Abstracts and program book for the 101st General Meeting of the American Society for Microbiology (Orlando).

227. **Noris, M., and G. Remuzzi.** 2005. Hemolytic uremic syndrome. J Am Soc Nephrol **16:**1035-50.

228. **Nougayrede, J. P., O. Marches, M. Boury, J. Mainil, G. Charlier, P. Pohl, J. De Rycke, A. Milon, and E. Oswald.** 1999. The long-term cytoskeletal rearrangement induced by rabbit enteropathogenic *Escherichia coli* is Esp dependent but intimin independent. Molecular Microbiology **31:**19-30.

229. **Obrig, T. G., C. B. Louise, C. A. Lingwood, B. Boyd, L. Barley-Maloney, and T. O. Daniel.** 1993. Endothelial heterogeneity in Shiga toxin receptors and responses. J Biol Chem **268:**15484-8.

230. **Ochman, H., E. Lerat, and V. Daubin.** 2005. Examining bacterial species under the specter of gene transfer and exchange. Proc Natl Acad Sci U S A **102 Suppl 1:**6595-9.

231. **Ogura, Y., T. Ooka, Asadulghani, J. Terajima, J. P. Nougayrede, K. Kurokawa, K. Tashiro, T. Tobe, K. Nakayama, S. Kuhara, E. Oswald, H. Watanabe, and T. Hayashi.** 2007. Extensive genomic diversity and selective conservation of virulence-determinants in enterohemorrhagic *Escherichia coli* strains of O157 and non-O157 serotypes. Genome Biol **8:**R138.

232. **Ohnishi, M., J. Terajima, K. Kurokawa, K. Nakayama, T. Murata, K. Tamura, Y. Ogura, H. Watanabe, and T. Hayashi.** 2002. Genomic diversity of enterohemorrhagic *Escherichia coli* O157 revealed by whole genome PCR scanning. Proc Natl Acad Sci U S A **99:**17043-8.

233. **Ostroff, S. M., P. I. Tarr, M. A. Neill, J. H. Lewis, N. Hargrett-Bean, and J. M. Kobayashi.** 1989. Toxin genotypes and plasmid profiles as determinants of systemic sequelae in *Escherichia coli* O157:H7 infections. J Infect Dis **160:**994-8.

234. **Palermo, M., F. Alves-Rosa, C. Rubel, G. C. Fernandez, G. Fernandez-Alonso, F. Alberto, M. Rivas, and M. Isturiz.** 2000. Pretreatment of mice with lipopolysaccharide (LPS) or IL-1beta exerts dose-dependent opposite effects on Shiga toxin-2 lethality. Clin Exp Immunol **119:**77-83.

235. **Pallen, M. J., S. A. Beatson, and C. M. Bailey.** 2005. Bioinformatics analysis of the locus for enterocyte effacement provides novel insights into type-III secretion. BMC Microbiol **5:**9.

236. **Paton, A. W., P. A. Manning, M. C. Woodrow, and J. C. Paton.** 1998. Translocated intimin receptors (Tir) of Shiga-toxigenic *Escherichia coli* isolates belonging to serogroups O26, O111, and O157 react with sera from patients with hemolytic-uremic syndrome and exhibit marked sequence heterogeneity. Infect Immun **66:**5580-6.

237. **Paton, A. W., and J. C. Paton.** 2002. Reactivity of convalescent-phase hemolytic-uremic syndrome patient sera with the megaplasmid-encoded TagA protein of Shiga toxigenic *Escherichia coli* O157. J Clin Microbiol **40:**1395-9.

238. **Paton, A. W., M. C. Woodrow, R. M. Doyle, J. A. Lanser, and J. C. Paton.** 1999. Molecular characterization of a Shiga toxigenic *Escherichia*

coli O113:H21 strain lacking eae responsible for a cluster of cases of hemolytic-uremic syndrome. J Clin Microbiol **37**:3357-61.

239. **Paton, J. C., and A. W. Paton.** 1998. Pathogenesis and diagnosis of Shiga toxin-producing *Escherichia coli* infections. Clin Microbiol Rev **11**:450-79.

240. **Pearson, G. R., K. J. Bazeley, J. R. Jones, R. F. Gunning, M. J. Green, A. Cookson, and M. J. Woodward.** 1999. Attaching and effacing lesions in the large intestine of an eight-month-old heifer associated with *Escherichia coli* O26 infection in a group of animals with dysentery. Vet Rec **145**:370-3.

241. **Perna, N. T., G. F. Mayhew, G. Posfai, S. Elliott, M. S. Donnenberg, J. B. Kaper, and F. R. Blattner.** 1998. Molecular evolution of a pathogenicity island from enterohemorrhagic *Escherichia coli* O157:H7. Infect Immun **66**:3810-7.

242. **Perna, N. T., G. Plunkett, 3rd, V. Burland, B. Mau, J. D. Glasner, D. J. Rose, G. F. Mayhew, P. S. Evans, J. Gregor, H. A. Kirkpatrick, G. Posfai, J. Hackett, S. Klink, A. Boutin, Y. Shao, L. Miller, E. J. Grotbeck, N. W. Davis, A. Lim, E. T. Dimalanta, K. D. Potamousis, J. Apodaca, T. S. Anantharaman, J. Lin, G. Yen, D. C. Schwartz, R. A. Welch, and F. R. Blattner.** 2001. Genome sequence of enterohaemorrhagic *Escherichia coli* O157:H7. Nature **409**:529-33.

243. **Persson, S., K. E. Olsen, S. Ethelberg, and F. Scheutz.** 2007. Subtyping method for *Escherichia coli* shiga toxin (verocytotoxin) 2 variants and correlations to clinical manifestations. J Clin Microbiol **45**:2020-4.

244. **Pfaffl, M. W.** 2001. A new mathematical model for relative quantification in real-time RT-PCR. Nucleic Acids Res **29**:e45.

245. **Phillips, A. D., S. Navabpour, S. Hicks, G. Dougan, T. Wallis, and G. Frankel.** 2000. Enterohaemorrhagic *Escherichia coli* O157:H7 target Peyer's patches in humans and cause attaching/effacing lesions in both human and bovine intestine. Gut **47**:377-81.

246. **Proulx, F., E. G. Seidman, and D. Karpman.** 2001. Pathogenesis of Shiga toxin-associated hemolytic uremic syndrome. Pediatr Res **50**:163-71.

247. **Pruimboom-Brees, I. M., T. W. Morgan, M. R. Ackermann, E. D. Nystrom, J. E. Samuel, N. A. Cornick, and H. W. Moon.** 2000. Cattle lack vascular receptors for *Escherichia coli* O157:H7 Shiga toxins. Proc Natl Acad Sci U S A **97**:10325-9.

248. **Quackenbush, J.** 2002. Microarray data normalization and transformation. Nat Genet **32 Suppl:**496-501.

249. **R/MAANOVA.** http://research.jax.org/faculty/churchill/software/Rmaanova/index.html.

250. **Rangel, J. M., P. H. Sparling, C. Crowe, P. M. Griffin, and D. L. Swerdlow.** 2005. Epidemiology of *Escherichia coli* O157:H7 outbreaks, United States, 1982-2002. Emerg Infect Dis **11:**603-9.

251. **Rashid, R. A., T. A. Tabata, M. J. Oatley, T. E. Besser, P. I. Tarr, and S. L. Moseley.** 2006. Expression of putative virulence factors of *Escherichia coli* O157:H7 differs in bovine and human infections. Infect Immun **74:**4142-8.

252. **Rasko, D. A., M. J. Rosovitz, G. S. Myers, E. F. Mongodin, W. F. Fricke, P. Gajer, J. Crabtree, M. Sebaihia, N. R. Thomson, R. Chaudhuri, I. R. Henderson, V. Sperandio, and J. Ravel.** 2008. The pangenome structure of *Escherichia coli*: comparative genomic analysis of *E. coli* commensal and pathogenic isolates. J Bacteriol **190:**6881-93.

253. **Recktenwald, J., and H. Schmidt.** 2002. The nucleotide sequence of Shiga toxin (Stx) 2e-encoding phage phiP27 is not related to other Stx phage genomes, but the modular genetic structure is conserved. Infect Immun **70:**1896-908.

254. **Reid, S. D., D. J. Betting, and T. S. Whittam.** 1999. Molecular detection and identification of intimin alleles in pathogenic *Escherichia coli* by multiplex PCR. J Clin Microbiol **37:**2719-22.

255. **Reid, S. D., C. J. Herbelin, A. C. Bumbaugh, R. K. Selander, and T. S. Whittam.** 2000. Parallel evolution of virulence in pathogenic *Escherichia coli*. Nature **406:**64-7.

256. **Reida, P., M. Wolff, H. W. Pohls, W. Kuhlmann, A. Lehmacher, S. Aleksic, H. Karch, and J. Bockemuhl.** 1994. An outbreak due to enterohaemorrhagic *Escherichia coli* O157:H7 in a children day care centre characterized by person-to-person transmission and environmental contamination. Zentralbl Bakteriol **281:**534-43.

257. **Reiss, G., P. Kunz, D. Koin, and E. B. Keeffe.** 2006. *Escherichia coli* O157:H7 infection in nursing homes: review of literature and report of recent outbreak. J Am Geriatr Soc **54:**680-4.

258. **Richardson, S. E., T. A. Rotman, V. Jay, C. R. Smith, L. E. Becker, M. Petric, N. F. Olivieri, and M. A. Karmali.** 1992. Experimental verocytotoxemia in rabbits. Infect Immun **60:**4154-67.

259. **Riley, L. W., R. S. Remis, S. D. Helgerson, H. B. McGee, J. G. Wells, B. R. Davis, R. J. Hebert, E. S. Olcott, L. M. Johnson, N. T. Hargrett, P. A. Blake, and M. L. Cohen.** 1983. Hemorrhagic colitis associated with a rare *Escherichia coli* serotype. N Engl J Med **308**:681-5.

260. **Ritchie, J. M., C. M. Thorpe, A. B. Rogers, and M. K. Waldor.** 2003. Critical roles for stx2, eae, and tir in enterohemorrhagic *Escherichia coli*-induced diarrhea and intestinal inflammation in infant rabbits. Infect Immun **71**:7129-39.

261. **Rivas, M., E. Miliwebsky, I. Chinen, C. D. Roldan, L. Balbi, B. Garcia, G. Fiorilli, S. Sosa-Estani, J. Kincaid, J. Rangel, and P. M. Griffin.** 2006. Characterization and epidemiologic subtyping of Shiga toxin-producing *Escherichia coli* strains isolated from hemolytic uremic syndrome and diarrhea cases in Argentina. Foodborne Pathog Dis **3**:88-96.

262. **Robins-Browne, R. M.** 2005. The relentless evolution of pathogenic *Escherichia coli*. Clin Infect Dis **41**:793-4.

263. **Robinson, C. M., J. F. Sinclair, M. J. Smith, and D. O'Brien A.** 2006. Shiga toxin of enterohemorrhagic *Escherichia coli* type O157:H7 promotes intestinal colonization. Proc Natl Acad Sci U S A.

264. **Roe, A. J., S. W. Naylor, K. J. Spears, H. M. Yull, T. A. Dransfield, M. Oxford, I. J. McKendrick, M. Porter, M. J. Woodward, D. G. Smith, and D. L. Gally.** 2004. Co-ordinate single-cell expression of LEE4- and LEE5-encoded proteins of *Escherichia coli* O157:H7. Mol Microbiol **54**:337-52.

265. **Russell, R. M., F. C. Sharp, D. A. Rasko, and V. Sperandio.** 2007. QseA and GrlR/GrlA regulation of the locus of enterocyte effacement genes in enterohemorrhagic *Escherichia coli*. J Bacteriol **189**:5387-92.

266. **Rutjes, N. W., B. A. Binnington, C. R. Smith, M. D. Maloney, and C. A. Lingwood.** 2002. Differential tissue targeting and pathogenesis of verotoxins 1 and 2 in the mouse animal model. Kidney Int **62**:832-45.

267. **Saeed, A. I., V. Sharov, J. White, J. Li, W. Liang, N. Bhagabati, J. Braisted, M. Klapa, T. Currier, M. Thiagarajan, A. Sturn, M. Snuffin, A. Rezantsev, D. Popov, A. Ryltsov, E. Kostukovich, I. Borisovsky, Z. Liu, A. Vinsavich, V. Trush, and J. Quackenbush.** 2003. TM4: a free, open-source system for microarray data management and analysis. Biotechniques **34**:374-8.

268. **Saito, S., J. Yatsuyanagi, Y. Kinouchi, H. Sato, Y. Miyajima, and M. Morita.** 1998. [A familial outbreak of verotoxin-producing *Escherichia coli* O103:H2 infection in which a calf was the suspected infectious source]. Kansenshogaku Zasshi **72**:707-13.

269. **Saitoh, T., S. Iyoda, S. Yamamoto, Y. Lu, K. Shimuta, M. Ohnishi, J. Terajima, and H. Watanabe.** 2008. Transcription of the ehx enterohemolysin gene is positively regulated by GrlA, a global regulator encoded within the locus of enterocyte effacement in enterohemorrhagic *Escherichia coli*. J Bacteriol **190**:4822-30.

270. **Sandkvist, M.** 2001. Type II secretion and pathogenesis. Infect Immun **69**:3523-35.

271. **Sandner, L., L. E. Eguiarte, A. Navarro, A. Cravioto, and V. Souza.** 2001. The elements of the locus of enterocyte effacement in human and wild mammal isolates of *Escherichia coli*: evolution by assemblage or disruption? Microbiology **147**:3149-58.

272. **Sandvig, K., and B. van Deurs.** 1994. Endocytosis and intracellular sorting of ricin and Shiga toxin. FEBS Lett **346**:99-102.

273. **Sayers, G., T. McCarthy, M. O'Connell, M. O'Leary, D. O'Brien, M. Cafferkey, and E. McNamara.** 2006. Haemolytic uraemic syndrome associated with interfamilial spread of *E. coli* O26:H11. Epidemiol Infect **134**:724-8.

274. **Schauder, S., K. Shokat, M. G. Surette, and B. L. Bassler.** 2001. The LuxS family of bacterial autoinducers: biosynthesis of a novel quorum-sensing signal molecule. Mol Microbiol **41**:463-76.

275. **Schimmer, B., K. Nygard, H. M. Eriksen, J. Lassen, B. A. Lindstedt, L. T. Brandal, G. Kapperud, and P. Aavitsland.** 2008. Outbreak of haemolytic uraemic syndrome in Norway caused by stx2-positive *Escherichia coli* O103:H25 traced to cured mutton sausages. BMC Infect Dis **8**:41.

276. **Schmidt, H., L. Beutin, and H. Karch.** 1995. Molecular analysis of the plasmid-encoded hemolysin of *Escherichia coli* O157:H7 strain EDL 933. Infect Immun **63**:1055-61.

277. **Schmittgen, T. D., and K. J. Livak.** 2008. Analyzing real-time PCR data by the comparative C(T) method. Nat Protoc **3**:1101-8.

278. **Schoonderwoerd, M., R. C. Clarke, A. A. van Dreumel, and S. A. Rawluk.** 1988. Colitis in calves: natural and experimental infection with a verotoxin-producing strain of *Escherichia coli* O111:NM. Can J Vet Res **52**:484-7.

279. **Serra-Moreno, R., S. Acosta, J. P. Hernalsteens, J. Jofre, and M. Muniesa.** 2006. Use of the lambda Red recombinase system to produce recombinant prophages carrying antibiotic resistance genes. BMC Mol Biol **7**:31.

280. **Serra-Moreno, R., J. Jofre, and M. Muniesa.** 2008. The CI repressors of Shiga toxin-converting prophages are involved in coinfection of *Escherichia coli* strains, which causes a down regulation in the production of Shiga toxin 2. J Bacteriol **190:**4722-35.

281. **Serra-Moreno, R., J. Jofre, and M. Muniesa.** 2007. Insertion site occupancy by stx2 bacteriophages depends on the locus availability of the host strain chromosome. J Bacteriol **189:**6645-54.

282. **Shariff, M., M. K. Bhan, S. Knutton, B. K. Das, S. Saini, and R. Kumar.** 1993. Evaluation of the fluorescence actin staining test for detection of enteropathogenic *Escherichia coli.* J Clin Microbiol **31:**386-9.

283. **Shiga, K.** 1898. Uber den Dysenteriebacillus (Bacillus dysenterie). Zentralblatt Bakteriologie, Parasitenkunde, Infektionskrankheiten und Hygiene **Abteilung I:**817-828.

284. **Shin, S., M. P. Castanie-Cornet, J. W. Foster, J. A. Crawford, C. Brinkley, and J. B. Kaper.** 2001. An activator of glutamate decarboxylase genes regulates the expression of enteropathogenic *Escherichia coli* virulence genes through control of the plasmid-encoded regulator, Per. Mol Microbiol **41:**1133-50.

285. **Siegler, R. L., T. G. Obrig, T. J. Pysher, V. L. Tesh, N. D. Denkers, and F. B. Taylor.** 2003. Response to Shiga toxin 1 and 2 in a baboon model of hemolytic uremic syndrome. Pediatr Nephrol **18:**92-6.

286. **Sinclair, J. F., and A. D. O'Brien.** 2002. Cell surface-localized nucleolin is a eukaryotic receptor for the adhesin intimin-gamma of enterohemorrhagic *Escherichia coli* O157:H7. J Biol Chem **277:**2876-85.

287. **Smith, J. L., P. M. Fratamico, and N. W. Gunther.** 2007. Extraintestinal pathogenic *Escherichia coli.* Foodborne Pathog Dis **4:**134-63.

288. **Sonntag, A. K., E. Zenner, H. Karch, and M. Bielaszewska.** 2005. Pigeons as a possible reservoir of Shiga toxin 2f-producing *Escherichia coli* pathogenic to humans. Berl Munch Tierarztl Wochenschr **118:**464-70.

289. **Spears, K. J., A. J. Roe, and D. L. Gally.** 2006. A comparison of enteropathogenic and enterohaemorrhagic *Escherichia coli* pathogenesis. FEMS Microbiol Lett **255:**187-202.

290. **Sperandio, V., J. L. Mellies, W. Nguyen, S. Shin, and J. B. Kaper.** 1999. Quorum sensing controls expression of the type III secretion gene transcription and protein secretion in enterohemorrhagic and enteropathogenic *Escherichia coli.* Proc Natl Acad Sci U S A **96:**15196-201.

291. **Sperandio, V., A. G. Torres, B. Jarvis, J. P. Nataro, and J. B. Kaper.** 2003. Bacteria-host communication: the language of hormones. Proc Natl Acad Sci U S A **100**:8951-6.

292. **Starr, M., V. Bennett-Wood, A. K. Bigham, T. F. de Koning-Ward, A. M. Bordun, D. Lightfoot, K. A. Bettelheim, C. L. Jones, and R. M. Robins-Browne.** 1998. Hemolytic-uremic syndrome following urinary tract infection with enterohemorrhagic *Escherichia coli*: case report and review. Clin Infect Dis **27**:310-5.

293. **Stevens, M. P., and Wallis, T. S.** 29 August 2005, posting date. Chapter 8.3.2.4, Adhesins of Enterohemorrhagic *Escherichia coli*. ASM Press http://www.ecosal.org. [Online.]

294. **Stevens, M. P., A. J. Roe, I. Vlisidou, P. M. van Diemen, R. M. La Ragione, A. Best, M. J. Woodward, D. L. Gally, and T. S. Wallis.** 2004. Mutation of toxB and a truncated version of the efa-1 gene in *Escherichia coli* O157:H7 influences the expression and secretion of locus of enterocyte effacement-encoded proteins but not intestinal colonization in calves or sheep. Infect Immun **72**:5402-11.

295. **Stevens, M. P., P. M. van Diemen, G. Frankel, A. D. Phillips, and T. S. Wallis.** 2002. Efa1 influences colonization of the bovine intestine by shiga toxin-producing *Escherichia coli* serotypes O5 and O111. Infect Immun **70**:5158-66.

296. **Stordeur, P., B. China, G. Charlier, S. Roels, and J. Mainil.** 2000. Clinical signs, reproduction of attaching/effacing lesions, and enterocyte invasion after oral inoculation of an O118 enterohaemorrhagic *Escherichia coli* in neonatal calves. Microbes Infect **2**:17-24.

297. **Strauch, E., J. A. Hammerl, A. Konietzny, S. Schneiker-Bekel, W. Arnold, A. Goesmann, A. Puhler, and L. Beutin.** 2008. Bacteriophage 2851 is a prototype phage for dissemination of the Shiga toxin variant gene 2c in *Escherichia coli* O157:H7. Infect Immun **76**:5466-77.

298. **Strauch, E., C. Schaudinn, and L. Beutin.** 2004. First-time isolation and characterization of a bacteriophage encoding the Shiga toxin 2c variant, which is globally spread in strains of *Escherichia coli* O157. Infect Immun **72**:7030-9.

299. **Surette, M. G., and B. L. Bassler.** 1998. Quorum sensing in *Escherichia coli* and *Salmonella typhimurium*. Proc Natl Acad Sci U S A **95**:7046-50.

300. **Surette, M. G., M. B. Miller, and B. L. Bassler.** 1999. Quorum sensing in *Escherichia coli*, *Salmonella typhimurium*, and Vibrio harveyi: a new family of genes responsible for autoinducer production. Proc Natl Acad Sci U S A **96**:1639-44.

301. **Takeda, T., S. Dohi, T. Igarashi, T. Yamanaka, K. Yoshiya, and N. Kobayashi.** 1993. Impairment by verotoxin of tubular function contributes to the renal damage seen in haemolytic uraemic syndrome. J Infect **27**:339-41.

302. **Tanaka, H., M. Ohseto, Y. Yamashita, N. Shinohara, H. Inoue, Y. Sasaki, Y. Kakihara, T. Tsukamoto, T. Yutsudo, Y. Oku, and et al.** 1989. [Bacteriological investigation on an outbreak of acute enteritis associated with verotoxin-producing *Escherichia coli* O111:H-]. Kansenshogaku Zasshi **63**:1187-94.

303. **Taneike, I., H. M. Zhang, N. Wakisaka-Saito, and T. Yamamoto.** 2002. Enterohemolysin operon of Shiga toxin-producing *Escherichia coli*: a virulence function of inflammatory cytokine production from human monocytes. FEBS Lett **524**:219-24.

304. **Tarr, C. L., T. M. Large, C. L. Moeller, D. W. Lacher, P. I. Tarr, D. W. Acheson, and T. S. Whittam.** 2002. Molecular characterization of a serotype O121:H19 clone, a distinct Shiga toxin-producing clone of pathogenic *Escherichia coli*. Infect Immun **70**:6853-9.

305. **Tarr, P. I., C. A. Gordon, and W. L. Chandler.** 2005. Shiga-toxin-producing *Escherichia coli* and haemolytic uraemic syndrome. Lancet **365**:1073-86.

306. **Tasara, T., and R. Stephan.** 2007. Evaluation of housekeeping genes in *Listeria monocytogenes* as potential internal control references for normalizing mRNA expression levels in stress adaptation models using real-time PCR. FEMS Microbiol Lett **269**:265-72.

307. **Tatsuno, I., M. Horie, H. Abe, T. Miki, K. Makino, H. Shinagawa, H. Taguchi, S. Kamiya, T. Hayashi, and C. Sasakawa.** 2001. toxB gene on pO157 of enterohemorrhagic *Escherichia coli* O157:H7 is required for full epithelial cell adherence phenotype. Infect Immun **69**:6660-9.

308. **Tauschek, M., R. A. Strugnell, and R. M. Robins-Browne.** 2002. Characterization and evidence of mobilization of the LEE pathogenicity island of rabbit-specific strains of enteropathogenic *Escherichia coli*. Mol Microbiol **44**:1533-50.

309. **Taylor, D. E.** 1999. Bacterial tellurite resistance. Trends Microbiol **7**:111-5.

310. **Taylor, D. E., M. Rooker, M. Keelan, L. K. Ng, I. Martin, N. T. Perna, N. T. Burland, and F. R. Blattner.** 2002. Genomic variability of O islands encoding tellurite resistance in enterohemorrhagic *Escherichia coli* O157:H7 isolates. J Bacteriol **184**:4690-8.

311. **Taylor, F. B., Jr., V. L. Tesh, L. DeBault, A. Li, A. C. Chang, S. D. Kosanke, T. J. Pysher, and R. L. Siegler.** 1999. Characterization of the baboon responses to Shiga-like toxin: descriptive study of a new primate model of toxic responses to Stx-1. Am J Pathol **154:**1285-99.

312. **Team, R. D. C.** 2005. R: A Language and Environment for Statistical Computing. R Foundation for Statistical Computing, Vienna, Austria.

313. **Tesh, V. L., J. A. Burris, J. W. Owens, V. M. Gordon, E. A. Wadolkowski, A. D. O'Brien, and J. E. Samuel.** 1993. Comparison of the relative toxicities of Shiga-like toxins type I and type II for mice. Infect Immun **61:**3392-402.

314. **Teunis, P., K. Takumi, and K. Shinagawa.** 2004. Dose response for infection by *Escherichia coli* O157:H7 from outbreak data. Risk Anal **24:**401-7.

315. **Thorpe C.M. , J. M. R., D.W.K. Acheson.** 2002. EHEC and other Shiga Toxin producing E.coli, p. 119-154. *In* M. Donnenberg (ed.), *E. coli*: Virulence mechanisms of a versatile pathogen. Elsevier Science.

316. **Tilden, J., Jr., W. Young, A. M. McNamara, C. Custer, B. Boesel, M. A. Lambert-Fair, J. Majkowski, D. Vugia, S. B. Werner, J. Hollingsworth, and J. G. Morris, Jr.** 1996. A new route of transmission for *Escherichia coli*: infection from dry fermented salami. Am J Public Health **86:**1142-5.

317. **Tobe, T., S. A. Beatson, H. Taniguchi, H. Abe, C. M. Bailey, A. Fivian, R. Younis, S. Matthews, O. Marches, G. Frankel, T. Hayashi, and M. J. Pallen.** 2006. An extensive repertoire of type III secretion effectors in *Escherichia coli* O157 and the role of lambdoid phages in their dissemination. Proc Natl Acad Sci U S A **103:**14941-6.

318. **Tomoyasu, T., A. Takaya, Y. Handa, K. Karata, and T. Yamamoto.** 2005. ClpXP controls the expression of LEE genes in enterohaemorrhagic *Escherichia coli*. FEMS Microbiol Lett **253:**59-66.

319. **Tozzi, A. E., A. Caprioli, F. Minelli, A. Gianviti, L. De Petris, A. Edefonti, G. Montini, A. Ferretti, T. De Palo, M. Gaido, and G. Rizzoni.** 2003. Shiga toxin-producing *Escherichia coli* infections associated with hemolytic uremic syndrome, Italy, 1988-2000. Emerg Infect Dis **9:**106-8.

320. **Trofa, A. F., H. Ueno-Olsen, R. Oiwa, and M. Yoshikawa.** 1999. Dr. Kiyoshi Shiga: discoverer of the dysentery bacillus. Clin Infect Dis **29:**1303-6.

321. **Tzipori, S., R. Gibson, and J. Montanaro.** 1989. Nature and distribution of mucosal lesions associated with enteropathogenic and

enterohemorrhagic *Escherichia coli* in piglets and the role of plasmid-mediated factors. Infect Immun **57**:1142-50.

322. **Tzipori, S., F. Gunzer, M. S. Donnenberg, L. de Montigny, J. B. Kaper, and A. Donohue-Rolfe.** 1995. The role of the eaeA gene in diarrhea and neurological complications in a gnotobiotic piglet model of enterohemorrhagic *Escherichia coli* infection. Infect Immun **63**:3621-7.

323. **Tzipori, S., K. I. Wachsmuth, J. Smithers, and C. Jackson.** 1988. Studies in gnotobiotic piglets on non-O157:H7 *Escherichia coli* serotypes isolated from patients with hemorrhagic colitis. Gastroenterology **94**:590-7.

324. **Untergasser, A., Nijveen H, Rao X, Bisseling T, Geurts R, and Leunissen JAM.** 2007. Primer3Plus, an enhanced web interface to Primer3. *Nucleic Acids Research* 2007 35: W71-W74; doi:10.1093/nar/gkm306.

325. **van Diemen, P. M., F. Dziva, A. Abu-Median, T. S. Wallis, H. van den Bosch, G. Dougan, N. Chanter, G. Frankel, and M. P. Stevens.** 2007. Subunit vaccines based on intimin and Efa-1 polypeptides induce humoral immunity in cattle but do not protect against intestinal colonisation by enterohaemorrhagic *Escherichia coli* O157:H7 or O26:H. Vet Immunol Immunopathol **116**:47-58.

326. **van Diemen, P. M., F. Dziva, M. P. Stevens, and T. S. Wallis.** 2005. Identification of enterohemorrhagic *Escherichia coli* O26:H- genes required for intestinal colonization in calves. Infect Immun **73**:1735-43.

327. **Vazquez-Juarez, R. C., J. A. Kuriakose, D. A. Rasko, J. M. Ritchie, M. M. Kendall, T. M. Slater, M. Sinha, B. A. Luxon, V. L. Popov, M. K. Waldor, V. Sperandio, and A. G. Torres.** 2008. CadA Negatively Regulates *Escherichia coli* O157:H7 Adherence and Intestinal Colonization
10.1128/IAI.00677-08. Infect. Immun. **76**:5072-5081.

328. **Vojdani, J. D., L. R. Beuchat, and R. V. Tauxe.** 2008. Juice-associated outbreaks of human illness in the United States, 1995 through 2005. J Food Prot **71**:356-64.

329. **Wade, W. G., B. T. Thom, and N. Evans.** 1979. Cytotoxic enteropathogenic *Escherichia coli*. Lancet **2**:1235-6.

330. **Wadolkowski, E. A., J. A. Burris, and A. D. O'Brien.** 1990. Mouse model for colonization and disease caused by enterohemorrhagic *Escherichia coli* O157:H7. Infect Immun **58**:2438-45.

331. **Wadolkowski, E. A., L. M. Sung, J. A. Burris, J. E. Samuel, and A. D. O'Brien.** 1990. Acute renal tubular necrosis and death of mice orally

infected with *Escherichia coli* strains that produce Shiga-like toxin type II. Infect Immun **58:**3959-65.

332. **Wagner, P. L., M. N. Neely, X. Zhang, D. W. Acheson, M. K. Waldor, and D. I. Friedman.** 2001. Role for a phage promoter in Shiga toxin 2 expression from a pathogenic *Escherichia coli* strain. J Bacteriol **183:**2081-5.

333. **Wales, A. D., M. J. Woodward, and G. R. Pearson.** 2005. Attaching-effacing bacteria in animals. J Comp Pathol **132:**1-26.

334. **Welch, R. A., V. Burland, G. Plunkett, 3rd, P. Redford, P. Roesch, D. Rasko, E. L. Buckles, S. R. Liou, A. Boutin, J. Hackett, D. Stroud, G. F. Mayhew, D. J. Rose, S. Zhou, D. C. Schwartz, N. T. Perna, H. L. Mobley, M. S. Donnenberg, and F. R. Blattner.** 2002. Extensive mosaic structure revealed by the complete genome sequence of uropathogenic *Escherichia coli*. Proc Natl Acad Sci U S A **99:**17020-4.

335. **Werber, D., A. Fruth, A. Liesegang, M. Littmann, U. Buchholz, R. Prager, H. Karch, T. Breuer, H. Tschape, and A. Ammon.** 2002. A multistate outbreak of Shiga toxin-producing *Escherichia coli* O26:H11 infections in Germany, detected by molecular subtyping surveillance. J Infect Dis **186:**419-22.

336. **Whittam, T. S.** 1998. Evolution of *E. coli* O157:H7 and other Shiga toxin-producing E.coli strains, p. 195-212. *In* J. B. Kaper and A. D. O'Brien (ed.), *E. coli* O157:H7 and other Shiga Toxin-Producing *E. coli* Strains. American Society for Microbiology, Washington.

337. **Whittam, T. S., Ake, S. E.** 1993. Genetic Polymorphisms and Recombination in Natural Populations of *E. coli*. *In* N. a. C. Takahata, A. G. (ed.), Mechanisms of molecular evolution. Japanese Scientific Society Press, Tokyo.

338. **Wick, L. M., W. Qi, D. W. Lacher, and T. S. Whittam.** 2005. Evolution of genomic content in the stepwise emergence of *Escherichia coli* O157:H7. J Bacteriol **187:**1783-91.

339. **Wieler, L. H., R. Bauerfeind, and G. Baljer.** 1992. Characterization of Shiga-like toxin producing *Escherichia coli* (SLTEC) isolated from calves with and without diarrhoea. Zentralbl Bakteriol **276:**243-53.

340. **Wieler, L. H., A. Schwanitz, E. Vieler, B. Busse, H. Steinruck, J. B. Kaper, and G. Baljer.** 1998. Virulence properties of Shiga toxin-producing *Escherichia coli* (STEC) strains of serogroup O118, a major group of STEC pathogens in calves. J Clin Microbiol **36:**1604-7.

341. **Wiles, S., S. Clare, J. Harker, A. Huett, D. Young, G. Dougan, and G. Frankel.** 2004. Organ specificity, colonization and clearance dynamics in vivo following oral challenges with the murine pathogen *Citrobacter rodentium*. Cell Microbiol **6**:963-72.

342. **Wray, C., I. M. McLaren, L. P. Randall, and G. R. Pearson.** 2000. Natural and experimental infection of normal cattle with *Escherichia coli* O157. Vet Rec **147**:65-8.

343. **Yona-Nadler, C., T. Umanski, S. Aizawa, D. Friedberg, and I. Rosenshine.** 2003. Integration host factor (IHF) mediates repression of flagella in enteropathogenic and enterohaemorrhagic *Escherichia coli*. Microbiology **149**:877-84.

344. **Zhang, W. L., M. Bielaszewska, A. Liesegang, H. Tschape, H. Schmidt, M. Bitzan, and H. Karch.** 2000. Molecular characteristics and epidemiological significance of Shiga toxin-producing *Escherichia coli* O26 strains. J Clin Microbiol **38**:2134-40.

345. **Zhu, C., T. S. Agin, S. J. Elliott, L. A. Johnson, T. E. Thate, J. B. Kaper, and E. C. Boedeker.** 2001. Complete nucleotide sequence and analysis of the locus of enterocyte Effacement from rabbit diarrheagenic *Escherichia coli* RDEC-1. Infect Immun **69**:2107-15.